Okinawa Institute of Science and Technology
Graduate University

Thesis submitted for the degree

Doctor of Philosophy

Forward genetic screen for *Caenorhabditis elegans* mutants with a progressive decline in adult locomotor function

by

Kazuto Kawamura

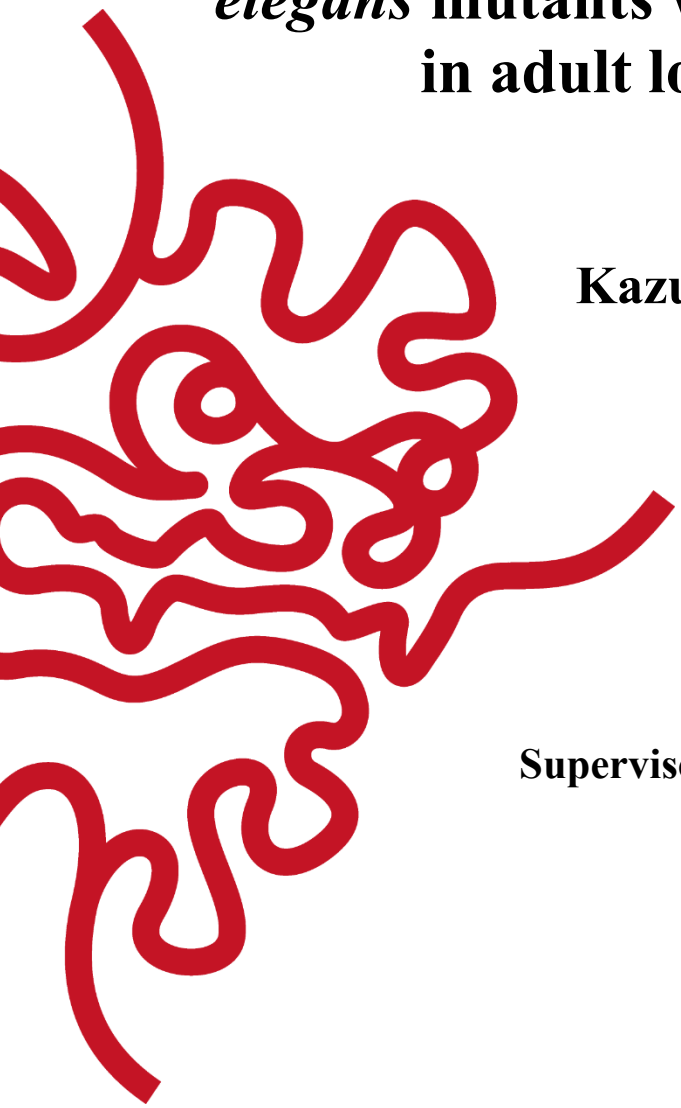

Supervisor: Ichiro Maruyama

January 2019

I, Kazuto Kawamura, declare that this thesis entitled "Forward genetic screen for *Caenorhabditis elegans* mutants with a progressive decline in adult locomotor function" and the data presented in it are original and my own work.

I confirm that:

- No part of this work has previously been submitted for a degree at this or any other university.
- References to the work of others have been clearly acknowledged. Quotations from the work of others have been clearly indicated, and attributed to them.
- In cases where others have contributed to part of this work, such contribution has been clearly acknowledged and distinguished from my own work.
- None of this work has been previously published elsewhere, with the exception of the following: (provide list of publications or presentations, or delete this part).
  (If the work of any co-authors appears in this thesis, authorization such as a release or signed waiver from all affected co-authors must be obtained prior to publishing the thesis. If so, attach copies of this authorization to your initial and final submitted versions, as a separate document for retention by the Graduate School, and indicate on this page that such authorization has been obtained).

Signature: 

Date: 12/14/2018

1. Abstract

Some inherited mutations can cause a delayed onset of toxic symptoms. These types of mutations can be the underlying cause of age-related diseases or more prevalent age-related functional impairments. The isolation of mutants and identification of mutations in model organisms that show delayed onset of toxic symptoms may provide insights into evolutionarily conserved genetic regulators that function during the maintenance of functional capacities. In this study, we carried out an unbiased forward genetic screen for *Caenorhabditis elegans* mutants that show progressive loss of locomotor function during adulthood. After screening 3,352 F2 worms from 1,000 haploid genomes, we isolated five mutant strains that progressively lose their ability to complete a locomotor assay. For one of the mutant strains, a nonsense mutation in Elongator Complex Protein Component 2 (*elpc-2)* causes the progressive decline in locomotor function. Other *C. elegans* mutants with mutations in subunits of the Elongator complex also showed progressive declines in adult locomotor function. The Elongator complex may play a critical role during the maintenance of adult locomotor function in *C. elegans*. The screening procedure, isolated mutants, and the Elongator complex are valuable tools to further explore how locomotor healthspan is maintained in animals.

Acknowledgements

I am grateful for the gracious support of many people who helped me during my PhD.

Ichi Maruyama, my PhD advisor, has always encouraged me to pursue an independent project, and has provided an environment where I could learn to think as an independent scientist. He has allowed me to pursue my own interests while providing guidance at critical decision-points to keep the project on track. I thank him for giving me such a generous opportunity.

Bernd Kuhn and Davie Van Vactor have always been generous with their time to provide advice on coursework and research as thesis committee members. Their kind support and advice has helped me grow as a researcher.

I am grateful to Monica Driscoll for traveling from the other side of the world to examine my thesis proposal. The discussion that took place during the thesis proposal has served as a compass while moving the project forward. I thank Rick Morimoto and Alex Parker for taking the time and effort to examine my thesis and providing valuable guidance and advice for my future.

I thank the Maruyama Unit members, especially Takashi Murayama and Eiichiro Saita, for being supportive throughout my PhD. Takashi handed me my first plate of *Caenorhabditis elegans* worms and taught me from how to pick a worm from one plate to another, to injecting DNA fragments into the miniscule gonad of the worm. Eiichiro has always been supportive and helped me with setting up the video recording system to measure the locomotor function of worms.

None of my experiments would have been possible without the administrative support of Hitomi Ohtaki. She has always been a positive presence, and has handled all of the administrative hoops and hurdles for me to obtain materials to carry out this thesis work.

I am grateful for the support of the OIST DNA sequencing section and Imaging section, especially Hiroki Goto and Koji Koizumi, for technical support as well as advice for my thesis project.

My first in-depth research experience came about because Takayuki Harada took a chance on me to work as a technician in his lab. This research experience motivated me to continue research and apply for a PhD. The encouragement and lessons that I learned while in the Harada Lab has remained with me through my PhD experience. Kazuhiko Namekata, Xiaoli Guo, Hayaki Watanabe, and Daiji Kittaka were great examples of researchers that I aspire to emulate.

I thank the Japan Society for the Promotion of Science and the Okinawa Institute of Science and Technology for providing funding for my PhD. The OIST graduate school staff has always been supportive from arranging my travel for the admissions workshop to coordinating the administrative support throughout my PhD.

Working on this thesis has been a growth experience for me. Sometimes I felt stuck or felt that I had chosen the wrong path in life. Through those times, I am happy to have had the support of my friends, especially Masakazu Igarashi, Tosif Ahamed, Tsai-Ming Luo, Ray Xin Lee, Yi-Jyun Luo, Yoriko Yamamura, Keisuke Ishihara, Alex Roertgen, Russ Hennessy, and Steve Asti.

Finally, I thank my family, Shoji, Mutsuko, and Yuko for their continued support. They have encouraged me to try new things and work hard toward my goals while enjoying life. My extended family, especially Ken, Kuniko, Toru, Jeremy, and Masatoshi have helped me with encouragement and understanding. My wife, Aya, has been a constant source of support. Without her support, I would not have been able to create this thesis.

List of Abbreviations

AD	Alzheimer's disease
ALS	amyotrophic lateral sclerosis
BC	backcrossed
bp	base pair
EDTA	Ethylenediaminetetraacetic acid
ELP	Elongator complex protein
ELPC	Elongator complex protein
EMS	ethyl methanesulfonate
EtOH	ethyl alcohol
FUDR	floxuridine
fALS	familial amyotrophic lateral sclerosis
HD	Huntington's disease
mcm	methoxycarbonylmethyl
ncm	carbamoylmethyl
NGM	nematode growth medium
RT	room temperature
SNP	single nucleotide polymorphism
SMA	spinal muscular atrophy
WT	wild type

Table of Contents

List of figures

List of tables

2. Problem Statement and Aims

What type of inherited mutation can cause delayed onset of disease symptoms? In inherited cases of adult-onset diseases such as Alzheimer's Disease (AD) or amyotrophic lateral sclerosis (ALS), the causative mutation is present from birth, but obvious disease symptoms occur later in life. In theory, delayed onset of disease symptoms can occur from mutations that cause a slow, cumulative form of toxicity or mutations in which its toxicity is triggered by changes related to aging or adulthood. The delayed onset of disease symptoms takes many years to study in humans. Therefore, the isolation of mutant model organisms that show delayed onset of disease symptoms may be a more practical approach to explore how an inherited mutation can cause adult-onset disease.

In this thesis, we addressed the following three aims:

Aim 1 (Chapter 1): Isolation of *Caenorhabdidtis elegans* mutants with progressive decline in adult locomotor function

Aim 2 (Chapter 2): Identification of the responsible gene for the progressive decline in locomotor function for the isolated mutants

Aim 3 (Chapter 3): Characterization of the *elpc-2* mutation

The accomplishment of these aims can provide new mutants to study the mechanisms of how an inherited mutation can lead to delayed onset of disease. The identified genes from the mutants may provide insights into the network of genes that are necessary for maintaining locomotor healthspan in *C. elegans*. These genes may also play a role in modifying the progression or age-of-onset of adult-onset diseases.

3. Chapter 1: Isolation of *C. elegans* mutants with progressive decline in adult locomotor function

3.1. Introduction

3.1.1 Inherited mutations can cause delayed onset of disease symptoms

As human life expectancy increases, there will be a greater need to understand the mechanisms of aging-related functional decline and aging-related disease. In some cases, mutations that are present from birth can cause a delayed onset of impairments that occur during normal aging or in adult-onset diseases.

An inherited mutation with strong immediate toxic effects will lead to a juvenile-onset disease (Fig. 3.1A; Table 3.1). If the mutation causes a slow, cumulative form of toxicity, the mutation can cause a delayed onset of disease symptoms (Fig. 3.1B; Table 3.1). A mutation in which its toxic effects are triggered by changes related to aging or adulthood may also cause delayed onset of disease symptoms (Fig. 3.1C; Table 3.1).

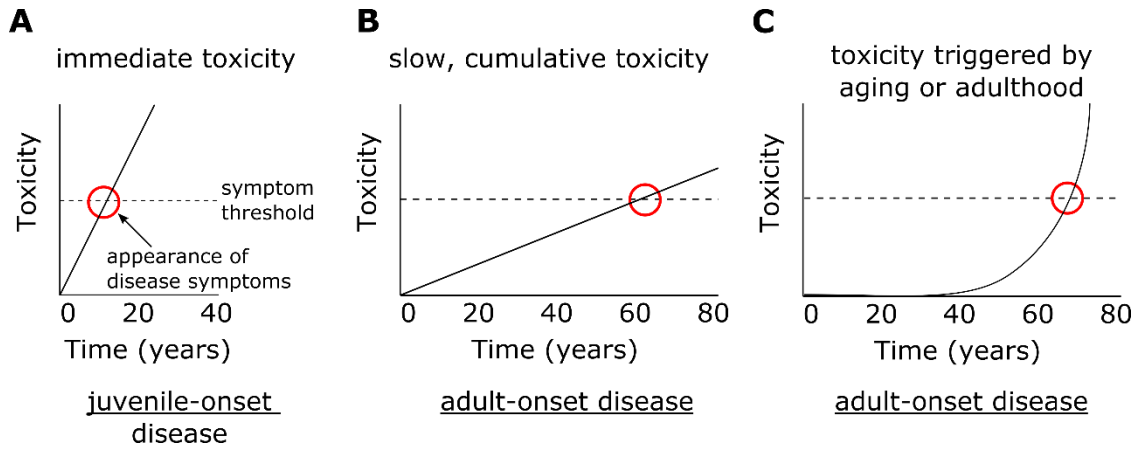

Figure 3.1 Mechanisms underlying immediate and delayed toxicity
(A) Mutations with immediate toxic effects causes symptoms during youth and leads to juvenile-onset disease. (B) Mutations with slow, cumulative forms of toxicity can cause a delayed onset of disease symptoms and lead to adult-onset disease. (C) Mutations in which its toxic effects are triggered by changes related to aging or adulthood can cause a delayed onset of disease symptoms and lead to adult-onset disease.

From a pathophysiological perspective, it may be difficult to distinguish disease symptoms caused by gradual accumulation of toxicity versus those that are caused by a trigger related to aging (Fig. 3.1B vs. Fig. 3.1C). However, distinguishing between the two cases may be important for medical diagnosis and treatment. If the disease occurs from gradual accumulation of toxicity, there should be small damages that can be measured even during early life. In these cases, biochemical markers or imaging approaches may potentially detect the early signs of disease. However, in cases where a mutation's toxic effects are triggered by changes related to aging, the disease will be very difficult to diagnose early in life. The use of genetic tests may be more prudent than biochemical or imaging approaches for diseases that are caused by mutations that are triggered by changes related to aging. In terms of treatment approaches, if a disease is of the age-related trigger type, certain aging pathways may be alternative therapeutic avenues along with targeting the disease mutation.

Table 3.1 Summary of types of inherited mutations and resulting phenotype

Mutation Toxicity	Cumulative toxicity	Toxicity increased by changes related to aging or adulthood	Phenotype
Strong	No	No	Child-onset disease
Strong	Yes	No	Child-onset disease
Strong	No	Yes	Child-onset disease
Strong	Yes	Yes	Child-onset disease
Weak	No	No	Subtle symptoms
Weak	Yes	No	Adult-onset disease
Weak	No	Yes	Adult-onset disease
Weak	Yes	Yes	Adult-onset disease

An example of a gain-of-function mutation that causes adult-onset symptoms is the polyglutamine repeat expansion that leads to Huntington's disease (HD) (Ross et al., 1999). Huntington's disease is characterized by loss of motor control and cognitive deficits that begin generally between 35 and 44 years of age (Gil and Rego, 2008). HD is caused by an autosomal dominant polyglutamine repeat expansion in the Huntingtin (*HTT*) gene (Gil and Rego, 2008). The polyglutamine repeat varies from 6 to 39 repeats in unaffected individuals and from 36 to 180 repeats in HD patients (Rubinsztein et al., 1996). A greater number of repeats correlates with earlier onset of disease, with some juvenile-onset cases (Andresen et al., 2007). If age-related changes are required for the onset of HD, there should not be any juvenile forms of the disease. This suggests that aging is not necessarily required to trigger the toxic effects of long polyglutamine repeats and that a gradual accumulation of toxicity may lead to the symptom onset in HD. However, age-related changes may interact with both strong and weak polyglutamine toxicity to alter the severity of symptoms and disease progression.

Loss-of-function mutations in molecular chaperones for protein folding can also cause adult-onset disease (Hartl et al., 2011). Chaperones are especially important for maintaining proper protein folding during adulthood (Labbadia and Morimoto, 2014a). Missense mutations in the αB-crystallin gene (*CRYAB*), a molecular chaperone for myofilaments, can cause familial forms of late-onset myopathy (Reilich et al., 2010; Zobel et al., 2003). Patients with mutations in *CRYAB* develop muscle weakness often associated with the neck, trunk, cardiomyopathy, and cataracts (Reilich et al., 2010). The onset of symptoms is variable between patients, and reported cases have ranged from 32 years to 68 years (Reilich et al., 2010; Selcen and Engel, 2003; Zobel et al., 2003). The reduced chaperone activity of αB-crystallin causes disorganization of desmin myofilaments and leads to the aggregation of desmin and αB-crystallin in muscle cells (Zobel et al., 2003). In this case, *CRYAB* may be a

gene that is not required during development, but is required for the maintenance of muscle function during adulthood. Whether the accumulation of toxicity is gradual, or is triggered by an age-related change is still unknown.

Spinal muscular atrophy (SMA) is a disease characterized by degeneration of motor neurons in the spinal cord (Coovert et al., 1997). The most common cases are caused by loss-of-function mutations in the *SMN1* gene, which leads to deficient SMN protein expression (Coovert et al., 1997). The disease is classified by the age of onset, which can range from infancy (Type 1) to adulthood (Type 4) (Coovert et al., 1997). *SMN2* is a gene that is closely related to *SMN1,* and can also express the SMN protein, but at lower levels (D'Amico et al., 2011). Symptoms that are caused by loss of *SMN1* are less severe for individuals with greater number of copies of the *SMN2* gene (D'Amico et al., 2011). In this case, the number of copies of the protective *SMN2* gene can explain the severity and age at onset of SMA. However, an open question is how the neuroprotective role of *SMN2* becomes diminished during adulthood in the late-onset cases of SMA. Transcription levels of *SMN2* may decrease with age, and thus reduce the neuroprotective effect, or the built-up toxicity from loss of *SMN1* may reach a threshold during adulthood that cannot be protected by *SMN2*.

3.1.2 Disease-related genes can be identified from forward genetic screens

Disease-related genes have been identified by studying human patients and animal models. Genetic sequencing of inherited cases of ALS led to the identification of ALS-causing mutations in genes such as *SOD1*, *TDP43*, and *C9ORF72* (Bruijn et al., 2004; Renton et al., 2011). An advantage of this approach is that the findings are directly relevant to human patients. However, evolutionarily conserved genes that are involved in aging-related impairments may also be important for understanding the basic mechanisms of aging-related

impairments. Such genes can potentially be identified from genetic screens using animal models.

Genetic studies using model organisms can generally be divided into reverse genetic approaches or forward genetic approaches. Reverse genetic approaches start with a specific gene of interest and study the phenotypic and molecular pathways that are affected by the gene. On the other hand, forward genetic approaches start with a phenotype of interest and search for genes that are involved in the phenotype. A candidate-based RNAi screening approach can also test the potential effects of genes that may be involved in a specific phenotype. However, in candidate-based screens, the selection of the candidate genes adds an element of bias in the genes that may be identified. RNAi approached are also limited in searching for phenotypes that result from decreased expression levels of a gene. Therefore, forward genetic approaches are suitable for searching for new genes involved in a phenotype in an unbiased way.

A classical forward genetic screen follows three steps: (1) Mutagenesis of animals, (2) Phenotypic screen to isolate mutants of a specific phenotype, and (3) Identification of the causative mutation site(s) in the isolated mutants. Further analysis of the causative mutation site may provide novel insights into how the mutation leads to the observed phenotype. Findings from model organisms may not be directly relevant to human patients but may provide basic insights that lead to generalizable findings.

A forward genetic screen can be carried out on wild-type animals, or on transgenic or mutant animals that already demonstrate a specific phenotype. In the latter case, it is referred to as a modifier or suppressor screen, in which genes that affect a specific genetic pathway can be identified. A modifier screen in *Drosophila melanogaster* identified J proteins as suppressors of polyglutamine toxicity (Kazemi-Esfarjani and Benzer, 2000). Modifier screens

in *C. elegans* have also identified genetic modifiers of polyglutamine toxicity (van Ham et al., 2010; Silva et al., 2011). Inactivation of MOAG-4 suppressed the formation of polyglutamine inclusion formations (van Ham et al., 2010). Silva and colleagues identified nine genes that suppress polyglutamine aggregation, improve the motility defect in *C. elegans*, and improve temperature-sensitive misfolding of proteins (Silva et al., 2011). The nine genes are reported to be involved in the mitochondrial respiratory chain, tricarboxylic acid cycle, rRNA processing, and transcription (Silva et al., 2011).

A forward genetic screen for modifiers of TDP-43 toxicity in yeast identified the yeast ortholog of Ataxin-2 (Elden et al., 2010). Greater numbers of polyglutamine repeats in human ATXN2 was found to be linked to the incidence of ALS (Elden et al., 2010). A drug screening carried out in *C. elegans* has identified the neuroleptic drug pimozide has protective effects in a pilot randomized double-blinded placebo-controlled randomized controlled trial for subjects with ALS (Patten et al., 2017). These studies indicate the potential of simple model organisms to provide insights into understanding and treating human diseases.

A forward genetic approach relies on a simple and reproducible screening procedure that can identify a specific phenotype of interest (Jorgensen and Mango, 2002). For an obvious phenotype such as abnormal body size, the screening procedure can be as simple as observing the mutants. However, screens for subtle phenotypes can be difficult to establish. The methodological challenge in screening for progressive disease phenotypes is distinguishing between degeneration that occurred during development versus after reaching adulthood. A paralytic phenotype that is observed in adulthood may have already been present begun during developmental stages. Adult-onset diseases are generally asymptomatic before adulthood, so the screening procedure must be able to separate developmentally

defective mutants from mutants that progressively lose their functional ability during adulthood.

3.1.3 *C. elegans* has been used successfully in forward genetic screens for complex phenotypes

Which animal model should be used for a forward genetic screen? The animal model used for mutagenesis must demonstrate the essential features of the target phenotype. Additional considerations include lifespan, genome size, and ease of handling. For this study, the basic features of the target phenotype are physiological aging and a locomotor circuit controlled by motor neurons and muscles.

C. elegans is a small, 1.5-mm nematode which moves by generating sinusoidal waveforms by contracting and relaxing its body wall muscles. The *C. elegans* motor circuit resembles major aspects of the human motor circuit: both are comprised of the motor neuron, muscle, and neuromuscular junction (Von Stetina et al., 2005). *C. elegans* also undergoes aging, with a lifespan of about two weeks (Kenyon et al., 1993). These features make *C. elegans* a suitable model to screen for mutants that show progressive declines in locomotor function. Sydney Brenner introduced *C. elegans* as an animal model and established its first forward genetic screen to identify genes involved in proper development and coordinated movement (Brenner, 1974). Many forward genetic screens have followed, providing the first examples of single gene mutations that regulate important biological processes such as apoptosis and lifespan (Friedman and Johnson, 1988; Hedgecock et al., 1983; Klass, 1983).

The *C. elegans* life cycle takes about three days from egg to adult and the mean adult lifespan lasts about two weeks. Despite this short lifespan, *C. elegans* undergo age-related changes such as neurodegeneration and sarcopenia that share signaling pathways with human

aging (Herndon et al., 2002; Toth et al., 2012). An unbiased forward genetic screen using *C. elegans* led to the isolation of long-lived mutant strains and identified a single mutation in the *age-1* gene that causes a 40% extension of mean lifespan (Friedman and Johnson, 1988; Klass, 1983). This discovery led to the characterization of the evolutionarily conserved insulin signaling pathway in aging, and demonstrated that regulators of complex biological phenomena can be identified from forward genetic screens in *C. elegans*. Low levels of insulin signaling have been implicated in cases of exceptional human longevity (Milman et al., 2014).

Animal models such as *C. elegans* may be advantageous to identify genes involved in complex disease processes due to their simple genetic architecture. In many cases, a family of human genes is represented by one gene in *C. elegans*. For example, the ErbB family of four genes in humans is represented by the single *let-23* gene in *C. elegans* (Aroian et al., 1990). If a loss-of-function mutation occurs in one of the four ErbB genes in humans, the effects of the mutation may be masked by functional rescue from the other three related genes. However, a loss-of-function mutation in *C. elegans let-23* will not be rescued due to the absence of homologs. Therefore, the functional contributions of some genes may be easier to identify in *C. elegans*. In some cases, mutations in genes that have many functions in higher organisms may cause lethality. These genes may have more simplified roles in *C. elegans*, leading to more subtle effects and allowing for their functional characterization.

3.1.4 *C. elegans* is used as a model for general mechanisms of neuromuscular aging and neuromuscular disease

C. elegans demonstrates signs of neuromuscular aging that are similar to humans. Sarcopenia, the loss of muscle mass and strength with age, is observed both in humans and *C.*

elegans (Herndon et al., 2002). Genes that are involved in the progression of sarcopenia are largely unknown. Kashyap and colleagues conducted a candidate-based RNAi screen using *C. elegans* and identified several genes that significantly reduce the prolonged locomotor activity of the long-lived *daf-2(e1370)* strain (Kashyap et al., 2012; Kenyon et al., 1993). Most of the genes that were identified were part of general cell maintenance pathways such as a vacuolar sorting protein, splicing factor, and fatty acid transport protein (Kashyap et al., 2012).

During aging, loss of motor neurons leads to the denervation of muscle fibers (Gonzalez-Freire et al., 2014). These muscle fibers can be re-innervated by nearby motor neurons, but age-related changes in the neuromuscular junction can prevent the re-innervation process (Gonzalez-Freire et al., 2014). Several mechanistic changes are implicated in the aged neuromuscular junction such as mitochondrial dysfunction, neurotransmitter dysfunction from presynaptic nerve terminals, and chronic systemic inflammation (Gonzalez-Freire et al., 2014; Rudolf et al., 2014). Several studies have focused on changes that occur in the *C. elegans* neuromuscular junction as a result of aging (Liu et al., 2013; Mulcahy et al., 2012). Liu and colleagues found that the first signs of neuromuscular deterioration in *C. elegans* is a deficit in synaptic vesicle fusion, followed by dysfunctions in neurotransmitter vesicle docking and priming (Liu et al., 2013). Muscle function defects are observed later in life (Liu et al., 2013). These findings implicate the neuromuscular junction as a critical location where interventions for neuromuscular deterioration may be most effective.

Reverse genetic models of various neuromuscular diseases have been developed in *C. elegans* (Table 3.1). Various types of disease models for both muscle and motor neuron diseases demonstrate the wide applicability of *C. elegans* for locomotor function studies. Disease phenotypes such as muscle degeneration, intracellular aggregate formation, and progressive paralysis have been described in *C. elegans* disease models (Table 3.1).

C. elegans models of ALS have been created by expressing human mutant SOD1 that has been implicated in familial ALS (fALS) (Oeda et al., 2001). *C. elegans* that express fALS-related mutant SOD1 show greater sensitivity to oxidative stress compared to *C. elegans* that express the wild-type version of SOD1 (Oeda et al., 2001). *C. elegans* mutants that express fALS-related FUS or TDP-43 showed progressive declines in locomotor function (Liachko et al., 2010; Murakami et al., 2012; Vaccaro et al., 2012). Deletion of *C. elegans alfa-1,* the ortholog of human C9ORF72 implicated in fALS, leads to progressive loss of locomotor function and sensitivity to osmotic stress (Therrien et al., 2013). The toxic effects of fALS-related proteins in *C. elegans* demonstrate the evolutionarily conserved effects of disease-related mutations.

Disruption or knockdown of endogenous *C. elegans* genes such as *dys-1*, *frh-1*, or *alfa-1* can cause progressive neuromuscular dysfunctions (Table 3.2). Therefore, targeting the phenotype of a progressive decline in locomotor function may uncover endogenous genes that work to maintain adult locomotor function in *C. elegans*.

Table 3.2 Reverse genetic disease models of neuromuscular disease in *C. elegans*

Disease	Transgenic Model	Phenotype	Refs
Amyotrophic Lateral Sclerosis	• Expression of human familial mutation versions of SOD1, TDP43, or FUS • Deletion of *C. elegans alfa-1,* ortholog of C9ORF72	• Progressive locomotion defects • Shortened lifespan in some cases	(Liachko et al., 2010; Murakami et al., 2012; Oeda et al., 2001; Therrien et al. 2013; Vaccaro et al. 2012)
Duchenne Muscular Dystrophy	Null mutation of *C. elegans dys-1* with weak mutation in *C. elegans MyoD* homolog *hlh-1*	• Progressive muscle degeneration • Progressive development of uncoordinated locomotion	(Gieseler et al., 2000)
Friedreich's Ataxia	RNAi knockdown of *C. elegans frh-1*	• Shortened lifespan • Lethargic behavior	(Vázquez-Manrique et al., 2006)
Inclusion Body Myositis	Expression of human Aβ(1-42)	• Progressive paralysis • Intracellular aggregate formation	(Link, 1995)
Spinal Muscular Atrophy	Deletion of *C. elegans smn-1*	• Larval lethality • Impaired locomotion	(Briese et al., 2009)

Over 90% of ALS cases are caused by unknown factors and the causes of polymyositis, a disease that causes adult-onset muscle weakness, are completely unknown (Bruijn et al., 2004; Dalakas and Hohlfeld, 2003). A recent study conducted whole-exome sequencing on 2869 ALS patients and 6405 controls and newly identified *TBK1* as an ALS associated gene (Cirulli et al., 2015). However, *TBK1* alone is unlikely to resolve all unexplained ALS cases. Searching for new potential target genes using *C. elegans* may lead to novel insights that would not be found in human studies and studies using other animal models.

3.1.5 Limitations in using *C. elegans* as the animal model

Neuromuscular diseases can be classified by their pathogenic origin. The major origins are the muscle, motor neuron, or neuromuscular junction. Neuromuscular diseases can also be classified by age of onset in which some diseases begin during infancy, while others begin after reaching old age.

The features of the *C. elegans* motor circuit determine the types of human diseases it can model. The *C. elegans* motor circuit is made of 113 motor neurons and 95 muscle cells (Von Stetina et al., 2005; White et al., 1986). Seventy-five motor neurons are located in the ventral nerve cord (VNC) (Von Stetina et al., 2005; White et al., 1986). VNC motor neurons are divided into five classes: A, B, D, VC, and AS. The A, B, and D classes are further divided into DA, VA, DB, VB, DD, and VD based on whether they innervate dorsal (D) or ventral (V) muscles (White et al., 1986). The A, B, VC, and AS motor neurons are cholinergic and excite muscle contraction while D motor neurons are GABAergic and inhibit muscle contraction in adulthood (Von Stetina et al., 2005; White et al., 1986).

Motor neurons in humans are also mainly cholinergic, demonstrating the evolutionary conservation of the motor circuit (Fambrough, 1979). However, *C. elegans* does not have an adaptive immune system and its neuronal axons are not surrounded by a myelin sheath. These differences preclude *C. elegans* from being used for specific neuromuscular diseases such as multiple sclerosis which is caused by loss of myelin (Glass et al., 2010).

3.2 Materials and Methods

C. elegans strains

C. elegans Bristol strain N2 was used as wild-type worms. Worms were cultivated on NGM plates with *Escherichia coli* strain OP50. *C. elegans* strains CB408 *unc-43 (e408),* CB190 *unc-54(e190),* MT7929 *unc-13(e51),* and AM725 *rmIs290 [unc-54*p*::Hsa-sod-1 (127X)::YFP]* were obtained from the *Caenorhabditis* Genetic Center (University of Minnesota, MN, USA). All animals were maintained at 20^{o}C.

Ethyl methanesulfonate (EMS) mutagenesis

Synchronized N2 young adult hermaphrodites were collected with 1 mL M9 buffer, and washed three times with 1 mL M9 buffer to remove bacteria. Animals were resuspended in 2 mL M9 buffer and mutagenized by adding 2 mL of 2x stock solution of 100 mM EMS to make a final concentration of 50 mM EMS. Animals were incubated in the 50mM EMS solution for 4 h. Animals were washed five times with 10 mL M9 buffer, then plated on OP50 seeded NGM plates.

Edge Assay

Edge Assay plates were prepared by pouring 16 mL of NGM agar into a circular 9 cm plate. NGM plates were dried overnight at room temperature (RT) with the lid on, then kept at 4°C until use. On the day before the Edge Assay, a total of 100µL of *E. coli* suspension was spotted on four spots near the edge of the NGM plate. The tip of a 50 mL serological pipette was briefly placed over a flame to smoothen the tip. The NGM plate was placed on an inoculating turntable and the smoothened pipette tip was held against the *E.coli* drop. The plate was slowly rotated while holding the pipette tip still. The plate was rotated 360° to spread the E.coli around the edge of the whole plate. Plates were incubated overnight at RT and used the next day. Synchronized worms were collected and washed twice with M9 buffer containing 0.1% aqueous gelatin. Worms were placed on the center of an Edge Assay plate and excess M9 buffer was removed with the edge of a Kimwipe tissue. The number of worms that reached and did not reach the edge were counted at various time points to measure the Edge Assay completion rate.

Measurements of maximum speed and travel distance

Worms were synchronized by picking five adult day 1 worms onto an NGM plate with food, and allowed to lay eggs for 3 h. When the offspring reached adult day 1, 15 worms were picked randomly onto a 6 cm NGM plate without bacteria. After the worms moved away from the initial location with residual food, worms were again moved onto a different NGM plate without bacteria. The plate with worms was placed under a camera, and recorded for one min. Images were analyzed using ImageJ and wrMTrck software (plugin for ImageJ: www.phage.dk/plugins) to produce maximum speed and total travel distance. Measurements were made with the lid on in a temperature-controlled room set at 20°C. At least three biological replicate plates of 15 worms each were measured for each strain. Representative locomotor tracks were also produced using wrMTrck software.

Lifespan Analysis

The lifespan of a population of worms was measured on NGM plates with food at 20°C. Worms that did not move after gentle prodding to the head and tail were counted as dead. Worms that were lost, died from an exploded vulva, or from the bag-of-worms phenotype were censored. For the *ix243* strain, many worms died from the bag-of-worms phenotype. Therefore, we measured lifespan on plates containing 25 µM floxuridine (FUDR), which is an inhibitor of germline proliferation. Worms were transferred from NGM plates to FUDR-containing plates after reaching the L4 stage.

Measurement of development time

The development time until adulthood was measured by allowing an adult day-1 worm to lay eggs for 1 h. The adult was then removed. The time until one of the offspring laid its first egg was measured as the development time.

3.3 Results

3.3.1 "Edge Assay" can test locomotor function of hundreds of worms

The first genetic screens that aimed to understand aging were focused on genetic or environmental interventions that affect lifespan. However, most scientists now agree that aging studies should place a stronger emphasis on "healthspan," or the period of time that a person can maintain a healthy level of functional activity (Burch et al., 2014). Recent studies have suggested that the genetic bases of lifespan and healthspan may not completely overlap (Bansal et al., 2015; Iwasa et al., 2010; Tissenbaum, 2012). Some genes or environmental interventions may have effects on healthspan without large effects on lifespan and vice versa. For example, lifelong spontaneous exercise was found to improve healthspan in mice without

any significant effects on lifespan (Garcia-Valles et al., 2013). A candidate-based genetic screen that searched for *C. elegans* worms with a prolonged swimming ability in adulthood found the epidermal growth factor signaling pathway to be involved in promoting locomotor healthspan without large effects on lifespan (Iwasa et al., 2010). Therefore, we also chose to focus on a healthspan-related phenotype: progressive loss of locomotor function during adulthood.

Loss of locomotor function is a sign of normal aging as well as a symptom of various age-related diseases. It is an evolutionarily conserved indicator of an animal's healthspan from worms, flies, mice, and humans (Cesari et al., 2009; Grotewiel et al., 2005; Hahm et al., 2015; Justice et al., 2014). We decided to search for mutants that demonstrate normal locomotor function during development and early adulthood, but lose their locomotor function much quicker than wild-type worms during adulthood. We addressed the issue of distinguishing mutants with developmental locomotor defects versus those with adult-onset locomotor deficits by establishing a sequential two-step screen in which we remove mutants that have strong developmental defects on the first day of adulthood and collect mutants that show locomotor deficits on the third and fifth days of adulthood. Our focus on locomotor function, a healthspan-related phenotype, aims to identify genes that are involved in the maintenance of healthspan.

In order to test the locomotor function of hundreds of worms at once, we established a procedure called the "Edge Assay." The Edge Assay is carried out on a 9-cm circular agar plate with *E. coli* OP50 strain bacterial feed spread only on the outer edge (Fig. 3.2). Up to several hundred synchronized adult worms are collected with M9 buffer and placed on the center of the plate. Motile worms reach the *E.coli* and remain close to the edge but slow or paralyzed worms can be found remaining in the center of the plate (Fig. 3.2B). Almost all worms that reached the *E. coli* bacterial feed remained in the edge.

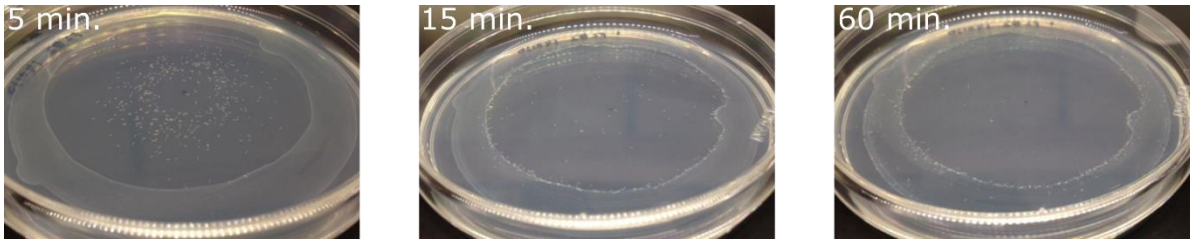

Figure 3.2 Photos of Edge assay

(Left) Photo of the Edge Assay after 5 min. (Center) Photo of the Edge Assay after 15 min. (Right) Photo of the Edge Assay after 60 min.

The Edge Assay completion rate is calculated by counting the number of worms on the edge of the plate divided by the total number of worms (Fig. 3.3A). We measured the completion rates of adult wild-type worms for seven days at 5, 10, 15, 30, and 60 min time points (Fig. 3.3B). Over 90% of wild-type worms completed the Edge Assay in 15 min on the first day of adulthood. If given 60 min, over 90% of wild-type worms completed the Edge Assay during the first five days of adulthood (Fig. 3.3B).

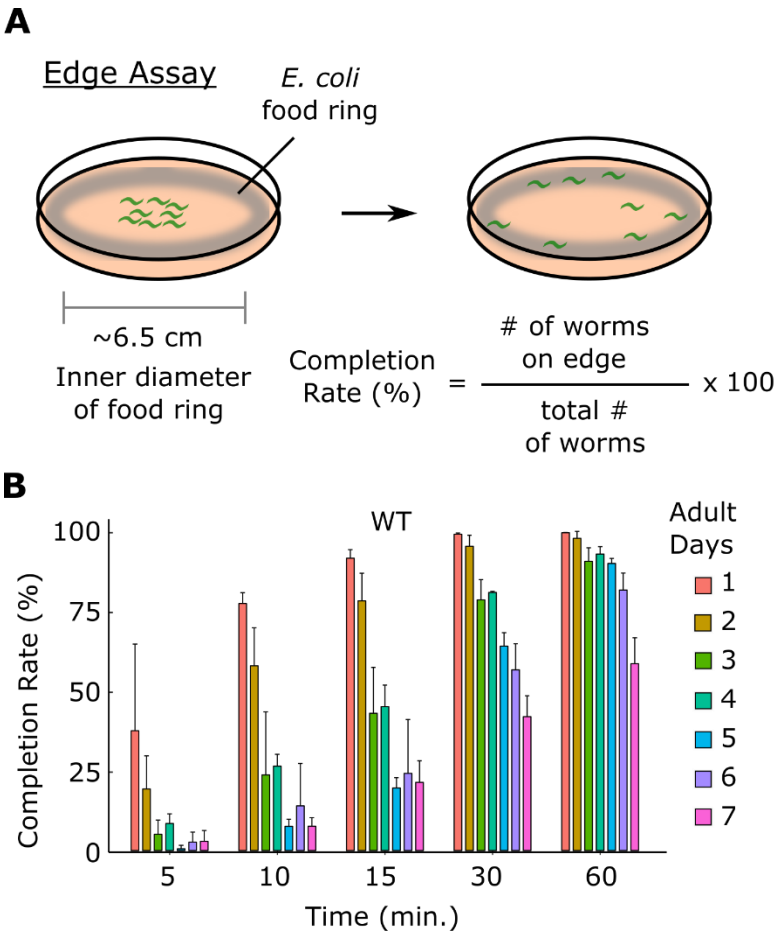

Figure 3.3 Edge Assay completion rates

(A) Schematic diagram of Edge Assay and method to calculate Edge Assay completion rate. (B) Completion rates of wild-type (WT) N2 *C. elegans* worms for the edge test from day 1 to day 7 of adulthood. Three biological replicate plates with approximately 100 worms per plate were assayed (n = 3). Error bars indicate 95% confidence intervals.

Large decreases in Edge Assay completion rate is observed from adult day 2 to 3 at the 10 and 15 min time points. In contrast, only minor decreases in the Edge Assay completion rate is observed from adult day 1 to 5 at the 60 min time point (Fig. 3.3B). Previous studies on the functional capacity of locomotor function and neuromuscular function suggest declines that begin around adult day 5 to day 6 (Hahm et al., 2015; Liu et al., 2013). *C. elegans* chemotaxis towards benzaldehyde, an attractive chemical cue, was

significantly diminished beginning on the fourth day of adulthood (Leinwand et al., 2015). Therefore, declines in Edge Assay completion rate that occurred on adult day 3 at the 10 and 15 min time points may indicate deficits in sensory perception or result from suboptimal search behavior. The adult day 3 worm may start to show deficits in sensing the food cue but still have fully functional neuromuscular activity.

3.3.2 Time points for distinguishing mutants with progressive locomotor decline from wild-type worms using the Edge Assay

We tested whether the Edge Assay can distinguish wild-type worms from mutants with a progressive decline in locomotor function. We tested *C. elegans* mutant strains that have been previously isolated and are defective in the function of neurons (*unc-13(e51)*, *unc-43(e408)*)) (Maruyama and Brenner, 1991; Reiner et al., 1999) or muscles (*unc-54(e190)*) (MacLeod et al., 1981) using the Edge Assay (Fig. 3.4A). On the first day of adulthood, all three mutant strains could not reach the edge in 15 min (Fig. 3.4A). After 60 min, 26% of *unc-54(e190)* mutants, 6.4% of *unc-43(e408)* mutants, and 0% of *unc-13(e51)* mutants reached the edge (Fig. 3.4A). In contrast, 91.3% of wild-type worms reached the edge in 15 min on the first day of adulthood and 99.6% reached the edge in 60 min (Fig. 1B). Therefore, carrying out the Edge Assay for 15 min on the first day of adulthood is a time point that can clearly distinguish wild-type worms from worms with strong developmental locomotor defects.

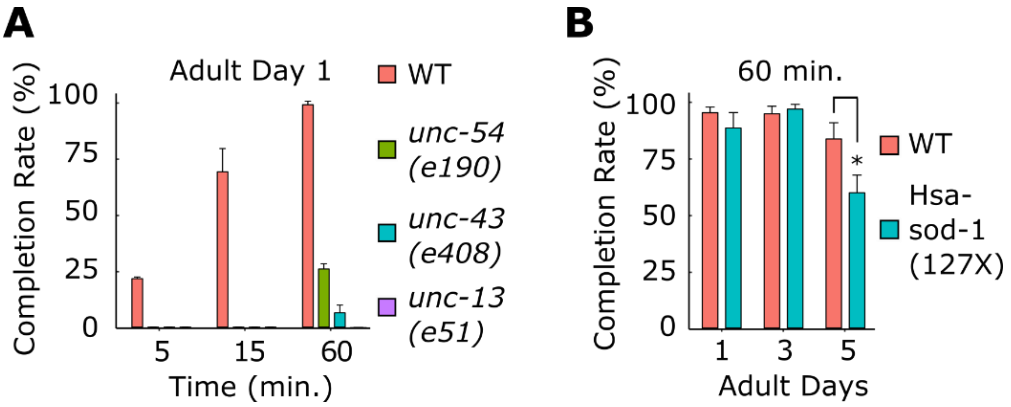

Figure 3.4 Edge Assay completion rates of known mutants

(A) Completion rates for WT and developmental motor deficit mutants (*unc-54(e190)*, *unc-43(e408)*, *(unc-13(e51)*) on the first day of adulthood. (B) Completion rates of WT and previously reported adult-onset motor deficit mutant (Hsa-sod-1(127X)). Three biological replicate plates with approximately 100 worms per plate were assayed (n = 3). Error bars indicate 95% confidence intervals. *$P < 0.05$; Unpaired Student's *t* test.

Next, we tested whether the Edge Assay can distinguish wild-type worms from worms that show progressive declines in locomotor function. A *C. elegans* model of amyotrophic lateral sclerosis that expresses a truncated version of human SOD1 (SOD1-G127insTGGGstop) was tested using the Edge Assay (Gidalevitz et al., 2009). The Hsa-sod-1(127X) mutant showed a significant reduction in the Edge Assay completion rate on the fifth day of adulthood compared to wild-type worms (Fig. 3.4B). Therefore, carrying out the Edge Assay for 60 min on the fifth day of adulthood is a time point that can distinguish wild-type worms from worms that show progressive declines in locomotor function.

3.3.3 Mutagenesis and screening procedure

Taking into account the Edge Assay completion rates of mutants with developmental and progressive locomotor deficits, we established a forward genetic screening procedure to isolate mutants that show progressive declines in locomotor function during adulthood (Fig. 3.5). The screening procedure removes mutants with developmental locomotor defects and isolates mutants that show a locomotor deficit in adulthood.

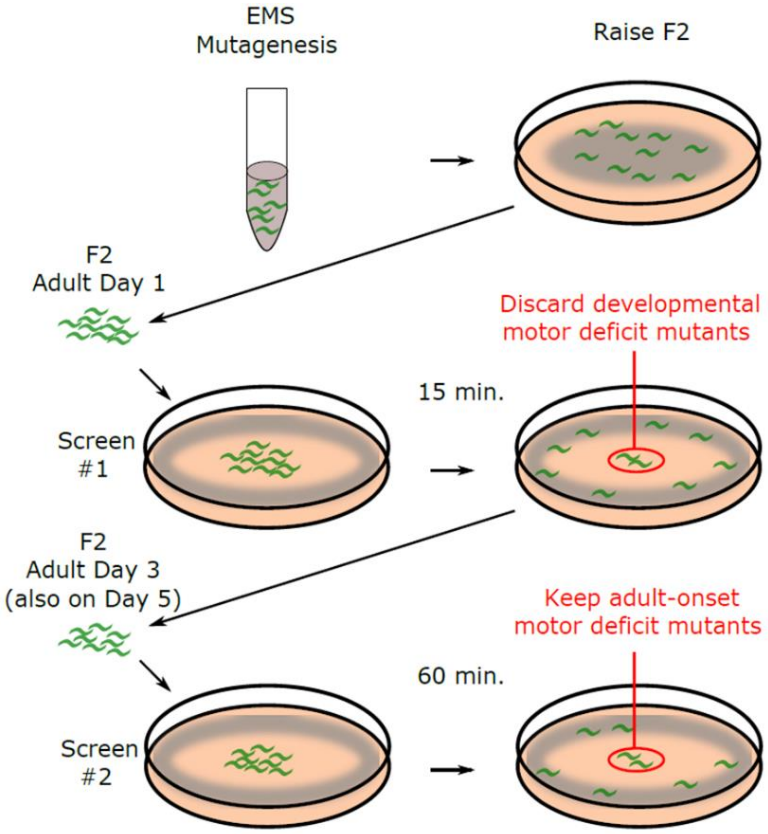

Figure 3.5 Schematic description of forward genetic screen
Schematic description of genetic screening procedure to isolate mutants that show a progressive decline in locomotor function.

We mutagenized worms using EMS and screened 3,352 F2 worms from 500 F1 worms (1,000 haploid genomes). We carried out a three-step screening procedure to isolate mutants with progressive locomotor deficits (Fig. 3.5). First, we carried out the Edge Assay

for F2 worms on the first day of adulthood to remove worms with developmental locomotor defects. Worms that were unable to reach the *E. coli* ring on the edge of the plate in 15 min were aspirated away. Second, we repeated the Edge Assay on the third day of adulthood using only the worms that were able to complete the Edge Assay on the first day. We collected the worms that remained in the central region of the Edge Assay plate after 60 min as mutants that show a progressive loss of locomotor function on the third day of adulthood. Third, we repeated the Edge Assay on the fifth day of adulthood using the worms that were able to complete the Edge Assay on the third day. We collected the worms that remained in the central region of the Edge Assay plate after 60 min as mutants that show a progressive loss of locomotor function on the fifth day of adulthood. We carried out two separate instances of the screening procedure and obtained 22 viable mutants (12 viable mutants on the third day of adulthood and 10 viable mutants on the fifth day of adulthood) (Table 3.3).

Table 3.3 Number of viable mutants obtained from screen

	EMS-A: 400 genomes		**EMS-B: 600 genomes**		
	Day 3	**Day 5**	**Day 3**	**Day 5**	**Total**
Adult-onset mutants	13	23	17	17	70
Viable adult-onset mutants	3	8	9	2	22

3.3.4 Isolated mutants

Five out of the 22 isolated mutants reproducibly showed progressive deficits in completing the Edge Assay (Fig. 3.6). Reductions in completing the Edge Assay may be caused by deficits in locomotor function, sensory perception, or search behavior. To determine whether the isolated mutants have deficits in locomotor function, we measured the locomotor function of individual worms on an agar plate without food. For each strain, we

recorded three plates of 15 worms on the first, third, and fifth days of adulthood. The videos were analyzed using ImageJ and wrMTrck software (www.phage.dk/plugins) to produce the instantaneous maximum velocity that the worm reached within a 1-second interval and the total travel distance of the worm during the 1-min recording. The *ix239* and *ix242* mutant strains showed significantly greater reductions in maximum velocity and travel distance compared to wild-type worms (Fig. 3.7A–D). However, *ix240* worms did not show a significant reduction in maximum velocity or travel distance from adult day 1 to 5 in comparison to wild-type worms (Fig. 3.7A–D). *ix240* worms may have progressive deficits in functions other than locomotor function, such as sensory perception or search behavior.

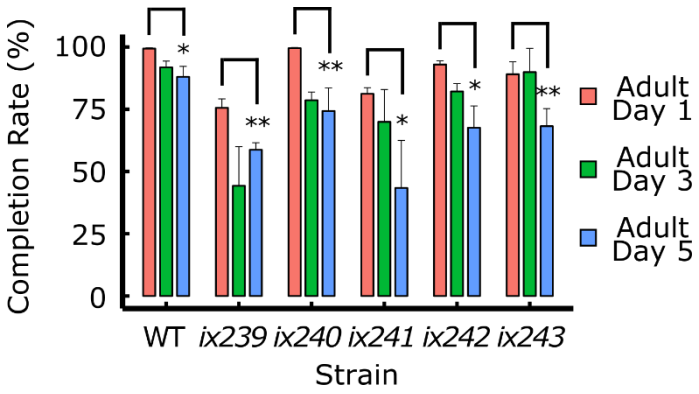

Figure 3.6 Edge Assay completion rates of isolated mutants

Edge Assay completion rates of isolated mutants for adult days 1, 3, and 5. Three biological replicate plates with approximately 100 worms per plate were assayed (n = 3). **P* < 0.05; ***P* < 0.01; Paired Student's *t* test vs. adult day 1 completion rate.

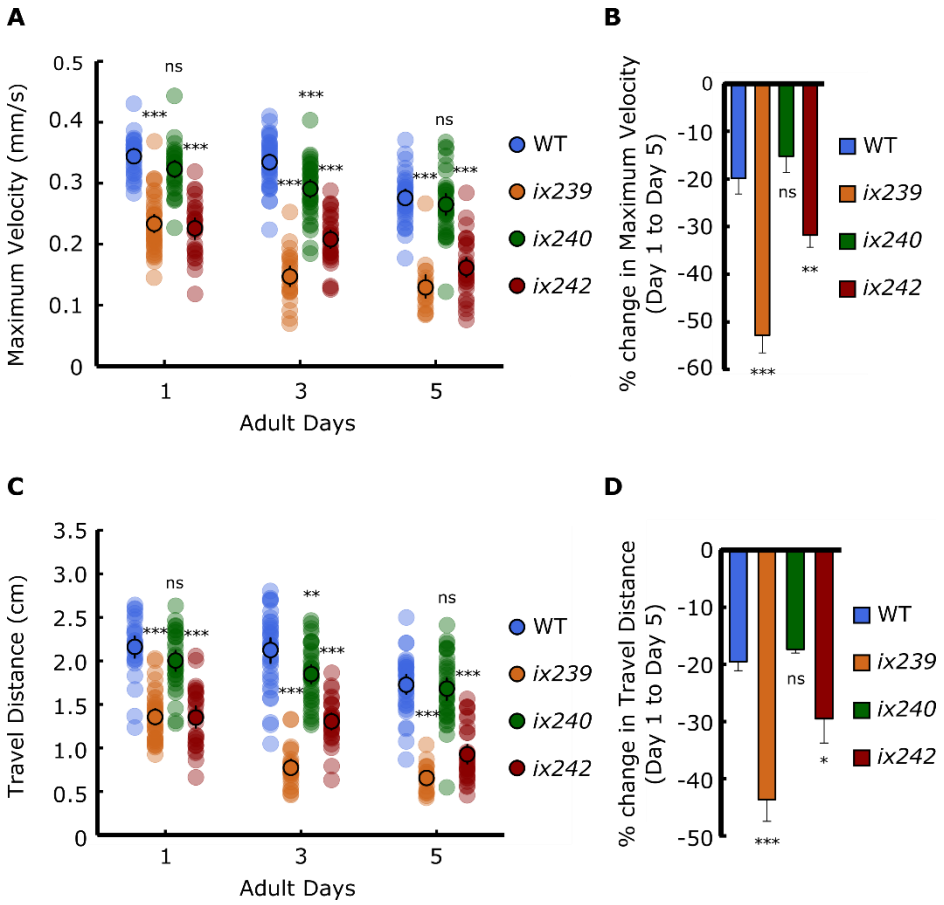

Figure 3.7 Maximum velocities of WT, *ix239*, *ix240*, and *ix242* worms

(A) Maximum velocity of WT, *ix239*, *ix240*, and *ix242* worms. (B) Percent change in maximum velocity of WT, *ix239*, *ix240*, and *ix242* worms. For maximum velocity and travel distance experiments, n = 30–45 worms per strain for each day (10–15 worms from 3 biological replicate plates). For percent change in maximum velocity graphs, n = 3 biological replicate plates. **P* < 0.05; ***P* < 0.01; ****P* < 0.001; ns, not significant; One-way ANOVA with Dunnett's post hoc test vs. WT.

To check whether the progressive decline in locomotor function is maintained after backcrossing, *ix241* and *ix243* worms were crossed with the parental N2 strain. After each backcross, we checked for lines that still showed the progressive decline in locomotor function by measuring the maximum velocity and travel distance of individual worms. Both *ix241* and *ix243* worms showed significant reductions in both travel distance and maximum velocity after four backcrosses (Fig. 3.8A-I).

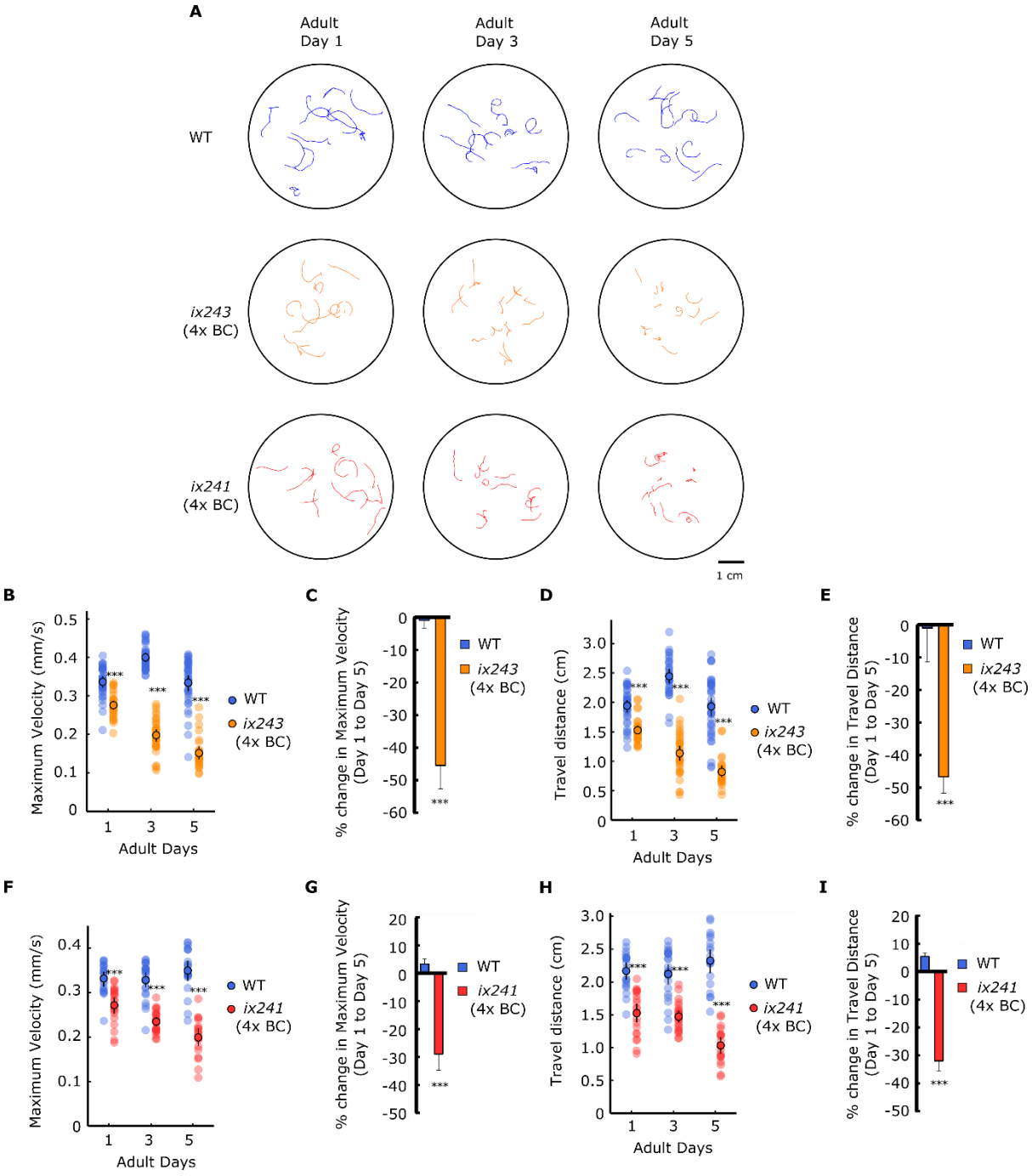

Figure 3.8 *ix241* and *ix243* strains show progressive decline in locomotor function after four backcrosses

(A) Representative tracks of WT, *ix241*, and *ix243* worms during 1-min video recording. n = 10–15 tracks per plate (some worms were unable to be tracked for the full minute, and were removed from analysis). (B) Maximum velocities of WT and *ix243* worms for adult days 1, 3, and 5. (C) Percent change in maximum velocity for *ix243* worms from adult day 1 to 5. (D) Travel distances of WT and *ix243* worms for adult days 1, 3, and 5. (E) Percent change in

travel distance for *ix243* worms from adult day 1 to 5. (F) Maximum velocities of WT and *ix241* worms for adult days 1, 3, and 5. (G) Percent change in maximum velocity for *ix241* worms from adult day 1 to 5. (H) Travel distances of WT and *ix241* worms for adult days 1, 3, and 5. (I) Percent change in travel distance for *ix241* worms from adult day 1 to 5. For maximum velocity and travel distance experiments, n = 30–45 worms per strain for each day (10–15 worms from 3 biological replicate plates). For percent change in maximum velocity and travel distance graphs, n = 3 biological replicate plates. ***$P < 0.001$; Unpaired Student's *t* test.

To check whether the *ix241* and *ix243* mutant strains were simply aging faster than wild-type worms, we measured the lifespans of the *ix241* and *ix243* worms (Fig. 3.9A, B, Table 3.4). The lifespan of the *ix241* worms was not significantly decreased compared to wild-type worms (Fig. 3.9B). The median lifespan of the *ix243* worms was decreased by two days (Fig. 3.9A). For the lifespan measurement of *ix243* worms, we used FUDR at low concentrations (25 µg/ml) for both *ix243* worms and WT worms since the *ix243* worms are slightly egg-laying deficient. *ix243* worms can lay eggs, but many worms die from the bag-of-worms phenotype in late adulthood. Although both *ix241* and *ix243* worms showed very little movement in adulthood, they were still able to move enough to orient its head to new patches of bacterial feed. We did not observe instances where the bacteria became absent near the head of *ix241* or *ix243* worms.

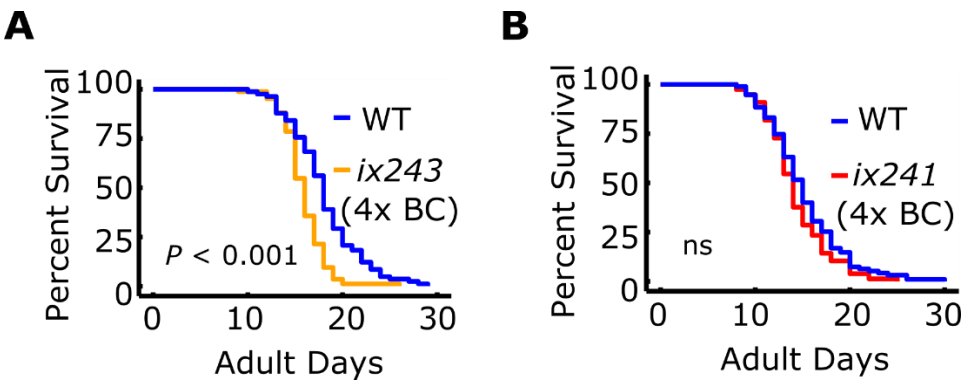

Figure 3.9 Lifespan of WT, *ix243*, and *ix241* worms

(A) Kaplan Meier survival curve of WT (n = 56) and *ix243* (n = 89) worms. (B) Kaplan Meier survival curve of WT (n = 94) and *ix241* (n = 77) worms. Log-rank test for lifespan comparisons.

Table 3.4 Lifespan measurements of WT (N2), *ix243*, and *ix241* worms

Strain	Median Lifespan (adult days)	*P* value vs WT (Log-rank test)	Worms (Counted/Total)	FUDR
N2	18		56/90	25 µg/ml
ix243 (4x backcrossed)	16	*P* = 0.00078	89/90	25 µg/ml
N2	18		82/90	25 µg/ml
ix243 (4x backcrossed)	16	*P* < 0.0001	84/90	25 µg/ml
N2	18		87/90	25 ug/ml
ix243 (4x backcrossed)	16	*P* < 0.0001	87/90	25 ug/ml
N2	17		94/120	0
ix241 (4x backcrossed)	16	*P* = 0.095	77/120	0
N2	14		66/90	0
ix241 (4x backcrossed)	15	*P* = 0.12	64/90	0
N2	12		67/90	0
ix241 (4x backcrossed)	14	*P* = 0.024	74/90	0

The *ix241* worms do not live shorter than wild-type worms. Therefore, the progressive decline in locomotor function is not due to a shorter lifespan. The *ix241* allele affects

locomotor healthspan, but not lifespan. This example suggests that the genetic bases of locomotor healthspan and lifespan may not completely overlap.

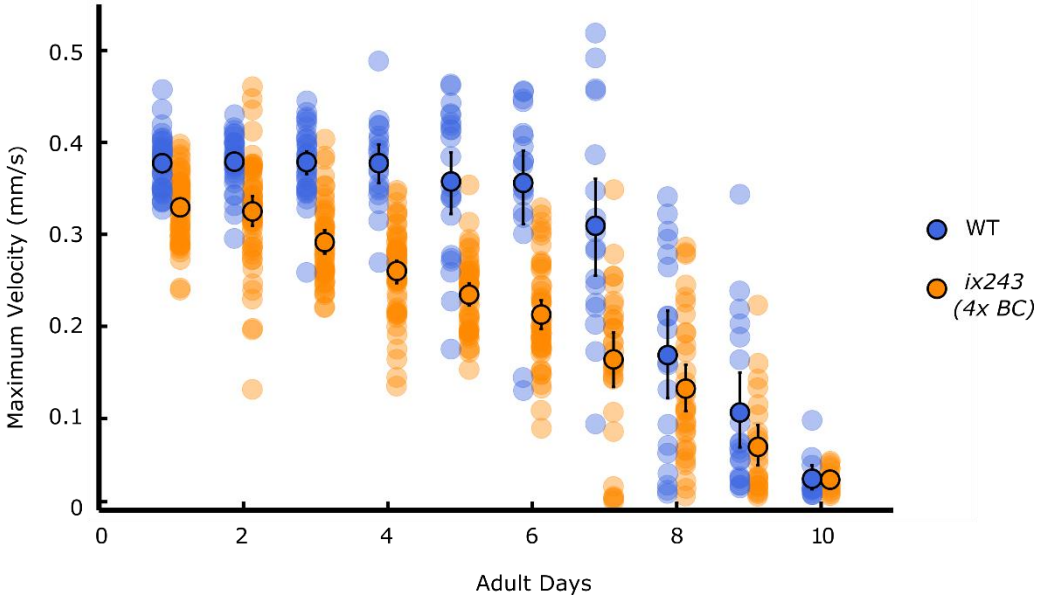

Figure 3.10 Maximum velocity of WT and *ix243* worms from adult day 1 to 10
Maximum velocities of individual WT and *ix243* worms from day 1 to day 10 of adulthood. n = 30–45 worms per strain for each day (10–15 worms from 3 biological replicate plates).

The *ix243* worms live two days shorter than wild-type worms. In order to compare the relative reductions in lifespan and locomotor healthspan, we quantified the reductions in lifespan and locomotor healthspan as compared to wild-type worms. The area under a healthspan curve has been suggested as a way to compare the relative changes in healthspan between individuals (Kaeberlein, 2018). We used this approach to quantify the reduction in lifespan and healthspan of *ix243* worms relative to wild-type worms. We measured the maximum velocity of wild type and *ix243* worms for 10 days and created a curve for locomotor healthspan (Fig. 3.10). We quantified the decrease in locomotor healthspan of *ix243* worms relative to wild-type worms by comparing the areas under the decline in maximum velocity curves (Fig. 3.11A). We quantified the decrease in lifespan of *ix243* worms relative to wild-type worms by comparing the areas under the survival curves (Fig.

3.11B). In the *ix243* worms, there is an average 11.5 percent decrease in lifespan, while there is a significantly greater decrease of 18.5 percent for locomotor healthspan (Fig. 3.11C). These results suggest that the *ix243* allele affects locomotor healthspan more than lifespan. The gene that is mutated in the *ix243* allele may play a more critical role for locomotor healthspan compared to lifespan. Other assays for healthspan-related phenotypes may provide insights into whether the *ix243* allele specifically affects locomotor healthspan, or affects healthspan in general.

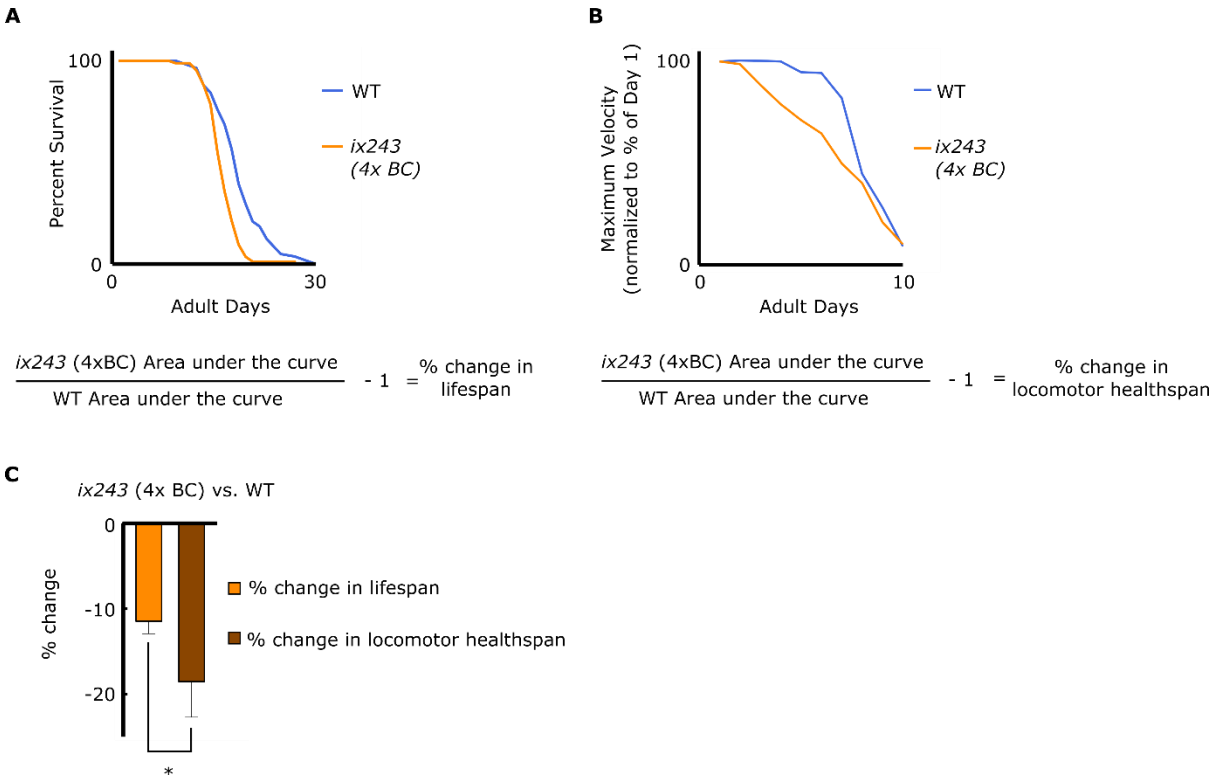

Figure 3.11 Percent change in lifespan and locomotor healthspan

(A) Calculation method for percent change in lifespan. (B) Calculation method for percent change in locomotor healthspan. (C) Percent change in lifespan and locomotor healthspan of *ix243* worms compared to wild-type worms. n = 3 biological replicate plates. **P* < 0.05; Unpaired Student's *t* test.

Four out of the five mutants that showed progressive deficits in completing the Edge Assay showed a progressive decline in locomotor function as measured by maximum velocity and travel distance. All four of those mutants showed slight but significant defects in locomotor function on the first day of adulthood. In order to check the developmental effects on the mutants, we measured the time it takes for the isolated mutant strains to reach development. Increases ranging from 1.1% to 13.9% were observed in our mutants, indicating that the induced mutations also have effects on development (Table 3.5).

Table 3.5 Development times of isolated mutant strains

Development time from egg to first egg-lay (n = 5 worms per strain).

Strain	Development Time (h)	% of WT
WT	70.4	100.0%
ix239	74.4	105.7%
ix240	71.2	101.1%
ix241 (4x backcrossed)	73.2	104.0%
ix242	71.8	102.0%
ix243 (4x backcrossed)	80.2	113.9%

3.4. Discussion

3.4.1 A new assay to measure *C. elegans* locomotor function

Here, we developed the "Edge Assay" to measure locomotor function of hundreds of worms at once. The Edge Assay can be used as an assay to compare the locomotor function of different populations of worms, or can be used to measure the decline in locomotor function of worms over time. We used *E. coli* bacterial feed on the edge of the plate as an attractant for the worms. Reductions in completion rate on the Edge Assay may represent deficits in locomotor function, sensory perception, or search behavior. Follow-up measurements are necessary to determine which modality was affected in worms with reduced completion rates. The Edge Assay can be used as a preliminary test or screen to measure the locomotor function of a population of worms. The main advantage of the Edge

Assay is its simplicity and that it can be conducted in any lab that has the facilities to maintain laboratory strains of *C. elegans*.

3.4.2 A new screening procedure to search for mutants with delayed onset of disease symptoms

The main difficulty in searching for mutants with progressive declines in adult functional capacity is distinguishing between mutants that had a developmental defect versus mutants that show a progressive decline in functional capacity. We overcome this issue by removing mutants with strong developmental locomotor defects on the first day of adulthood. Using only the mutant worms that completed the locomotor assay on the first day of adulthood, we collect mutants that show a loss of locomotor function on the third and fifth days of adulthood. To our knowledge, our screening procedure is the first unbiased screen using *C. elegans* that focuses on the progressive decline of adult locomotor function.

Many *C. elegans* models of neurodegenerative diseases show progressive deficits in locomotor function (Table 3.1). A *C. elegans* model of inclusion body myositis that expresses human beta amyloid, the protein that comprises the aggregates found in Alzheimer's disease, is reported to undergo age-dependent paralysis (Wu et al., 2006). *C. elegans* worms that express green fluorescent protein (GFP) preceded by polyglutamine repeats show age-dependent accumulations of GFP aggregates (Morley et al., 2002). However, the accumulation of protein aggregations does not always correlate with the severity of locomotor dysfunction (Silva et al., 2011). In those cases, locomotor function may serve as a better indicator of the severity of symptoms compared to protein aggregation levels.

Simple methods to test the locomotor function of many worms can accelerate the implementation of suppressor screens using previously created *C. elegans* models of neurodegenerative disease. For example, mutagenesis can be carried out on *C. elegans* mutants that carry human beta amyloid, and the Edge Assay can be used to isolate mutants that show improvements in locomotor function. The best age to carry out the screening procedure to enrich for mutants with a suppressed phenotype will depend on the severity of the locomotor deficit in each *C. elegans* disease model.

The *E. coli* bacterial lawn can be replaced with specific chemical cues to test the sensory functions of *C. elegans*. It may be possible to carry out forward genetic screens to isolate mutants with progressive loss of specific sensory functions by carrying out the Edge Assay with a repellent on the edge of the plate. First, mutagenized adult day 1 worms that remain in the center and are repelled by the repellent are collected. Those worms can be tested again on adult day 3 and day 5 for mutants that then cannot sense the repellent and move towards the edge of the plate. In addition to these examples, the Edge Assay may be a valuable assay for various types screening paradigms.

3.4.3 Isolation of five mutants with progressive deficits in completing the Edge Assay

Typically, the frequency that a loss-of-function allele occurs for a particular gene following EMS is 1/2000 (Brenner, 1974; Jorgensen and Mango, 2002). This equals 10 null-mutations per genome since there are 20,000 genes. If we screen 2,000 genomes, we will have caused approximately one mutation in each gene. Since we screened 1,000 genomes, we caused loss-of-function mutations in approximately 10,000 genes. Therefore, there may be genes that are involved in our specific phenotype that were not mutagenized in our screenings. Another screening of 1,000 genomes may identify more genes that are involved

in this phenotype. A saturation screen would theoretically test all 20,000 genes, so we can roughly estimate that our current screen is halfway towards saturation. However, even if a screen is saturated, genes may not be found if they have redundant functions or are small in size. Therefore, a saturation screen will not be able to test all *C. elegans* genes. Generally, a screen is considered saturated when multiple alleles of the same gene are identified.

3.4.4 Slight defects in development may cause strong deficits during adulthood

Four out of the five mutants that we isolated in our screen showed a progressive decline in locomotor function as measured by maximum velocity and travel distance in 1 min on an agar plate without food. All four of those mutants showed slight but significant defects in locomotor function on the first day of adulthood, indicating signs of developmental neuromuscular deficits. Those four mutants also showed slight delays in development. The slight effects on development may be analogous to the early signs of dysfunction in brains of young adults with risk alleles for Alzheimer's Disease (Mormino et al., 2016). Potential links between genes implicated in development and those implicated in aging or age-related impairments may provide clues for early diagnosis of late-onset diseases.

3.4.5 Genetic bases of lifespan and locomotor healthspan may not completely overlap

In the *ix241* mutant strain, a progressive decline in locomotor function was observed without a reduction in lifespan. In the *ix243* mutant strain, there was a significantly greater negative effect on locomotor healthspan compared to lifespan. These results support the notion that the genetic bases of lifespan and locomotor healthspan may not completely overlap (Bansal et al., 2015; Tissenbaum, 2012). Although genetic regulators of lifespan in many cases may also affect healthspan, some genes may affect lifespan without largely

affecting locomotor healthspan and vice versa (Fig. 3.12). Therapeutic targets to improve healthspan should therefore target genes that have disproportionate effects on healthspan instead of genes that have the most robust effects on lifespan.

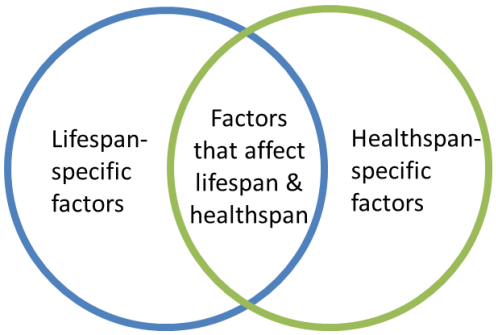

Figure 3.12 Genetic factors that affect lifespan and healthspan may not completely overlap

Conserved genetic regulators of specific aspects of healthspan may be easier to identify from model organisms compared to conserved genetic regulators of lifespan. Lifespan is regulated by various causes of death, which may be very different from one organism to another. For example, one of the major causes of death in *C. elegans* is bacterial colonization of the gut (Podshivalova et al., 2017; Zhao et al., 2017). Pharyngeal swelling is caused by bacterial infection by *E. coli*, which is an innocuous food source until later stages of adulthood (Zhao et al., 2017). Since the leading cause of death in humans is heart disease, the improvement of heart function may be the most effective way to prolong lifespan in the human population (Heron, 2013).

In contrast, the genetic factors that affect specific domains of healthspan are functionally conserved. For example, locomotor healthspan in humans and *C. elegans* are maintained by the neuromuscular system in both species. Therefore, genetic factors related to healthspan that are found from model organisms may have a greater probability of having similar effects in humans.

4. Chapter 2: Identification of the causative mutation site in the isolated mutants

4.1 Introduction

4.1.1 Strategies to identify the causative mutation site in mutants isolated from forward genetic screens

There are several strategies to identify the causative mutation of mutants isolated from forward genetic screens. The development and reduced cost of next generation sequencing enables new approaches to identify the causative mutation. Broadly, there are three methods: (1) Hawaiian variant mapping by outcrossing to a polymorphic Hawaiian strain (CB4856), (2) EMS variant density mapping by backcrossing to the original parent strain, and (3) EMS variant density mapping by bulk segregation (Doitsidou et al., 2010; Minevich et al., 2012; Zuryn and Jarriault, 2013). The advantages and disadvantages of each approach are described in Table 4.1.

Table 4.1 Advantages and disadvantages of mutation identification strategies

	Advantage	Disadvantage
Hawaiian	• Only one outcross • Higher mapping resolution	• Hawaiian background may have an effect on the phenotype
EMS backcross	• Crossing back to original strain should not have any large effects on the phenotype	• Multiple backcrosses necessary • Lower mapping resolution
EMS bulk backcross	• Only one backcross • Crossing back to original strain should not have any large effects on the phenotype	• Still need to backcross for phenotype analysis • Lower mapping resolution

The Hawaiian variant mapping method relies on single nucleotide polymorphisms (SNPs) that exist between the N2 Bristol strain and Hawaiian CB4856 strain. An isolated mutant from EMS-mutagenesis is outcrossed with the Hawaiian strain and F2 progeny that

demonstrate the mutant phenotype are selected. These F2 mutants are maintained as independent populations and pooled together for whole-genome sequencing. The SNP frequency of the N2 and Hawaiian strains are distributed equally in the F2 genomes except for SNPs that are genetically linked to the causative mutation in the N2 strain. Therefore, there should be a high frequency of N2 SNPs and a low frequency of Hawaiian SNPs in the

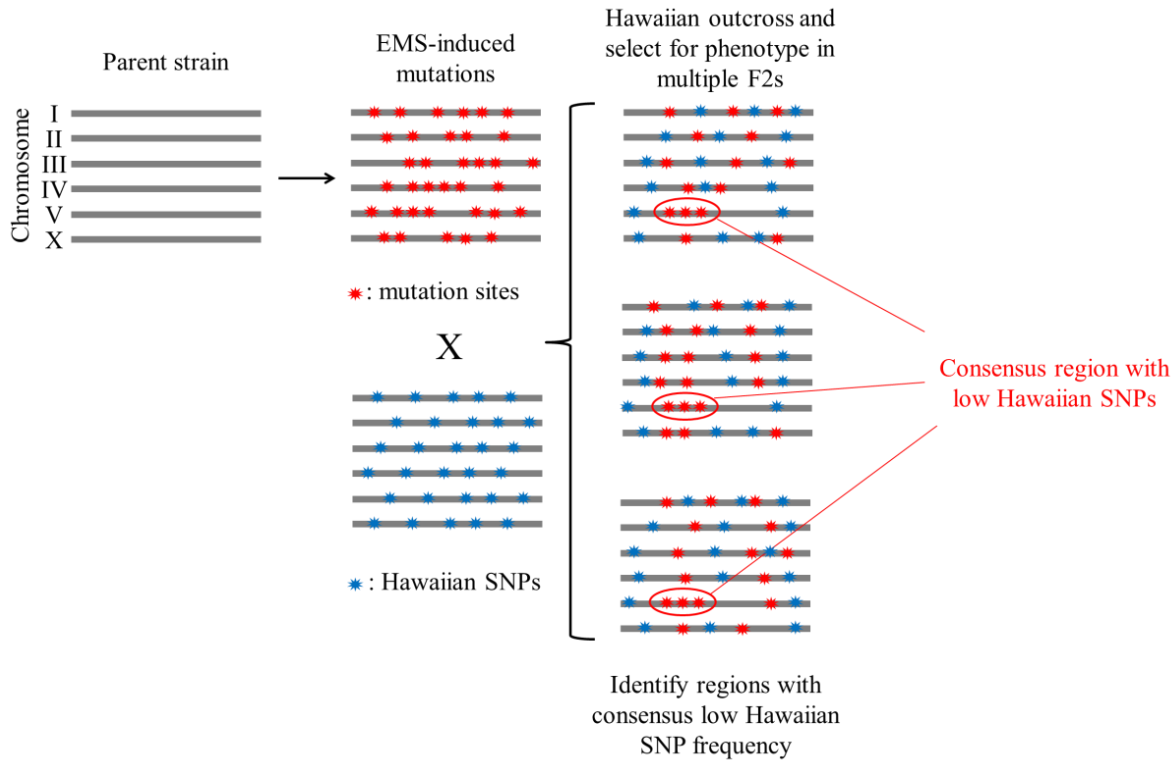

region close to the causative mutation (Doitsidou et al., 2010).

Figure 4.1 Schematic diagram of Hawaiian variant mapping strategy
The isolated mutant is outcrossed to the Hawaiian strain. F2 animals that demonstrate the phenotype are kept as individual populations. Mutation sites that are not involved in the phenotype should be lost randomly. However, the causative mutation site should remain in all independent strains. DNA sequencing of pooled DNA of the independent lines should show a consensus region with low Hawaiian SNPs and high N2 SNPs.

One difficulty of using a divergent strain for mapping the mutation is that the presence of many SNPs in the Hawaiian strain can have an effect on the target phenotype.

This makes it difficult to determine whether the mutant phenotype is present in individual F2 animals. The Hawaiian strain shows a burrowing behavior on NGM agar plates, and thus makes it difficult to use as a mapping strain for a study that measures locomotor activity.

EMS variant density mapping by backcrossing is carried out by crossing the mutant strain with the parent strain and selecting animals that still show the mutant phenotype in the F2 generation. By repeating this procedure for multiple backcrosses, mutations that are not involved in the mutant phenotype can be removed. After several backcrosses, the mutant line will contain a smaller number of mutations. Due to a lower frequency of homologous recombinations between physically close genomic regions, there should be a higher density of EMS mutations near the causative mutation site (Fig. 4.2). The frequency of EMS-induced mutations can be measured by whole-genome sequencing.

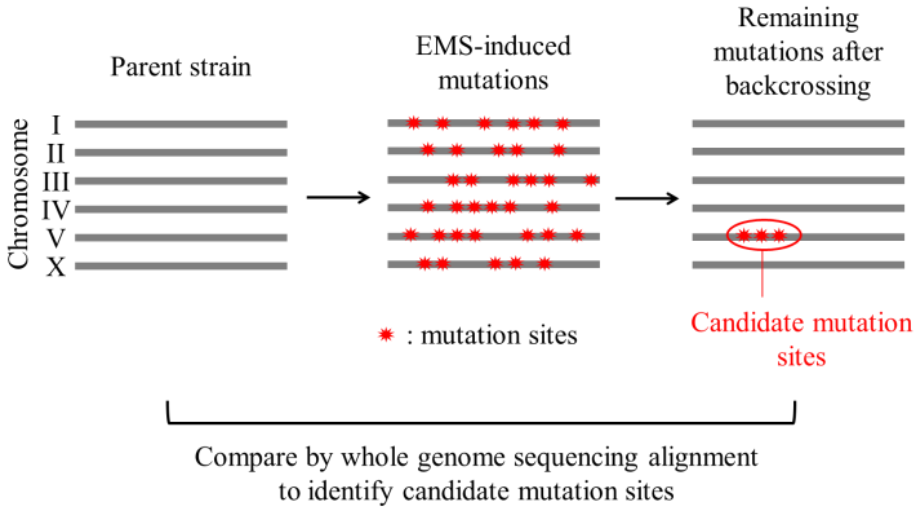

Figure 4.2 EMS variant density mapping by backcrossing

The isolated mutant is backcrossed to the parent strain at least four times. This removes mutations that are not involved in the target phenotype. Due to genetic linkage, there is a higher number of EMS-induced mutations near the causative mutation site.

EMS variant density mapping by bulk segregation is carried out by backcrossing the mutant strain only once to the parent strain. In this approach, approximately 50 independent backcrossed lines that show the phenotype will be established after the first backcross. The DNA from each population will be pooled together for sequencing. The causative mutation should be found in all backcrossed F2 populations, while other mutation sites should not be present in all populations. Therefore consensus mutation sites that are present in the pooled DNA sample indicates potential candidate causative mutation sites (Fig. 4.3).

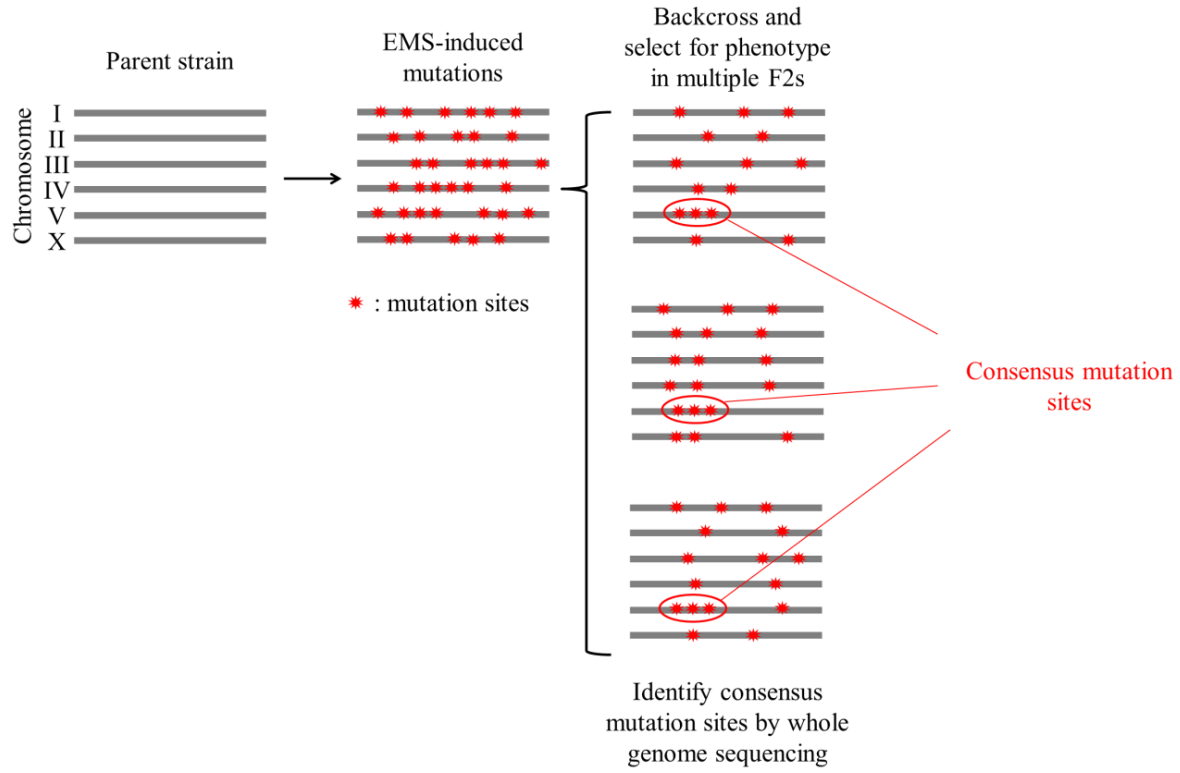

Figure 4.3 EMS variant density mapping by bulk segregation

The isolated mutant is backcrossed once to the parent strain. F2 animals that demonstrate the phenotype are kept as individual populations. Mutation sites that are not involved in the phenotype should be lost randomly. However, the causative mutation site should remain in all independent strains. DNA sequencing of pooled DNA of the independent lines should show a consensus region where EMS-induced mutations remained.

Mapping of the mutation site can also be carried out using a combination of the backcrossing method and the bulk segregation method. The sibling subtraction method for mapping is one example of combining the two approaches (Joseph et al., 2018). In the sibling subtraction method, backcrossed lines that show the phenotype and lost the phenotype are kept and sequenced separately (Joseph et al., 2018). The mutations that are present in the backcrossed lines that do not show the phenotype can be ruled out as candidate mutation sites. This method has the advantage of having a higher mapping resolution, without having to sequence as many mutants as the bulk segregation approach. This approach also takes advantage of the genetic information of mutants that do not show the phenotype.

4.1.2 Strategies to confirm the causative mutation site

Once there are candidate mutation sites for a mutant strain, the mutation site can be confirmed by various methods. Broadly, there are four ways to confirm a candidate mutation site: (1) Rescue with microinjection of WT version of gene, (2) Phenocopy with mutation induced by CRISPR/Cas9, (3) Phenocopy by RNAi gene knockdown, and (4) Complementation with other mutant alleles of the same gene. The advantages and disadvantages of each strategy are listed in Table 4.2. The best approach can depend on the candidate mutation site. For example, some genes may be too large to PCR amplify for rescue with the WT version of the gene.

Table 4.2 Advantages and disadvantages of mutation confirmation strategies

	Advantage	Disadvantage
Rescue with microinjection of WT version of gene	• Can specifically test the effect of one gene	• Overexpression may cause different phenotype • Can only rescue mutations that are loss-of-function
Phenocopy with mutation induced by CRISPR	• Can create specific mutations within a gene • Can create a mutant line that does not contain other EMS-induced mutations	• Unintended mutations may occur in genome • CRISPR gRNA may be inefficient for specific genomic regions
Phenocopy by RNAi gene knockdown	• Can perform by feeding • Can test multiple gene knockdowns at once	• Off-target effects may occur • RNAi efficiency is variable • Some cell-types are difficult to target, such as neurons
Complementation with other mutant alleles of the same gene	• One mating can be sufficient to test the effect of a gene	• Need a different mutant allele • In some cases intragenic complementation can occur • Need to make males, and males need to be able to mate

C. elegans can incorporate and pass along genetic material as extrachromosomal arrays (Mello et al., 1991). Mutant phenotypes that occur as a result of a loss-of-function of a gene can be rescued by re-introducing the wild-type version of the gene as an extrachromosomal array. Genetic material is injected into the gonad of an adult hermaphrodite worm. Some germ cells will uptake and express the genetic material. Co-injection of visible injection markers such as GFP or RFP under the control of tissue-specific promoters allow the simple identification of worms that incorporated the introduced genetic material. Extrachromosomal arrays will likely contain multiple copies of the gene and lead to overexpression of the gene. Therefore, if overexpression of a gene leads to negative phenotypes, microinjection of the WT version of a gene may not be a suitable approach to rescue the mutant phenotype. Additionally, gain-of-function mutations would not be rescued by overexpressing the wild-type version of a gene. In this case, the comparison of worms

overexpressing the wild-type version of the gene versus worms that overexpress the gene with the gain-of-function mutation may suggest whether the mutation has toxic effects.

The CRISPR/Cas9 system can create targeted mutations in many organisms including *C. elegans* (Cong et al., 2013). Once a candidate mutation site is found in a mutant strain, the mutation can be re-created in a wild-type strain to see if the same phenotypic effects are observed. Additionally, the candidate mutation site can be reversed back to the wild-type allele in the mutant strain to test if the phenotype can be rescued. However, the CRISPR/Cas9 system can also cause off-target mutations (Zhang et al., 2015). It also may have decreased efficiency for certain mutation sites due to the chromosomal structure.

C. elegans can uptake small fragments of double-stranded RNA through its intestine (Gönczy et al., 2000). If *C. elegans* are fed bacteria that express double-stranded RNA that is complementary to a gene, it can reduce the mRNA levels of the gene transcript (Gönczy et al., 2000). This reduction of function may recapitulate some loss-of-function mutations in a gene. RNAi can be used as a strategy to test the phenotypic effects of reduced function of many genes. However, RNAi does not cause complete loss-of-function in many cases. RNAi is also not efficient in neuronal tissues, and specific strains that are more sensitive to neuronal RNAi should be used such as the SID-1 overexpressing strain (Calixto et al., 2010). RNAi can have off-target effects, so additional experiments are necessary to confirm the phenotypic results from RNAi.

Genetic complementation is an approach that can be used to test whether the phenotypes of two mutants are a result of disruption in the same gene. In most cases, one copy of the WT version of a gene can complement, or be sufficient, for the general functions of an organism. Therefore, if a mutant strain with a loss-of-function mutation is mated with the wild-type strain, the F1 offspring will be heterozygous for the mutation site and carry one

copy of the wild-type version of the gene. These F1 offspring should show a wild-type phenotype. However, if a mutant strain with a loss-of-function mutation in a gene is mated with a separate mutant strain with a different loss-of-function mutation in the same gene, the offspring will carry two loss-of-function alleles. In this case, the two mutant strains do not complement each other, and the F1 offspring should all show the mutant phenotype. Genetic complementation can be used to test whether the phenotypes of two mutants are caused by loss-of-function mutations in the same gene.

4.2 Materials and Methods

C. elegans strains

C. elegans Bristol strain N2 was used as wild-type. Animals were cultivated on NGM plates with *E. coli* strain OP50. All animals were maintained at 20°C. *C. elegans* strain VC1937 *elpc-3(ok2452)* was obtained from the *Caenorhabditis* Genetic Center (University of Minnesota, MN, USA). *C. elegans* strain *elpc-1(tm2149)* was obtained from the National BioResource Project (Japan). *C. elegans* strains *elpc-2(ix243), elpc-2(ix243);elpc-3(ok2452),* and *elpc-1(ok2452);elpc-2(ix243)* were created in this study.

DNA extraction

C. elegans populations were maintained on 6-cm plates until the bacterial feed was exhausted. Worms were collected using lysis buffer (5 mM Tris-HCl pH 8.0, 2.5 mM KCl, 0.23% Tween-20) and washed three times in a 1.5mL Eppendorf tube with 1.0 mL lysis buffer. After the final wash, 500 µL lysis buffer with 200 µg/mL final concentration Proteinase K was added to the worms. The tube was incubated at 55^{O}C overnight. Next, 800

µg/mL RNase A was added and incubated at 37^{o}C for 30 min. After incubation, 125 µL saturated NaCl was added to the solution. The tube was centrifuged at 15,000 rpm for 15 min. The supernatant was transferred to a new 1.5 mL Eppendorf tube without disturbing the pellet. Next, 1.0 mL 100% ethyl alcohol (EtOH) was added to the supernatant. The tube was then centrifuged at 15,000 rpm for 20 min. The supernatant was discarded and 1.0 mL of 70% EtOH was added to the tube. The tube was centrifuged at 15,000 rpm for 20 min. The supernatant was discarded and the precipitant was air-dried, then re-constituted in Tris-Ethylenediaminetetraacetic acid (EDTA) buffer.

Whole-genome sequencing

The extracted DNA was sequenced by MiSeq (Illumina, San Diego, CA, USA). Libraries were prepared with the Illumina TruSeq Library Prep Kit. Mapping was conducted with BWA software (Li and Durbin, 2009). WBcel235 was used as the reference *C elegans* genome. Resulting files were converted to a bam file, then to pileup format by Samtools (Li et al., 2009). Variant analysis was conducted using varscan and snpeff available on the Galaxy platform (Blankenberg et al., 2010; Cingolani et al., 2012; Giardine et al., 2005; Goecks et al., 2010; Koboldt et al., 2009). Mutation frequencies along each chromosome were calculated and visualized using CloudMap.(Minevich et al., 2012)

Sanger sequencing of elpc-2 *mutation site*

A PCR fragment flanking the *elpc-2* mutation site was amplified using the following primers:

5' *elpc-2* snp: 5’-aaatgaatttttcgccacaaaacccaaaaa-3’

3' *elpc-2* snp: 5’-ttcgcgaaaactctcgtagtctgatcctg-3’

The PCR fragment was purified using Wizard SV Gel and PCR Clean-Up System (Promega, Madison, WI). The sequence of the amplified PCR fragment was determined using cycle sequencing with BigDye v3.1 reagents (Applied Biosystems, Foster City, CA). Sequencing products were purified by EtOH/EDTA precipitation. Sequencing was performed by capillary sequencing using ABI3700 (Applied Biosystems, Foster City, CA). Sequences were visualized using ApE software.

Preparation of agar pads

Agar pads were created by placing a clean slide between two glass slides with masking tape taped over both sides to serve as spacers. One drop of molten 2% agar was dropped on the surface of the clean slide using a Pasteur pipette. The drop of agar was covered by another clean glass slide. After the agar solidified, the glass slides were pulled apart, with the agar remaining on one of the glass slides. The glass slide with the agar was dried in a 60°C incubator overnight. The dried agar pads were stored at RT until use.

Creation of ix243(4x Backcrossed (4xBC));Ex[elpc-2(+)] *worms*

The wild-type version of *elpc-2* including 2090 base pairs (bp) upstream of the start codon and 851 bp downstream of the stop codon was amplified using the following primers:

5' *elpc-2*p (2090 bp upstream): 5'-gataagtgacatgccgctgcgtccttac-3'

3' *elpc-2*UTR (851 bp downstream): 5'-aagagacagcgtctgattcttgaaacggta-3'

The PCR product was purified using Wizard SV Gel and PCR Clean-Up System (Promega, Madison, WI). One-day old hermaphrodite *ix243*(4x BC) adults were used for microinjection. One drop of liquid paraffin was placed on 2% agar pads. One worm was placed in the liquid

paraffin. The purified PCR product was injected into the distal gonad at a concentration of 10 ng/µL with a *lin-44*p*::RFP* injection tail marker at a concentration of 50 ng/µL. M9 buffer was added immediately after injection, and the worm was placed on an OP50-seeded NGM plate to recover.

Measurements of Maximum Speed, Average Speed, and Total Distance Traveled

Described in Section 3.2 Material and Methods

Genetic crosses and backcrosses

C. elegans strains *elpc-2(ix243);elpc-3(ok2452),* and *elpc-1(ok2452);elpc-2(ix243)* were created by genetic crossing. Males were made by incubating 7 L4 stage hermaphrodite worms at 30 °C for 4-6 h, and checking their offspring. Males were isolated and maintained by crossing with hermaphrodites of the same genotype. Double mutants were checked by extracting their DNA, amplifying a genomic fragment flanking the mutation site by PCR, and sequencing the PCR product by Sanger sequencing. *ix243*(4x BC) strains were created in a similar way except wild-type N2 males were used. The following primers were used to check whether a line carried a mutation site.

5' *elpc-2* snp: 5'-aaatgaatttttcgccacaaaacccaaaaa-3'

3' *elpc-2* snp: 5'-ttcgcgaaaactctcgtagtctgatcctg-3'

5' *elpc-1* del: 5'-gaaaagcatcgagttgtccacttgaatcac-3'

3' *elpc-1* del: 5'-cttttcagttgaattctggcatctctccaa-3'

5' *elpc-3* del: 5'-taatagaacccagatcgagtttggcagatg-3'

3' *elpc-3* del: 5’-aatgcatcgtatgtggttaggcggtaaaac-3’

Transcriptional reporter expression

A genomic fragment of 2090 bp immediately upstream of the start codon of the *elpc-2* gene was PCR-amplified using “5' elpc-2p overlap ppd95.79 107-” and “3' elpc-2p overlap ppd95.79 138-” primers, which have 15 bp overhangs that anneal with immediately upstream of the GFP sequence in the pPD95.79 vector. The pPD95.79 vector containing GFP was linearized by PCR using the “5' ppd95.79 107-” and “3' ppd95.79 138-” primers.

5' elpc-2p overlap ppd95.79 107-: 5’-gggtaccggtagaaaaaatgaaaatcgaagaagaatttatctctgctag-3’

3' elpc-2p overlap ppd95.79 138-: 5’-agttcttctcctttactcatctgggaaacattaaagattctcaatttcgc-3’

5' ppd95.79 107-: 5’-atgagtaaaggagaagaacttttcactggag-3’

3' ppd95.79 138-: 5’-tttttctaccggtaccctccaagcaagggtc-3’

The template vector was digested with restriction enzyme *Dpn*I (New England Biolabs, Ipswich, MA), and the linearized vector was purified by Wizard SV Gel and PCR Clean-Up System (Promega, Madison, WI). The pure linearized vector and the *elpc-2* promoter were fused using In-Fusion HD Cloning Kit (Takara, Kusatsu, Japan) to make the *elpc-2*p*::GFP* transcriptional reporter construct. The construct was microinjected into the gonad of wild-type worms at a concentration of 50 ng/µL. Worms that expressed the reporter construct were immobilized in 25 mM sodium azide and observed under confocal microscope LSM710 (Carl Zeiss, Oberkochen, Germany). A z-stack image was created from images taken at 1µm increments.

4.3. Results

4.3.1 Whole genome sequencing of *ix243* mutant strain

We used a modified version of the sibling subtraction method to identify the causative mutation site in the *ix243* strain (Fig. 4.4) (Joseph et al., 2018; Minevich et al., 2012). The whole genome of the *ix243* mutant strain was sequenced before and after backcrossing to identify the mutation that causes the progressive decline in locomotor function. The WBcel235 genome was used as the reference *C. elegans* genome. An even distribution of mutations were present on all chromosomes in the *ix243* mutant strain before backcrossing (Fig. 4.5A). After the fourth backcross, we found three strains that show a progressive decline in locomotor function, and two strains that did not show the progressive decline in locomotor function. In order to narrow down the candidate mutation sites, we compared the mutation sites that were present in the *ix243* strain before backcrossing and the three strains that showed the progressive decline in locomotor function after four backcrosses. From the list of shared mutation sites, we subtracted the mutation sites found in the two strains that did not show the progressive decline in locomotor function after the fourth backcross. A high frequency of mutations remained on Chromosome III (Fig. 4.5B).

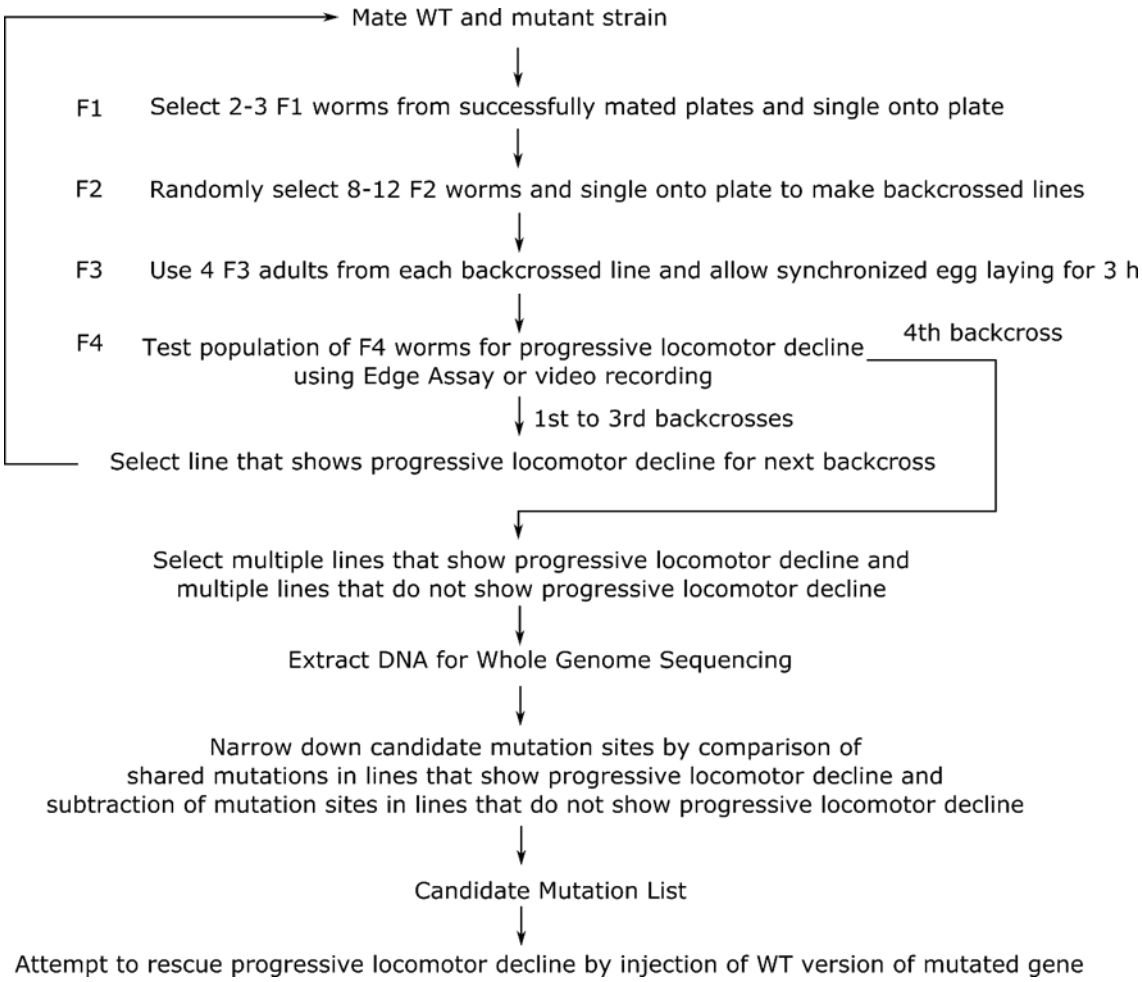

Figure 4.4 Mutation identification strategy for *ix243* strain

A strategy to map the causative mutation site in the *ix243* strain.

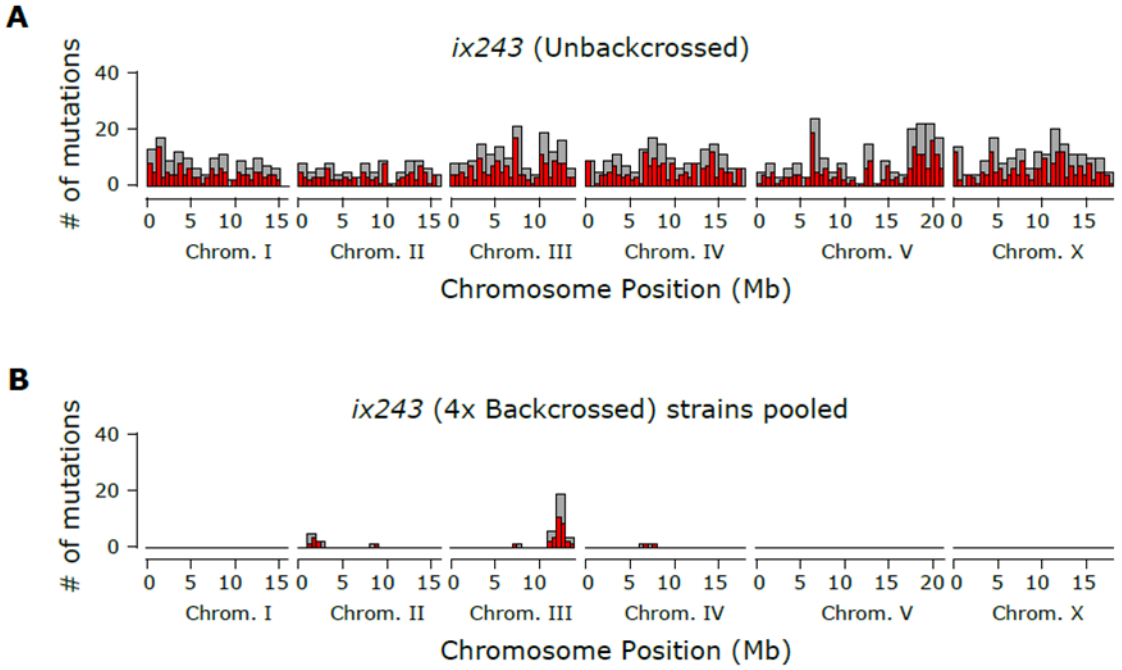

Figure 4.5 Mutation frequencies of *ix243* mutant strain

(A) Frequency of mutations along each chromosome for *ix243* strain before backcrossing. (B) Frequency of mutations along each chromosome for *ix243* strain after backcrossing, and comparing shared mutations among backcrossed strains that show the phenotype, and subtracting mutations in backcrossed strains that lost the phenotype.

A nonsense mutation from TGG to TAG within the protein coding region of *elpc-2* was the mutation that was predicted to have the strongest effect on protein function among the candidate mutation sites (Table 4.3; Table 4.4). The mutation changes the 373rd amino acid of ELPC-2 from tryptophan to the Amber stop codon (Fig. 4.6A). We confirmed the presence of the *elpc-2* mutation site by Sanger sequencing of DNA extracted from the *ix243* mutant worms (Fig. 4.6B).

Table 4.3 Remaining mutations in *ix243* mutant strains

Chrom.	Pos.	Ref.	Alt.	Gene	Mutation Type	Effect*
I	3428548	A	AGGCAGACCTAGCCCACCCTG GGCAGACCTAGCCCACCCTG	K03E5.2	downstream gene variant	modifier
I	14448378	G	GCGTCCGGTTTTGGGGTAGGTTT CCACGGCGGCCGACAATTTCCG AGTTTCGCCACTCACTATACTTA ATCAGCAATTTTATAGTGAGTTG CGAAACTCGGAAATTGTCGGCC GTCGTGGATAACTACCCCAAAA CCGGACGACCGGA	Y105E8A.27	downstream gene variant	modifier
II	1465622	C	T	Y51H7C.13	missense variant	moderate
II	1602489	C	T	bath-47	downstream gene variant	modifier
II	1717193	C	T	btb-7	downstream gene variant	modifier
II	1915528	C	T	math-31	upstream gene variant	modifier
II	2339259	G	T	F43C11.6	upstream gene variant	modifier
II	2428896	C	T	F42G2.2	downstream gene variant	modifier
II	2477652	T	A	tsr-1	upstream gene variant	modifier
II	8975684	G	T	tomm-40	upstream gene variant	modifier
III	577387	TAAAAATTT AACAAAA	T	Y55B1AL.1	downstream gene variant	modifier
III	1704981	A	T	Y22D7AR.10	upstream gene variant	modifier
III	7406703	A	T	linc-165	upstream gene variant	modifier
III	7439448	C	T	linc-165-alh-12	intergenic region	modifier
III	11024784	G	A	Y48A6B.16	upstream gene variant	modifier
III	11416475	G	A	Y47D3B.13	upstream gene variant	modifier
III	11549303	G	A	Y66D12A.14	downstream gene variant	modifier
III	11816202	G	A	C18D11.1	upstream gene variant	modifier
III	11895783	G	A	faah-5	upstream gene variant	modifier
III	12134837	G	A	Y75B8A.6	upstream gene variant	modifier
III	12156042	G	A	linc-87	upstream gene variant	modifier
III	12190456	G	A	Y75B8A.54	upstream gene variant	modifier
III	12200963	G	A	Y75B8A.44	downstream gene variant	modifier
III	12223827	G	A	Y75B8A.16	missense variant	moderate
III	12407309	G	A	tat-1	missense variant	moderate
III	12427755	G	A	Y49E10.16	upstream gene variant	modifier
III	12476529	G	A	Y49E10.33	upstream gene variant	modifier
III	12498064	C	T	Y111B2A.3	synonymous variant	low
III	12678743	G	A	elpc-2	stop gained	high
III	12701690	G	A	spin-4	downstream gene variant	modifier
III	12750669	A	T	irld-60	missense variant	moderate
III	12810002	G	A	BE10.5	upstream gene variant	modifier
III	12838123	G	A	Y37D8A.4	synonymous variant	low
III	12892115	G	A	unc-71	upstream gene variant	modifier
III	12923518	G	A	Y37D8A.16	upstream gene variant	modifier
III	12924071	G	A	mrps-10	upstream gene variant	modifier
III	13352002	G	A	F53A2.9	downstream gene variant	modifier
III	13453318	G	A	cua-1	upstream gene variant	modifier
III	13578898	G	A	T05D4.5	upstream gene variant	modifier
IV	6722231	C	T	Y73B6A.6-Y73B6A.2	intergenic region	modifier
IV	7597770	G	A	tag-80	synonymous variant	low
IV	7597783	T	A	tag-80	missense variant	moderate
IV	17276360	A	AT	gln-5	upstream gene variant	modifier

*Ranked in order of putative impact of the mutation (high > moderate > low > modifier)

Table 4.4 Description of mutation types (from SnpEff manual (Cingolani et al., 2012))

Mutation Type	Description
downstream gene variant	Variant is downstream of a gene (default length: 5K bases)
intergenic region	The variant is in an intergenic region
missense variant	Variant causes a codon that produces a different amino acid
stop gained	Variant causes a STOP codon
synonymous variant	Variant causes a codon that produces the same amino acid
upstream gene variant	Variant is upstream of a gene (default length: 5K bases)

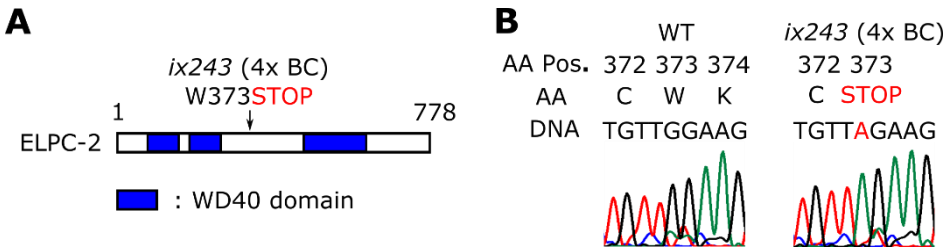

Figure 4.6 Candidate mutation site

(A) Schematic description of mutation effect in *ix243* worms for the amino acid sequence of ELPC-2. (B) Confirmation of mutation site in *ix243* worms by Sanger sequencing.

4.3.2 Wild-type version of *elpc-2* rescues progressive loss of locomotor function in *ix243* worms

To check whether the *elpc-2(ix243)* mutation causes the progressive decline in locomotor function, we expressed the wild-type version of *elpc-2* including 2090-bp upstream of the start codon and 851-bp downstream of the stop codon in the *ix243* worms. The wild-type version of *elpc-2* rescued the progressive loss of adult locomotor function in *ix243* worms as measured by maximum velocity and travel distance (Fig. 4.7). These results demonstrate that *elpc-2* plays a necessary role during the maintenance of adult locomotor function in *C. elegans*. The *elpc-2(ix243)* mutant strain is the first reported mutant of the *elpc-2* gene in *C. elegans*.

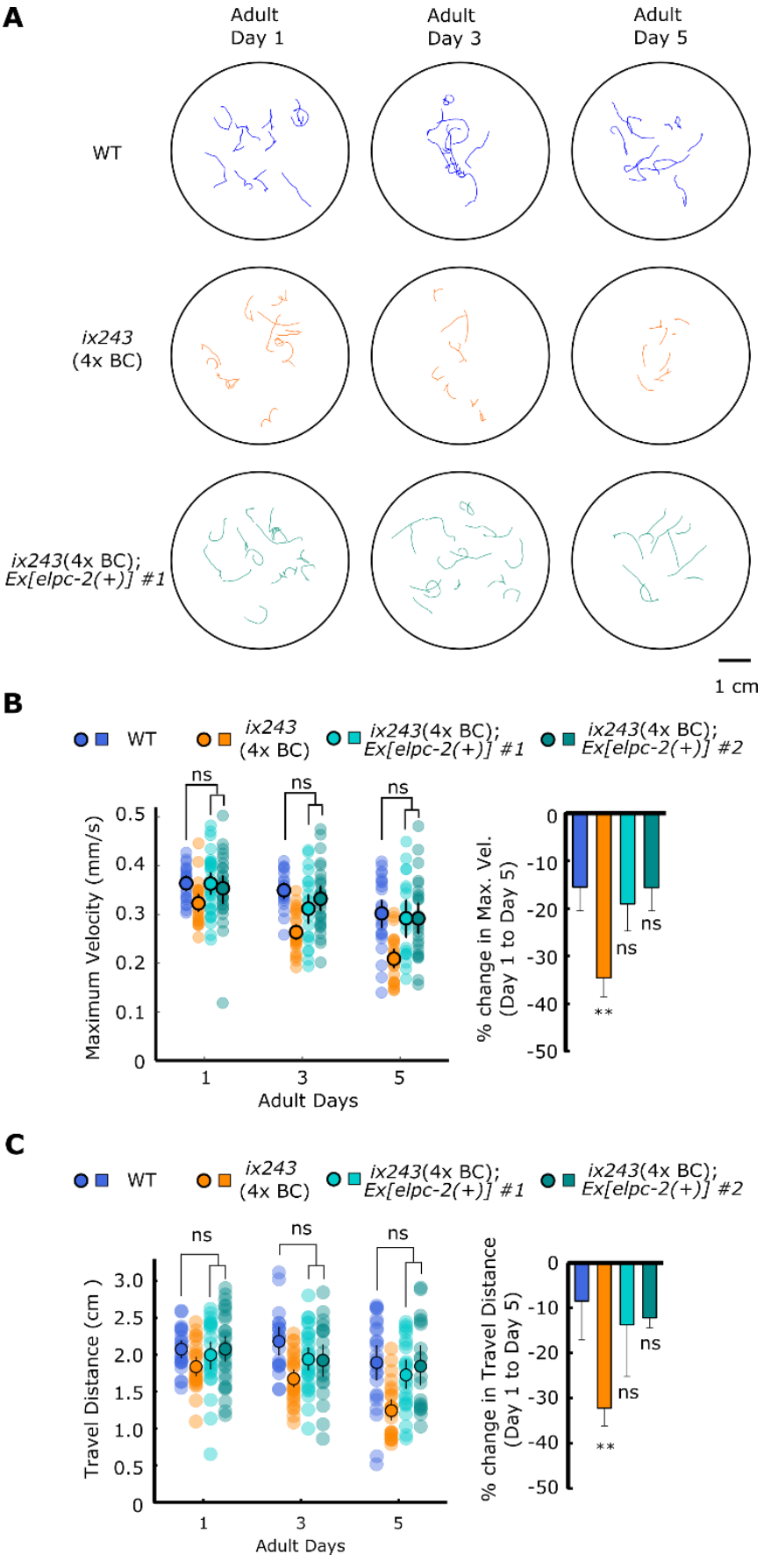

Figure 4.7 *elpc-2* rescues progressive loss of locomotor function in *ix243* worms

(A) Representative locomotor tracks of WT, *ix243*(4x BC), and *ix243*(4x BC)*;Ex[elpc-2(+)] #1* worms from 1-min video recording on agar plate without food. n = 10–15 tracks per plate. (B) (*Left*) Maximum velocities of WT, *ix243*(4x BC), *ix243*(4x BC)*;Ex[elpc-2(+)] #1, and ix243*(4x BC)*;Ex[elpc-2(+)] #2*. (*Right*) Change in maximum velocity of strains from left panel. (C) (*Left*) Travel distances of WT, *ix243*(4x BC), *ix243*(4x BC)*;Ex[elpc-2(+)] #1, and ix243*(4x BC)*;Ex[elpc-2(+)] #2*. (*Right*) Change in travel distance of strains from left panel. For maximum velocity and travel distance experiments, n = 30–45 worms per strain for each day (10–15 worms from 3 biological replicate plates). For percent change in maximum velocity and travel distance graphs, n = 3 biological replicate plates. Error bars indicate 95% confidence intervals. ***P* < 0.01; ns, not significant; One-way ANOVA with Dunnett's post hoc test vs. WT.

4.3.3 Other *C. elegans* Elongator mutants show progressive loss of locomotor function

C. elegans ELPC-2 is a functional component of the Elongator complex, an evolutionarily conserved protein complex that consists of six subunits in *S. cerevisiae*, *A. thaliana*, *M. musculus*, and humans (Creppe and Buschbeck, 2011). In *S. cerevisiae* and humans, ELP1–ELP3 form the core complex, and ELP4–ELP6 form a sub-complex (Creppe and Buschbeck, 2011). There are only four predicted components of the Elongator complex (ELPC1–4) in *C. elegans* (Solinger et al., 2010). In *C. elegans*, functioning of the core ELP1–ELP3 complex may only be necessary, or orthologs of ELP5 and ELP6 are not yet found. The phenotypes of *C. elegans elpc-1* and *elpc-3* mutants have been studied in the context of tRNA modifications (Chen et al., 2009a) and tubulin acetylation (Solinger et al., 2010). However, it is unknown whether *elpc-1* and *elpc-3* are involved in the maintenance of locomotor function.

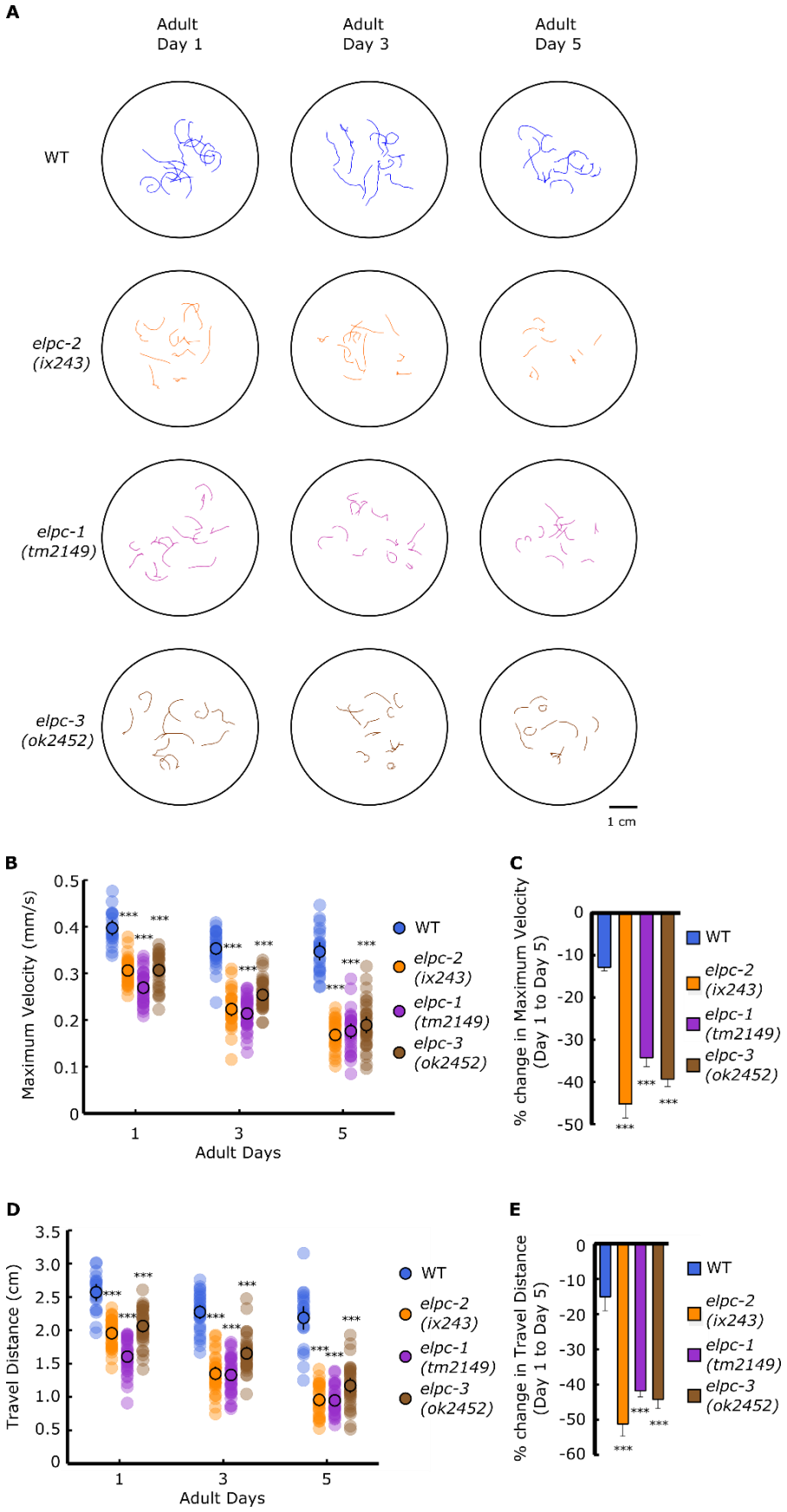

Figure 4.8 The Elongator complex is required to maintain locomotor function

(A) Representative locomotor tracks of WT, *elpc-1(tm2149)* and *elpc-3(ok2452)* worms. n = 10–15 tracks per plate. (B) Maximum velocities of WT and *elpc* mutant strains. (C) Change in maximum velocity of WT and *elpc* mutant strains. (D) Travel distances of WT and *elpc* mutant strains. (E) Change in travel distance of WT and *elpc* mutant strains. For maximum velocity and travel distance experiments, n = 30–45 worms per strain for each day (10–15 worms from 3 biological replicate plates). For percent change in maximum velocity and travel distance graphs, n = 3 biological replicate plates. Error bars indicate 95% confidence intervals. ***$P < 0.001$; One-way ANOVA with Dunnett's post hoc test vs. WT.

We wondered whether functional loss of *elpc-2* causes the progressive decline in locomotor function independently or as a component of the Elongator complex. We measured the maximum velocities and travel distances of strains carrying deletions in *elpc-1* and *elpc-3*. We found that *elpc-1(tm2149)* and *elpc-3(ok2452)* mutant strains also could not maintain their locomotor function during adulthood (Fig. 4.8A–E). The percent decline in locomotor function in the *elpc-1(tm2149)* and *elpc-3(ok2452)* mutants resemble the locomotor decline of the *elpc-2(ix243)* mutant strain (Fig. 4.8A–E).

4.3.4 No additive effects are seen in Elongator double mutants

We tested whether double mutants carrying both *elpc-2* and *elpc-3* mutations would show additive deficiencies in locomotor function. We created *elpc-2(ix243);elpc-3(ok2452)* double mutants and measured maximum velocity and travel distance of the worms. The *elpc-2(ix243);elpc-3(ok2452)* double mutant strain did not show additive deficiencies in maximum velocity or travel distance compared to either of the single mutants (Fig. 4.9 A–D). These results suggest that the Elongator complex works as a protein complex, and loss-of-function

of one component of the complex is sufficient to abolish the function of the Elongator complex.

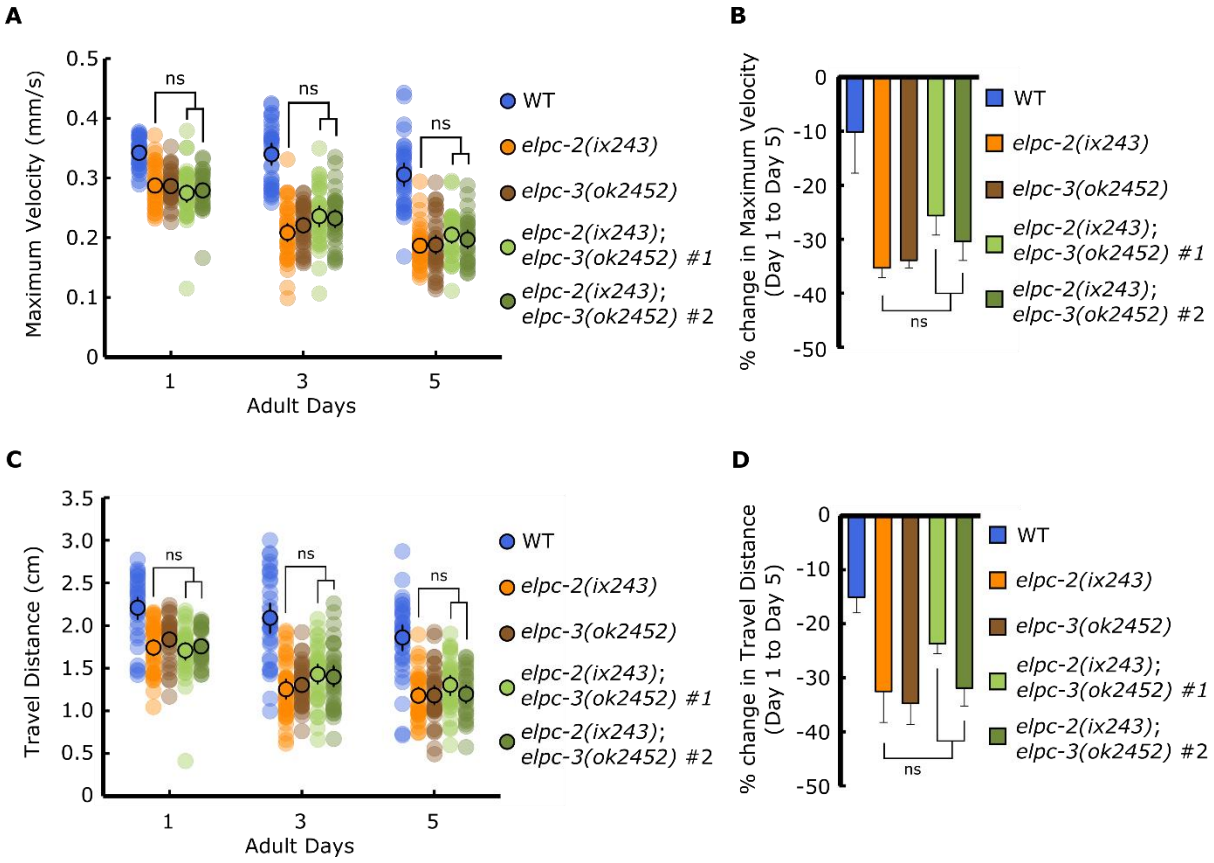

Figure 4.9 *elpc-3* mutation does not cause additive effects in *elpc-2* mutant
(A) Maximum velocities of WT, *elpc-2(ix243)*, *elpc-3(ok2452)*, and *elpc-2(ix243);elpc-3(ok2452)* double mutant strains. (B) Change in maximum velocity of strains from A. (B) Travel distances of WT, *elpc-2(ix243)*, *elpc-3(ok2452)*, and *elpc-2(ix243);elpc-3(ok2452)* double mutant strains. (D) Change in travel distance of strains from C. For maximum velocity and travel distance experiments, n = 30–45 worms per strain for each day (10–15 worms from 3 biological replicate plates). For percent change in maximum velocity and travel distance graphs, n = 3 biological replicate plates. Error bars indicate 95% confidence intervals. ns, not significant; One-way ANOVA with Tukey's post hoc test.

We also tested whether double mutants carrying both *elpc-2* and *elpc-1* mutations would show additive deficiencies in locomotor function. We created a *elpc-1(ok2452);elpc-*

2(ix243) double mutant strain and measured the maximum velocity and travel distance of the worms. The *elpc-1(ok2452);elpc-2(ix243)* double mutant worms did not show additive deficiencies in the progressive decline in locomotor function compared to either of the single mutants (Fig. 4.10A–D). The results are similar to what we observed in the *elpc-2(ix243);elpc-3(ok2452)* double mutants. Both double mutant experiments support the notion that loss of one part of the complex will prevent proper functioning of the Elongator complex.

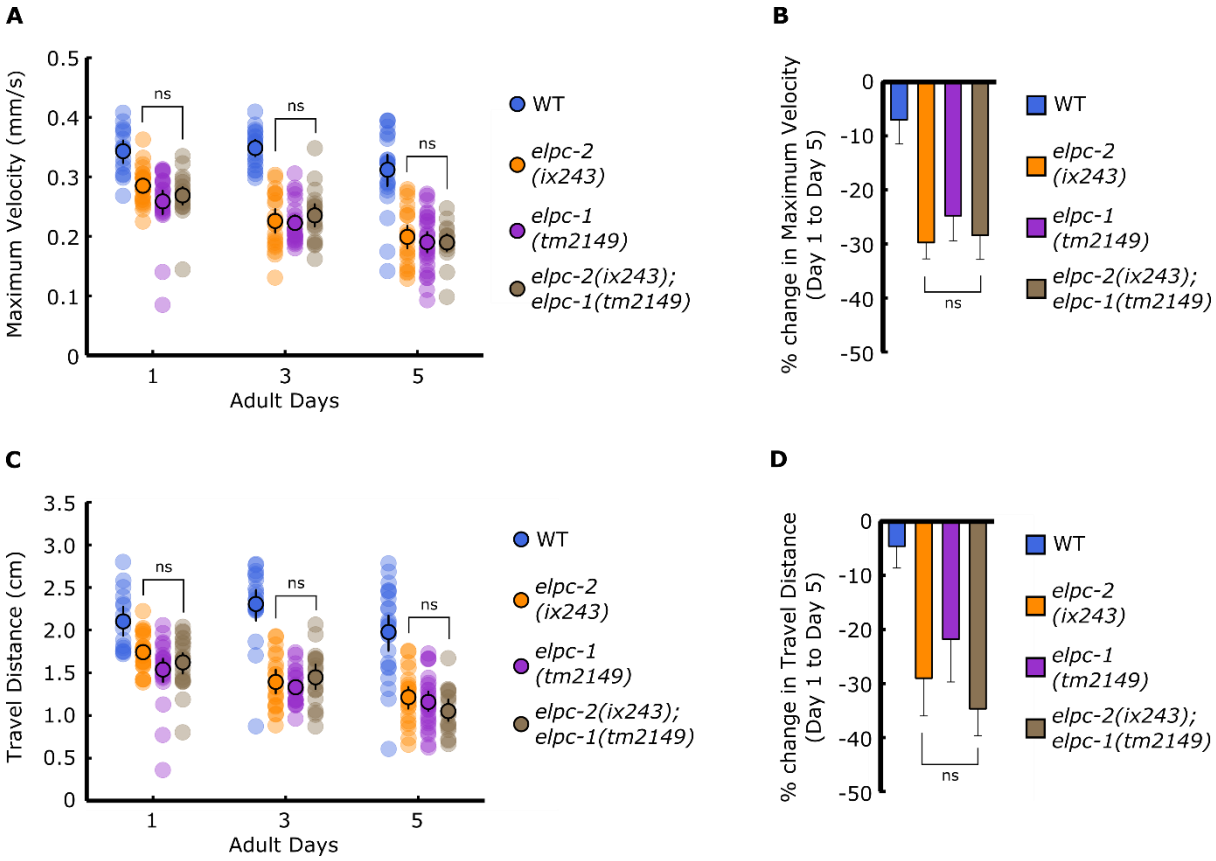

Figure 4.10 *elpc-1* mutation does not cause additive effects in *elpc-2* mutant

(A) Maximum veolcities of WT, *elpc-2(ix243), elpc-1(tm2149), and elpc-1(tm2149);elpc-2(ix243)* double mutant strains. (B) Change in maximum velocity of strains from E. (C) Travel distances of WT, *elpc-2(ix243), elpc-1(tm2149), and elpc-1(tm2149);elpc-2(ix243)* double mutant strains. (D) Change in travel distance of strains from G. For maximum velocity and travel distance experiments, n = 30–45 worms per strain for each day (10–15 worms from 3 biological replicate plates). For percent change in maximum velocity and

travel distance graphs, n = 3 biological replicate plates. Error bars indicate 95% confidence intervals. ns, not significant; One-way ANOVA with Tukey's post hoc test.

4.3.5 Expression pattern of *elpc-2* transcriptional reporter

A transcriptional reporter of *elpc-2*p::*GFP* was created using 2090 bp upstream of the *elpc-2* start codon as the promoter sequence. The transcriptional reporter showed a broad expression pattern including head and body wall muscles, head neurons, pharynx, canal cell, coelomocytes, intestine, and tail. The expression pattern of *elpc-2* overlaps in the pharynx, body wall muscles, and neurons with a previously reported expression pattern of *elpc-1* (Chen et al., 2009a). The Elongator complex may have broad functions across many different cell types.

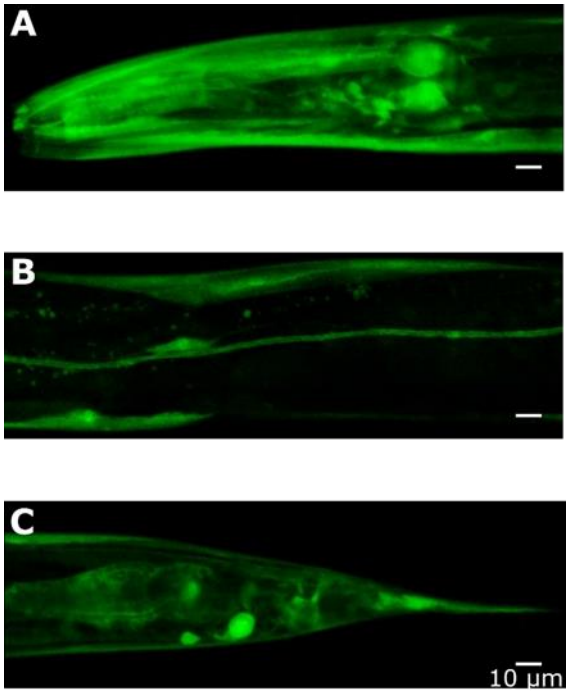

Figure 4.11 Expression pattern of *elpc-2* transcriptional GFP fusion
(A) *elpc-2*p*::GFP* expression in pharynx, neurons, and head muscles. (B) *elpc-2*p*::GFP* expression in body wall muscles and canal cell. (C) *elpc-2*p*::GFP* expression in coelomocytes, intestine, and tail. Scale bars: 10 µm.

4.3.6 Whole genome sequencing of *ix241* mutant strain

In order to identify the causative mutation site in the *ix241* worms, we sequenced the whole genome of the *ix241* worms before and after backcrossing (Fig. 4.12A–C). Mutations were evenly induced across all chromosomes prior to backcrossing (Fig. 4.12A). After backcrossing four times, mutation peaks remained on chromosomes I, IV, and X (Fig. 4.12B).

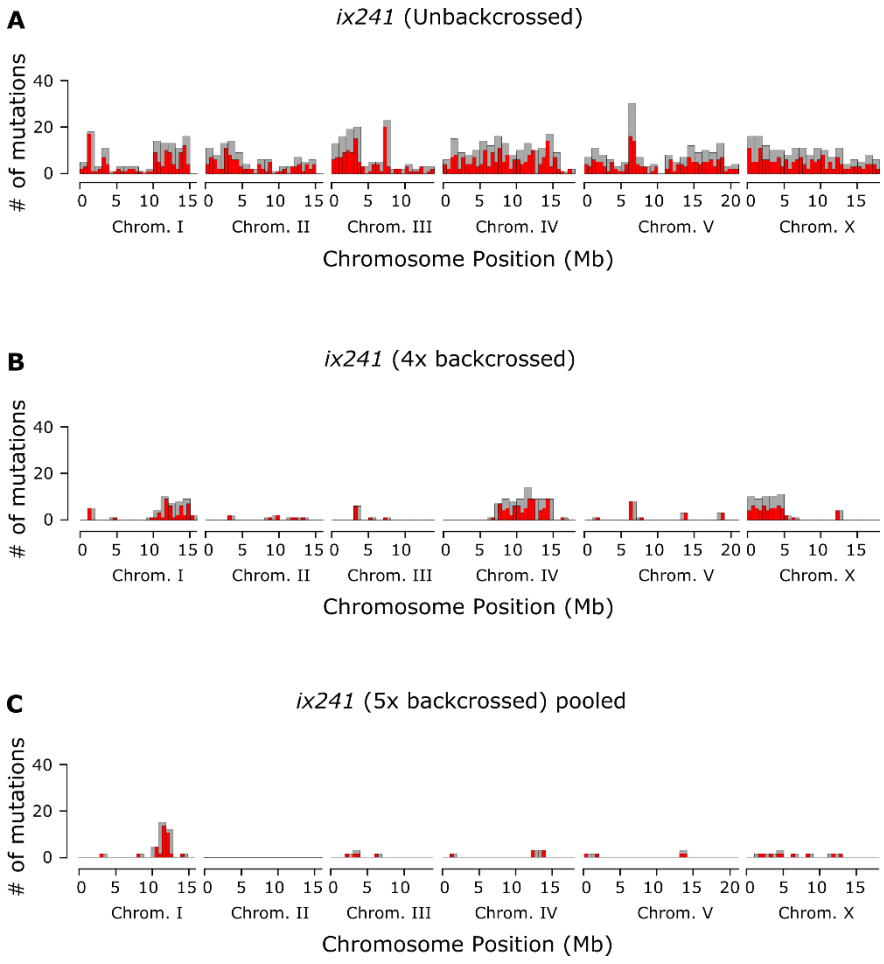

Figure 4.12 Mutation frequency of *ix241* mutant strain

(A) Frequency of mutations along each chromosome for *ix241* strain before backcrossing. (B) Frequency of mutations along each chromosome for *ix241* strain after the fourth backcross. (C) Frequency of mutations along each chromosome for *ix241* strains after the fifth backcross. Red bars indicate 0.5-Mb bins and grey bars indicate 1.0-Mb bins.

Since there were multiple mutation peaks remaining after the fourth backcross, we carried out a fifth backcross. We sequenced five strains that showed the progressive decline in locomotor function after the fifth backcross. Only a peak on chromosome I remained (Fig. 4.12C). The mutation that causes the progressive decline in locomotor function in the *ix241* mutant strain most likely lies within the mutation peak on chromosome I. The mutations that were shared among the strains that showed the progressive decline in locomotor function after the fifth backcross are shown in Table 4.5.

Within the mutation peak on Chromosome I, the mutation that was predicted to have the strongest effect on protein function was a splice acceptor mutation in *dys-1* (Table 4.5, Table 4.6). *dys-1* is an ortholog of human dystrophin, which is the mutated gene in Duchenne and Becker muscular dystrophies (Hoffman et al., 1987). Depending on the severity of the dystrophin mutation, the onset of disease symptoms can occur during childhood (Duchenne muscular dystrophy), or during early adulthood (Becker muscular dystrophy) (Koenig et al., 1989). *C. elegans* strains carrying deletions in *dys-1* show progressive declines in locomotor function (Gieseler et al., 2000; Oh and Kim, 2013). In addition, *C. elegans dys-1* mutants bend their head and neck ("overbent" phenotype) more than wild-type animals when moving forward (Bessou et al., 1998). We also observe the overbent phenotype in the *ix241* worms. Therefore, the splice site mutation in *dys-1* is a strong candidate for the causative mutation site that leads to the progressive decline in locomotor function in the *ix241* strain.

Table 4.5 Remaining mutations in *ix241* mutant strains

Chrom.	Pos.	Ref.	Alt.	Gene	Mutation Type	Effect*
I	3258592	CA	C	Y54E10A.20	upstream gene variant	modifier
I	8160530	TTATA	T	T28B8.3	downstream gene variant	modifier
I	10731034	C	T	rpn-10	missense variant	moderate
I	10766899	C	T	daf-16	intron variant	modifier
I	10974485	C	T	Y52B11A.3	intron variant	modifier
I	11307424	C	T	H25P06.5	synonymous variant	low
I	11536456	C	T	dys-1	splice acceptor variant	high
I	11644705	C	T	W04G5.9	intron variant	modifier
I	11726250	C	T	F35E2.9	missense variant	moderate
I	11808061	G	T	T02G6.2-T02G6.4	intergenic region	modifier
I	11832340	C	T	Y47H9C.1	missense variant	moderate
I	11864150	T	A	ced-1	intron variant	modifier
I	11896398	C	T	Y47H9C.12	upstream gene variant	modifier
I	11914682	C	T	hda-3	missense variant	moderate
I	11927975	C	T	wve-1	upstream gene variant	modifier
I	12008815	C	T	fbxa-122	downstream gene variant	modifier
I	12176794	C	T	R05D7.3	intron variant	modifier
I	12298210	C	T	F56H6.7	missense variant	moderate
I	12341691	C	T	nhr-217	intron variant	modifier
I	12343381	T	A	T09E11.11	upstream gene variant	modifier
I	12414199	C	T	E03H4.5	intron variant	modifier
I	12493515	C	T	T27F6.6	synonymous variant	low
I	12970406	G	A	eif-6	downstream gene variant	modifier
I	14083393	A	C	gadr-6	upstream gene variant	modifier
III	2340737	A	C	Y54F10BM.1	intron variant	modifier
III	3385124	A	AG	hecw-1	upstream gene variant	modifier
III	3786851	T	TTC	acy-3	upstream gene variant	modifier
III	6301707	T	TC	F47D12.9	upstream gene variant	modifier
IV	1226960	T	C	W09G12.8	intron variant	modifier
IV	12319292	TG	T	F19B6.9	downstream gene variant	modifier
IV	12319295	T	A	F19B6.9	upstream gene variant	modifier
IV	13506453	GA	G	nlp-17	upstream gene variant	modifier
IV	13823462	A	AACTCGGCTGTCGGCTGGCGCCGACAGCCGAGTCCATTTCGCT	H08M01.74	downstream gene variant	modifier
V	363225	C	CTACTGTAGTGCTTGTGTCGATTTACGGGATCGATTTCCTAAATGAACCGTAAATCGACACAAGCACTACAGTAGTCATTTAAAGGAT	T22H9.1	intron variant	
V	1500601	G	A	sru-27	missense variant	moderate
V	13231585	T	G	C34D1.8	downstream gene variant	modifier
V	13697695	C	T	T01D3.1	missense variant	moderate
X	1519515	A	ATCCGACATTTTTATAGCAATGCGCAGAACCCAAAAAATGTCGGACGCGGAGCCAAGGCTGCACCAAATAGTGCGATAGGGTATGGCATTATTTGGTGCAAACTTGGCTTCGCG	toca-1	intron variant	modifier
X	2008595	TA	T	Y40A1A.1-Y102A11A.9	intergenic region	modifier
X	3314891	A	AT	F11D5.12	upstream gene variant	modifier
X	4241974	A	G	W01H2.t1	upstream gene variant	modifier
X	4674025	G	GT	F16H11.1	downstream gene variant	modifier
X	6357781	C	CCCAT	C03B1.10	frameshift variant	high
X	8191585	G	GT	C17H11.6	intron variant	modifier
X	11646516	A	C	T04F8.15	upstream gene variant	modifier
X	12502801	T	TACGAAAAATAGATTGTTAC	sdz-19	intron variant	modifier

*"Effect" is ranked in order of putative impact of the mutation (high > moderate > low > modifier)

Table 4.6 Description of mutation types (from SnpEff manual (Cingolani et al., 2012))

Mutation Type	Description
downstream gene variant	Variant is downstream of a gene (default length: 5K bases)
frameshift variant	Insertion or deletion causes a frame shift
intergenic region	The variant is in an intergenic region
intron variant	Variant is in an intron
missense variant	Variant causes a codon that produces a different amino acid
splice acceptor variant	The variant hits a splice acceptor site (defined as two bases before exon start, except for the first exon).
synonymous variant	Variant causes a codon that produces the same amino acid
upstream gene variant	Variant is upstream of a gene (default length: 5K bases)

The splice acceptor mutation in *dys-1* was confirmed by Sanger sequencing (Fig. 4.13A). In the *ix241* worms, the main effect of the *dys-1* mutation is the retention of the intron between exon 33 and 34 (Fig. 4.13B). However, a small fraction of transcripts are spliced between exon 33 and exon 34 (Fig. 4.13B). Sanger sequencing of the spliced product indicated that the splice site is shifted by two base pairs, and would cause a frameshift in the protein sequence (Fig.4.13B). Therefore, proper *dys-1* transcripts are not formed in the *ix241* worms, and would likely cause loss of DYS-1 function.

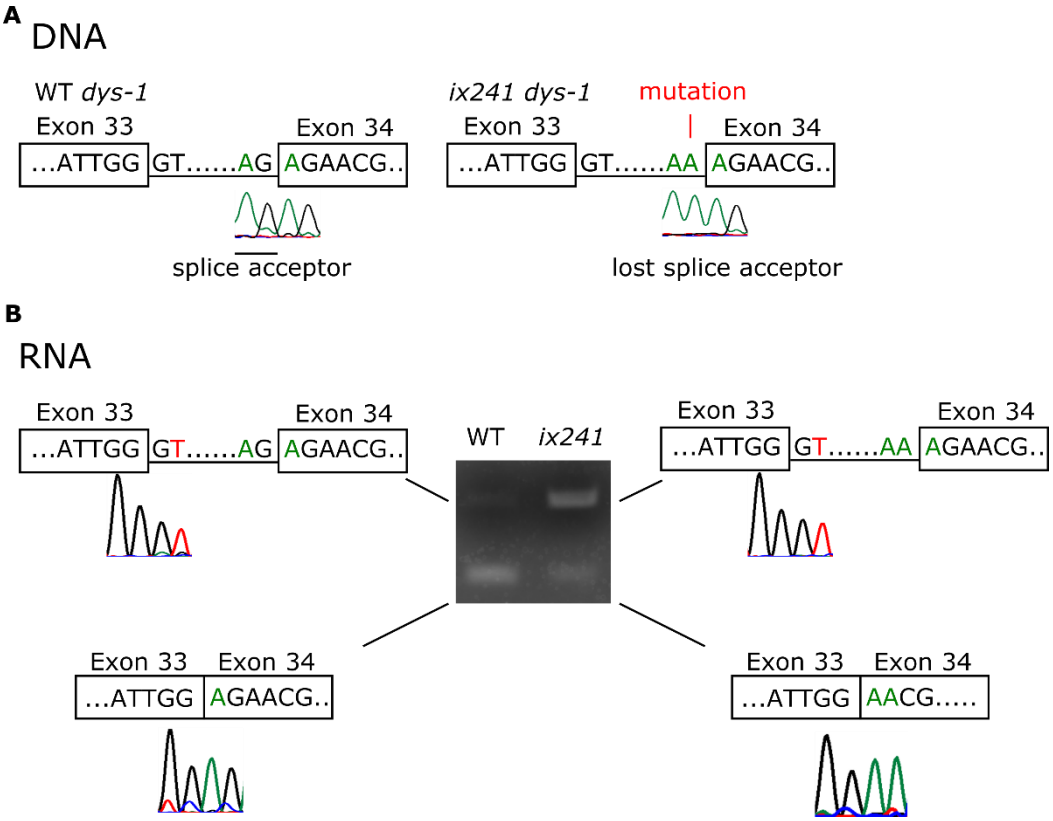

Figure 4.13 Confirmation of *dys-1* mutation site in *ix241* worms

(A) Sanger sequencing of DNA extracted from WT and *ix241* worms at *dys-1* mutation site. (B) Sanger sequencing of cDNA extracted from WT and *ix241* worms at *dys-1* mutation site.

4.3.7 *ix241*(5x BC) #23 strain carries *dys-1* mutation but maintains locomotor function

While backcrossing for the first four times, we noticed that the locomotor deficit phenotype of the *ix241* strain segregates with the overbent phenotype, where mutant worms bend their head and neck more than wild-type worms when moving forward. This phenotype was readily observable using a stereoscopic microscope. Therefore, for the fifth backcross, we selected worms that showed the overbent phenotype. This enabled us to obtain a greater number of backcrossed lines. We observed a locomotor decline from adult day 2 to day 5 in 22 out of 23 lines that showed the overbent phenotype. However, one strain showed the overbent phenotype, but did not show a locomotor deficit from adult day 2 to day 5 (Fig. 4.14). We refer to this strain as the *ix241*(5x BC) #23 strain.

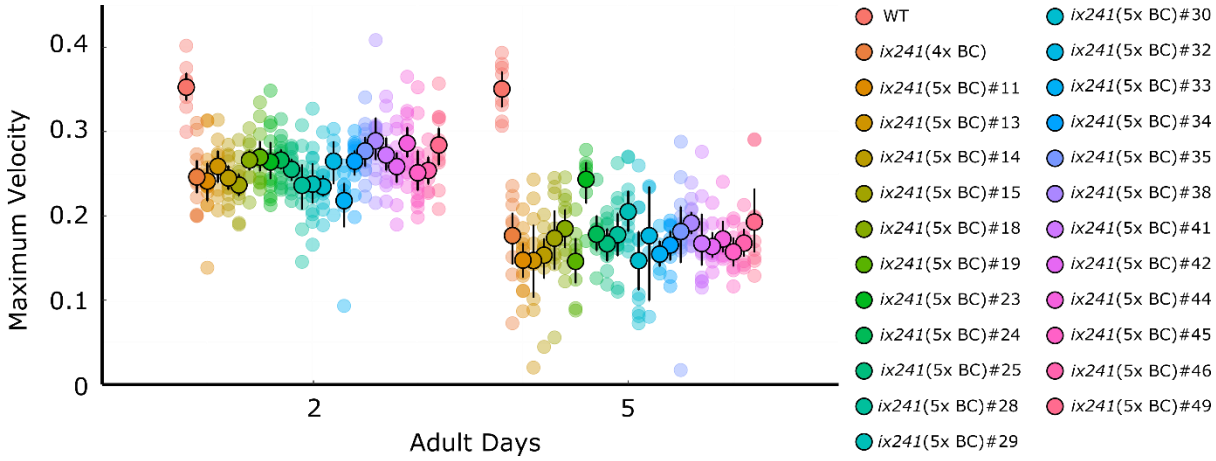

Figure 4.14 Locomotor function of ix241 worms after the fifth backcross
Maximum velocities of *ix241* worms after the fourth backcross and *ix241* worms after the fifth backcross. n = 10–15 worms per strain. Error bars indicate 95% confidence intervals.

The *ix241*(5x BC) #23 strain demonstrates the overbent head phenotype and shows a slight deficit in locomotor function on the first day of adulthood compared to wild-type worms (Fig. 4.14). This strain may have acquired a gain-of-function mutation that prevents the progressive loss of locomotor function, or may have lost a loss-of-function mutation that may have also been required to cause the progressive loss of locomotor function. In the case of a loss of a mutation, since only one strain was found out of 23, the mutation may lie in a region close to the *dys-1* mutation site.

In order to identify the mutation site that is involved in the lack of progressive decline in locomotor function in the *ix241*(5x BC) #23 strain, we backcrossed the *ix241*(5x BC) #23 strain to the WT strain. Backcrossed strains of the *ix241*(5x BC) #23 strain that carried the *dys-1* mutation also showed a lack of progressive decline in locomotor function. We sequenced the whole genomes of the *ix241*(5x BC) #23 strain and two backcrossed strains *ix241*(6x BC) #1 and *ix241*(6x BC) #2.

In the case of a loss of loss-of-function mutation, the causative mutation would have been lost in the *ix241*(5x BC) #23, *ix241*(6x BC) #1, and *ix241*(6x BC) #2 strains. In order to identify the candidate mutation sites, we subtracted the mutation sites found in the *ix241*(5x BC) #23, *ix241*(6x BC) #1, and *ix241*(6x BC) #2 strains from the shared mutations in strains that show the progressive decline in locomotor function (*ix241*(4x BC), *ix241*(5x BC) #1, *ix241*(5x BC) #11, *ix241*(5x BC) #33, *ix241*(5x BC) #45, *ix241*(5x BC) #46). The mutations that remained after analysis are shown in Table 4.7.

Table 4.7 Candidate mutation sites involved in maintained locomotor function in *ix241*(5x BC) #23 strain: Assuming loss of a loss-of-function mutation

Chrom.	Pos.	Ref.	Alt.	Gene	Mutation Type	Effect*
I	10731034	C	T	rpn-10	missense variant	moderate
I	10766899	C	T	daf-16	intron variant	modifier
I	10974485	C	T	Y52B11A.3	intron variant	modifier
I	11307424	C	T	H25P06.5	synonymous variant	low
I	11864150	T	A	ced-1	intron variant	modifier
I	11896398	C	T	Y47H9C.12	upstream gene variant	modifier
I	11914682	C	T	hda-3	missense variant	moderate
I	11927975	C	T	wve-1	upstream gene variant	modifier
I	12008815	C	T	fbxa-122	downstream gene variant	modifier
I	12176794	C	T	R05D7.3	intron variant	modifier
I	12298210	C	T	F56H6.7	missense variant	moderate
I	12341691	C	T	nhr-217	intron variant	modifier
I	12343381	T	A	T09E11.11	upstream gene variant	modifier
I	12414199	C	T	E03H4.5	intron variant	modifier
I	12493515	C	T	T27F6.6	synonymous variant	low
I	12970406	G	A	eif-6	downstream gene variant	modifier

*"Effect" is ranked in order of putative impact of the mutation (high > moderate > low > modifier)

Table 4.8 Description of mutation types (from SnpEff manual (Cingolani et al., 2012))

Mutation Type	Description
downstream gene variant	Variant is downstream of a gene (default length: 5K bases)
intron variant	Variant is in an intron
missense variant	Variant causes a codon that produces a different amino acid
synonymous variant	Variant causes a codon that produces the same amino acid
upstream gene variant	Variant is upstream of a gene (default length: 5K bases)

If the lack of progressive decline in locomotor function is caused by a gain-of-function mutation, the causative mutation would be present in the *ix241*(5x BC) #23, *ix241*(6x BC) #1, and *ix241*(6x BC) #2 strains, but not in the *ix241*(4x BC), *ix241*(5x BC) #1, *ix241*(5x BC) #11, *ix241*(5x BC) #33, *ix241*(5x BC) #45, and *ix241*(5x BC) #46 strains. The mutations that remained are shown in Table 4.9.

Table 4.9 Candidate mutation sites involved in maintained locomotor function in *ix241*(5x BC) #23 strain: Assuming gain of function mutation

Chrom.	Pos.	Ref.	Alt.	Gene	Mutation Type	Effect*
I	2500953	C	A	Y23H5B.5	intron variant	modifier
I	3562207	T	C	Y47G6A.22	intron variant	modifier
I	5078741	G	A	linc-156	non coding transcript exon variant	modifier
I	5681015	C	G	unc-40	missense variant	moderate
I	8839955	A	T	F29D10.1	upstream gene variant	modifier
I	10765117	C	A	daf-16	upstream gene variant	modifier
I	11043947	ATTT	A	Y52B11A.10	intron variant	modifier
I	11044000	C	G	Y52B11A.10	intron variant	modifier
I	11044002	A	AT	Y52B11A.10	intron variant	modifier
I	11044010	A	AG	Y52B11A.10	intron variant	modifier
I	11044013	GAA	G	Y52B11A.10	intron variant	modifier
I	11044022	C	CT	Y52B11A.10	intron variant	modifier
I	11044029	A	AATATAT	Y52B11A.10	intron variant	modifier
I	11044035	T	G	Y52B11A.10	intron variant	modifier
I	11044054	TCA	T	Y52B11A.10	intron variant	modifier
I	11044061	A	T	Y52B11A.10	intron variant	modifier
I	11044069	A	G	Y52B11A.10	intron variant	modifier
I	11044075	C	A	Y52B11A.10	intron variant	modifier
I	11044093	T	A	Y52B11A.10	intron variant	modifier
I	11044095	G	T	Y52B11A.10	intron variant	modifier
I	14633990	A	ATTACATGTGCATGTG	exoc-8	downstream gene variant	modifier
II	12484251	A	T	fbxb-102	3 prime UTR variant	modifier
II	14523996	A	T	btb-20	upstream gene variant	modifier
II	15013592	T	G	Y53F4B.51	missense variant	moderate
V	6940649	C	G	Y57E12B.10-Y57E12B.4	intergenic region	modifier
V	6940659	C	T	Y57E12B.10-Y57E12B.4	intergenic region	modifier
X	1296462	T	TC	dop-4	intron variant	modifier
X	2726891	ACCCCC	A	unc-2	intron variant	modifier
X	4345596	T	A	F14H12.3	3 prime UTR variant	modifier
X	9101324	AG	A	ajm-1	intron variant	modifier

*"Effect" is ranked in order of putative impact of the mutation (high > moderate > low > modifier)

Table 4.10 Description of mutation types (from SnpEff manual (Cingolani et al., 2012))

Mutation Type	Description
downstream gene variant	Variant is downstream of a gene (default length: 5K bases)
intergenic region	The variant is in an intergenic region
intron variant	Variant is in an intron
missense variant	Variant causes a codon that produces a different amino acid
non coding transcript exon variant	A sequence variant that changes non-coding exon sequence.
synonymous variant	Variant causes a codon that produces the same amino acid
upstream gene variant	Variant is upstream of a gene (default length: 5K bases)
3 primer UTR variant	Variant hits 3'UTR region

Further experiments are necessary to identify the causative mutation that is responsible for the maintained locomotor healthspan in the *ix241*(5x BC) #23 strain. The causative mutation may work together with the *dys-1* mutation to cause progressive decline in locomotor function, or the causative mutation may be a gain-of-function mutation that can ameliorate the toxic effects of the *dys-1* mutation.

4.4 Discussion

4.4.1 Elongator Complex is important for maintaining adult locomotor function in *C. elegans*

The Elongator complex is an evolutionarily conserved protein complex that consists of six subunits (Creppe and Buschbeck, 2011). The catalytic subunit, ELP3, possesses a radical *S*-adenosylmethionine (SAM) domain and a histone acetyltransferase (HAT) domain (Boal et al., 2011; Creppe and Buschbeck, 2011). The SAM domain is predicted to be responsible for the enzymatic transfer of methoxycarbonylmethyl (mcm) and carbamoylmethyl (ncm) modifications to tRNA (Boal et al., 2011). The HAT domain is responsible for the acetylation of target proteins (Creppe and Buschbeck, 2011). In *C. elegans*, there are currently only four predicted homologs (*elpc-1*, *elpc-2*, *elpc-3*, *elpc-4*) of

the Elongator complex (Solinger et al., 2010). From our study, loss-of-function mutations in *elpc-1*, *elpc-2,* and *elpc-3* caused a shortened locomotor healthspan. Proper functioning of the Elongator complex may require multiple or all components of the complex (Dauden et al., 2017). Our work suggests that the Elongator complex is required to maintain locomotor function during adulthood.

4.4.2 ELP1 is implicated in familial dysautonomia

Familial dysautonomia (FD), or Riley-Day syndrome, is a familial neurodevelopmental disorder that affects the development, survival, and progressive degeneration of the sensory and autonomic nervous system. The disorder is characterized by symptoms that include reduced pain sensation, episodic hypertension, excessive sweating, and an absence of tears (Rubin and Anderson, 2017). The disorder begins during development, and only 50% of patients reach 30 years of age (Slaugenhaupt et al., 2001). The major causative mutation site for familial dysautonomia was found to be located in the donor splice site of intron 20 in *ELP1* (Anderson et al., 2001; Slaugenhaupt et al., 2001). This mutation causes variable skipping of exon 20, leading to lower levels of the normal ELP1 transcript in affected patients compared to unaffected individuals (Hims et al., 2007). Heterozygous carriers of the mutation do not show any symptoms, suggesting that FD is caused by a loss-of-function mutation (Rubin and Anderson, 2017).

Mice with complete loss of *ELP1* or loss of exon 20 of *ELP1* were both embryonic lethal (Chen et al., 2009b; Dietrich et al., 2011). This indicates that complete loss of ELP1 protein function is not tolerated in mice. Since *C. elegans* can tolerate the loss of *elpc-1,* cellular and biochemical changes that occur from loss of ELP1 may be characterized using the *C. elegans elpc-1(tm2149)* mutant.

4.4.3 ELP2 is involved in inherited neurodevelopmental disease

A mutation in *ELP2* was reported to be the causative mutation in a familial form of neurodevelopmental disability (Cohen et al., 2015). The two affected patients are brothers with parents that have different missense mutations in ELP2 (H271R and R527W) (Cohen et al., 2015). The brothers are both compound heterozygotes for the two *ELP2* mutations (Cohen et al., 2015). The patients demonstrate a lack of motor control starting in early development, severe intellectual disability, and progressive loss of locomotor function (Cohen et al., 2015). The parents are unaffected carriers of the *ELP2* mutation. The compound heterozygous mutations may enable some activity of the Elongator complex, but may cause the loss of many functions.

Loss of ELP2 protein function may lead to more severe defects in humans compared to *C. elegans*, since we only saw minor effects on development in the *elpc-2(ix243)* mutant strain. However, we also see deficits in locomotor function on the first day of adulthood and a 13.9% delay in the time it takes for development in the *elpc-2(ix243)* mutant strain. Therefore, it may be possible to model some of the neurodevelopmental dysfunctions that result from the human ELP2 mutation in our *C. elegans elpc-2(ix243)* mutant. The amino acid sequences of *C. elegans* ELPC-2 and human ELP2 are highly conserved. Both amino acid residues that are mutated in the human patients are conserved in *C. elegans.* Therefore, our *elpc-2(ix243)* mutant may be used as a disease model for aspects of familial neurodevelopmental disease caused by mutations in human *ELP2*. The *elpc-2(ix243)* strain can be used for therapeutic drug screenings or suppressor screens that may reverse the negative effects of loss of *elpc-2.*

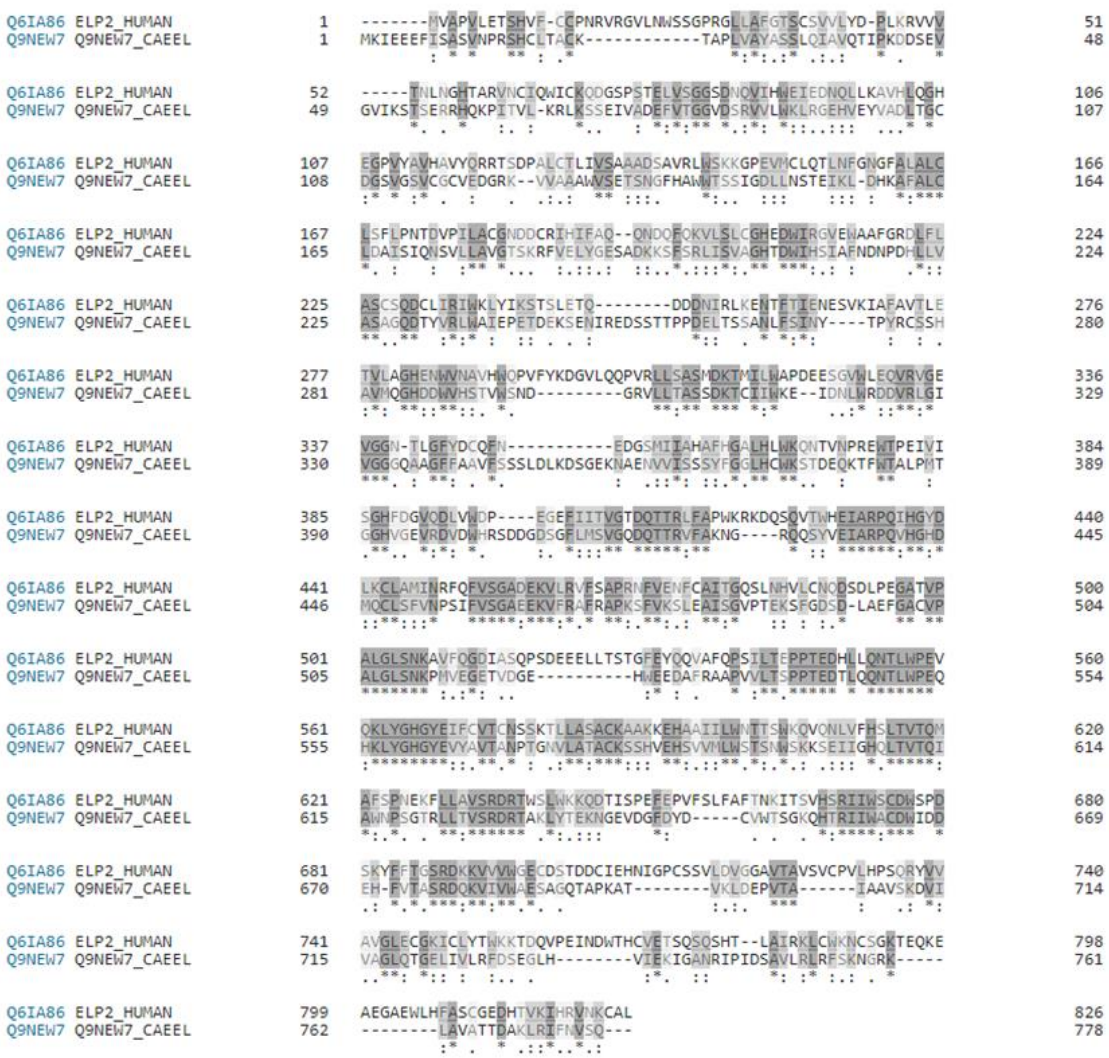

Figure 4.15 Amino acid alignment of *C. elegans* ELPC-2 and human ELP2

C. elegans ELPC-2 and human ELP2 were aligned using Clustal Omega (Sievers et al., 2011). An asterisk (*) indicates positions that are conserved; colon (:) indicates positions that are strongly similar (> 0.5 in the Gonnet PAM 250 matrix); period (.) indicates positions that are weakly similar (< 0.5 in the Gonnet PAM 250 matrix).

4.4.4 ELP3 is implicated in amyotrophic lateral sclerosis

Allelic variants of *ELP3*, the gene encoding the catalytic subunit of the Elongator complex, were found to be associated with amyotrophic lateral sclerosis (ALS) in three human populations (Simpson et al., 2009). Risk-associated alleles have lower levels of ELP3 in the cerebellum and motor cortex of ALS patients, and protection-associated alleles have

higher levels of ELP3 (Simpson et al., 2009). Overexpression of ELP3 reduced the levels of axonopathy in the $SOD1^{A4V}$ zebrafish model of ALS and $SOD1^{G93A}$ mouse model of ALS (Bento-Abreu et al., 2018). The Elongator complex may play a role in ameliorating the toxic effects of fALS-related SOD1. Our work complements studies that have been performed in the context of ALS, and show that loss of the Elongator complex alone can cause locomotor deficits during adulthood in *C. elegans*. Future therapies that target multiple subunits of the Elongator complex may provide more robust effects than therapies that target only the catalytic ELP3 subunit.

4.4.5 ELP4 is implicated in rolandic epilepsy

Rolandic epilepsy is the most common form of human epilepsy, characterized by seizures that affect the vocal tract (Strug et al., 2009). The onset of seizures occurs during childhood (3-12 years) (Strug et al., 2009). A genome-wide linkage study that focused on rolandic epilepsy found that *ELP4* may be implicated in the disease (Strug et al., 2009). Three SNPs in introns 5, 6, and 9 of *ELP4* showed the highest linkage with rolandic epilepsy. The SNPs may affect the expression level or function of ELP4. Reduced levels of ELP4 may affect the catalytic activity of ELP3 or may have independent functions outside of supporting the formation of the Elongator complex.

4.4.6 ELP6 causes larval lethality in *Drosophila melanogaster*

The *Drosophila melanogaster poly* gene shows protein sequence similarity with human *ELP6*. Loss-of-function mutation in *poly* causes larval lethality in *Drosophila* due to a downregulation of insulin-signaling (Bolukbasi et al., 2012). The *poly* mutant carries a P-element insertion in an intron which led to an absence of *poly* mRNA and Poly protein

(Bolukbasi et al., 2012). Poly acts downstream of the insulin receptor, but upstream of Akt kinase and TOR signaling in the regulation of cell metabolism and growth (Bolukbasi et al., 2012).

4.4.7 Differences and commonalities among ELP-related diseases

In all disease cases related to the Elongator complex, neuronal functions are affected in the patients. To our knowledge, there have not been any reported cases of human patients with complete loss of any of the Elongator Complex genes. Therefore, the Elongator complex may be required during developmental processes in humans. However, missense mutations in the protein sequence or mutations that affect the expression levels of Elongator components are tolerated in humans, but with dysfunctions of varying severity (Anderson et al., 2001; Bento-Abreu et al., 2018; Cohen et al., 2015). The disease phenotypes of patients with mutations in *ELP1, ELP2,* and *ELP3* are not identical. Mutation in *ELP1* causes sensory and autonomic defects; mutation in *ELP2* causes intellectual and motor defects; and mutation in *ELP3* affects the vulnerability of the motor neurons in ALS patients. The differences in disease phenotypes may suggest that Elongator subunits have different roles aside from functioning as part of the Elongator complex. Another possibility is that different Elongator subunits may facilitate the recruitment of cell-type specific substrates to the catalytic ELP3 subunit.

We observe that *C. elegans* can tolerate the loss of various components of the Elongator complex. This characteristic may make *C. elegans* a suitable animal model to study how loss of Elongator complex function affects development and phenotypes related to the aging process. More careful analysis of the phenotypic differences among the *C. elegans*

elpc-1, *elpc-2*, and *elpc-3* mutants may provide insights into the different functions of each subunit of the Elongator complex.

5. Chapter 3: Characterization of the *elpc-2* gene

5.1 Introduction

5.1.1 DAF-16 and HSF-1 are transcription factors that regulate aging in *C. elegans*

C. elegans is a model organism that has pioneered the research of genetic and molecular pathways that play a role in longevity. Two well-characterized transcription factors involved in longevity are DAF-16 and HSF-1 (Hsu et al., 2003). Both transcription factors induce the expression of pro-longevity genes involved in many processes including immune and stress responses, protein folding, and autophagy (Samuelson et al., 2007; Taylor and Dillin, 2011). DAF-16 and HSF-1 not only regulate lifespan, but also alter the progression of symptoms in *C. elegans* models of age-related diseases (Cohen et al., 2006). From our forward genetic screen in *C. elegans*, we identified a nonsense mutation in the *elpc-2* gene that causes a progressive decline in adult locomotor function. *elpc-2* is a component of the Elongator complex, which is implicated in modifying tRNA (Dauden et al., 2017). Since DAF-16 and HSF-1 have been implicated in the maintenance of healthy aging, we focused on whether effects of the *elpc-2* mutation may overlap with either of these pathways in the context of locomotor healthspan.

5.1.2 Insulin-signaling pathway involvement in locomotor healthspan and aging

A forward genetic screen for long-lived mutants in *C. elegans* has isolated mutants that can live twice as long as wild-type worms (Klass, 1983). Follow-up studies have found that a reduction-of-function mutation in the DAF-2 insulin-like signaling receptor is responsible for prolonging lifespan (Kimura et al., 1997). DAF-16 is a major transcription factor that acts downstream of DAF-2 to induce the expression of proteins that prolong longevity (Kimura et al., 1997).

Various studies have found that long-lived insulin-signaling mutants also show a prolonged healthspan (Ewald et al., 2018). However, whether the extent of the positive effect on healthspan is the same or more as the extent of the positive extent on lifespan has been a subject of debate (Ewald et al., 2018). *daf-2(e1370)* mutant worms were found to spend a larger proportion of life in gerospan (less than 50% of maximum functional capacity) compared to wild-type worms for movement capacity and other measures of healthspan (Bansal et al., 2015). However, when locomotor function of worms was measured in the absence of food, the proportion of time spent in gerospan was not changed compared to wild-type worms (Hahm et al., 2015). This may be due to the greater expression level of odorant receptor ODR-10 in *daf-2(e1370)* mutant worms (Hahm et al., 2015). The higher expression of ODR-10 may cause a hypersensitive response to food signals and inhibit the movement of worms. The ratio of healthspan to lifespan is also regulated by how long the worm can prevent "causes of death" such as bacterial colonization in the intestine (Podshivalova et al., 2017). For the *daf-2* mutants, the prevention of bacterial colonization increases the time spent in "end-of-life decrepitude", which affects the proportion of time spent in gerospan versus healthspan (Podshivalova et al., 2017).

Insulin-signaling has also been implicated in the locomotor healthspan of *Drosophila*. Decreased expression of phosphoinositide-dependent kinase 1 (PDK1) was found to delay the progression of age-related locomotor impairments of adult flies (Jones et al., 2009). PDK1 acts downstream of phosphatidylinositol 3-kinase (PI3K) and upstream of AKT in the canonical insulin-signaling pathway (Jones et al., 2009).

5.1.3 Heat-shock factor involvement in locomotor healthspan and aging

The heat shock response is a cellular response to stressors such as heat stress, toxic chemicals, and oxidative stress (Morimoto, 1993). In response to these stressors, heat shock factor 1 (HSF1) induces the expression of a variety of molecular chaperones that aid protein folding (Hartl et al., 2011). There are various classes of heat shock proteins that are induced by HSF1, including Hsp100, Hsp90, Hsp70, Hsp60, Hsp40, and small heat shock proteins (Hartl et al., 2011).

Loss of *hsf-1* leads to a shortened lifespan in *C. elegans* (Hsu et al., 2003). *hsf-1* mutant worms also lose their locomotor function much quicker than wild-type worms (Rollins et al., 2017). These findings suggest that the maintenance of protein folding is not only important for longevity, but also for locomotor healthspan.

5.1.4 tRNA modifications are involved in optimal protein translataion

Transfer RNA, or tRNA, is an adaptor molecule involved in protein translation. tRNAs are charged with specific amino acids at its 3' end (Phizicky and Hopper, 2010). tRNA associates with codons of messenger RNA (mRNA) through its anticodon loop located at nucleotide positions 34, 35, and 36 (Phizicky and Hopper, 2010). When a uridine is present at the 34 position, it is frequently post-transcriptionally modified to allow wobble base pairing (Huang et al., 2005). The loss of wobble base pairing may lead to slower translation speeds and may affect the co-translational folding of the newly synthesized protein.

In yeast, the Elongator complex is required for the addition of methoxycarbonylmethyl (mcm) and carbamoylmethyl (ncm) modifications to the wobble uridine of tRNA (Huang et al., 2005). Following the mcm modification, some tRNAs can be further modified by thiolation (Huang et al., 2005). In yeast, thiolation is carried out by a

sulfur transfer pathway which requires Uba4, Urm1, Ncs2, and Ncs6 (Leidel et al., 2009). *tut-1*, the *C. elegans* ortholog of Ncs6, was found to be involved in wobble uridine thiolation in *C. elegans* (Chen et al., 2009a). The *tut-1(tm1297)* mutant worms lacked the mcm^5s^2U modification that is normally present in wild-type worms (Chen et al., 2009a).

In most cases, slower translation speeds promote proper protein folding. For example, slower translation rates promote proper folding of eukaryotic proteins in *E.coli* (Siller et al., 2010). However, some computational studies have indicated that fast translation speeds can increase the probability of proper co-translational folding by avoiding misfolded intermediate states (Wang et al., 2015). Therefore, slower translation speeds caused by loss of wobble uridine modifications may cause higher levels of misfolded proteins.

5.2 Materials and Methods

C. elegans strains

C. elegans Bristol strain N2 was used as wild-type. Animals were cultivated on NGM plates with *E. coli* strain OP50. All animals were maintained at 20°C. *C. elegans* strains CF1038 *daf-16(mu86) I,* PS3551 *hsf-1(sy441) I,* and TJ375 *hsp-16.2p::GFP* were obtained from the *Caenorhabditis* Genetic Center (University of Minnesota, MN, USA). *C. elegans* strain *tut-1(tm1297)* was obtained from the National BioResource Project (Japan). *elpc-2(ix243)* was isolated from this study.

Measurements of Maximum Speed and Total Distance Traveled

Described in Section 3.2 Material and Methods

Quantification of fluorescence

Fluorescence was quantified from images taken with confocal microscope LSM710 (Carl Zeiss, Oberkochen, Germany). A z-stack image was created from images taken at 1µm increments, encompassing the entire section of the worm. The fluorescence intensity was quantified using ImageJ software. A region of the head from the base of the pharynx to the tip of the nose was selected using the freehand selection tool. The built-in "Measure" tool was used to measure the fluorescence intensity from the image.

Genetic crosses

hsf-1(sy441);elpc-2(ix243), elpc-2(ix243);tut-1(tm1297), and *elpc-2(ix243);hsp-16.2*p*::GFP* double mutants were made by genetic crossing. The following primers were used to check whether a line carried a mutation site.

5' *hsf-1(sy441)* snp: 5'-agaaaattccgggaaaaactttcaagaagc-3'

3' *hsf-1(sy441)* snp: 5'-gcaatagaagatcagcatcatccaacgact-3'

5' *elpc-2* snp: 5'-aaatgaatttttcgccacaaaacccaaaaa-3'

3' *elpc-2* snp: 5'-ttcgcgaaaactctcgtagtctgatcctg-3'

5' *tut-1* del: 5'-gattttggttgaggctctcagaatttttgg-3'

3' *tut-1* del: 5'-agtaattcagatggaaaaacgccgaggac-3'

Application of heat shock

Worms were placed in a temperature-controlled incubator HB-100 (TAITEC, Saitama, Japan) set at 30°C for 3 h. The incubator was turned on 30 min before the worms were placed in the incubator to create a stable temperature setting.

Measurement of development time

Described in Section 3.2 Materials and Methods

5.3. Results

5.3.1 Adult locomotor function of *daf-16(mu86)* and *hsf-1(sy441)* worms

We tested the locomotor functions of *daf-16(mu86)* and *hsf-1(sy441)* mutant strains by measuring the maximum velocity and total travel distance of worms for one min on an agar plate without food. We did not see significant locomotor declines in the percent change in maximum velocity or travel distance for *daf-16(mu86)* worms compared to that of WT worms (Fig. 5.1A–D). Other studies have also found that locomotor function is not strongly affected in the *daf-16(mu86)* mutant during early adulthood (Hahm et al., 2015; Newell Stamper et al., 2018). *hsf-1(sy441)* worms showed significant reductions in maximum velocity and travel distance on all tested days and showed a significantly greater reduction in percent change in maximum velocity and travel distance from adult day 1 to 5 compared to WT worms (Fig. 5.1A–D). The *hsf-1* signaling pathway may be required during the maintenance of locomotor function beginning in early adulthood.

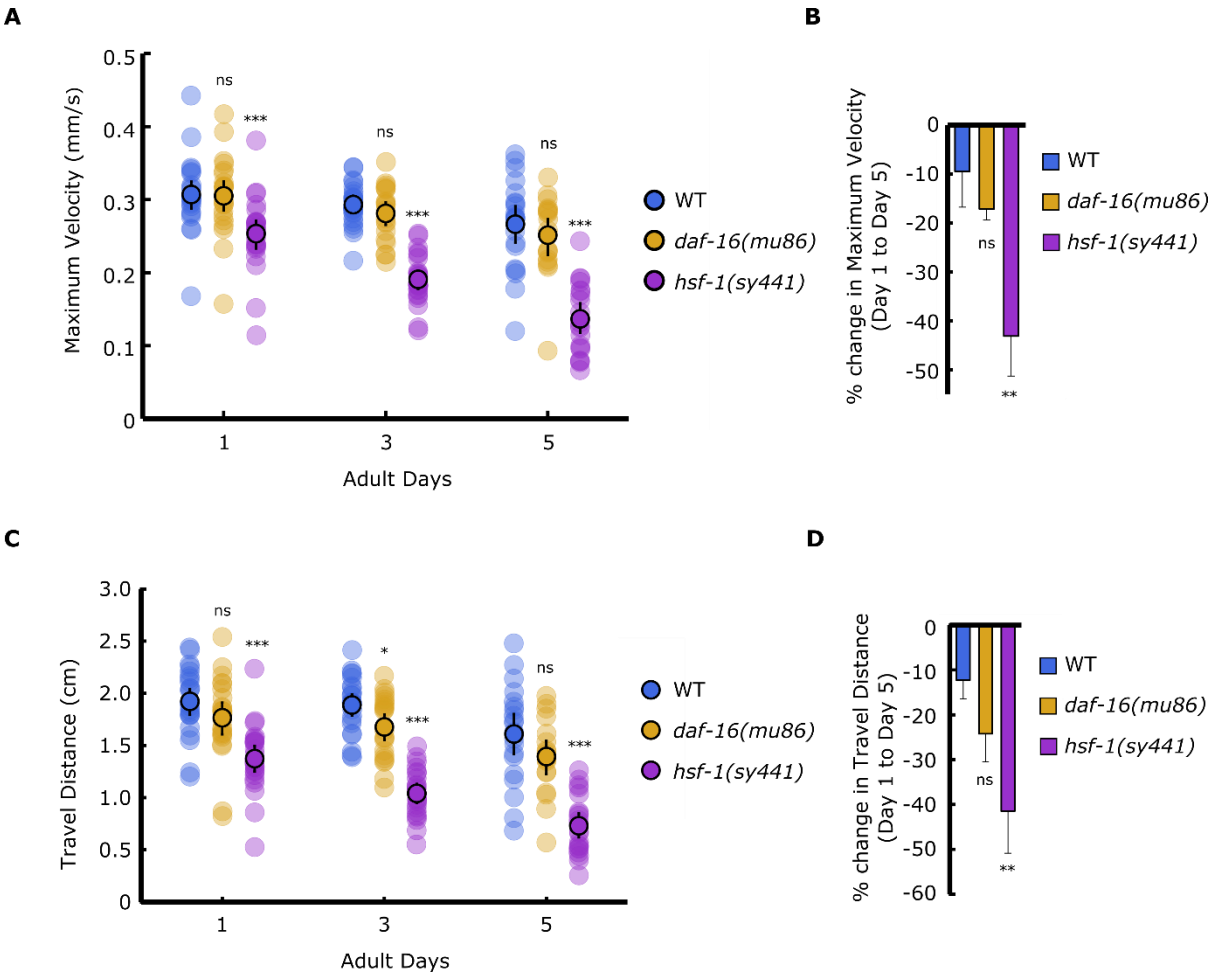

Figure 5.1 Locomotor function of known aging mutants

(A) Maximum velocities of WT, *daf-16(mu86)*, and *hsf-1(sy441)* mutants. (B) Percent change in maximum velocity of strains from A. (C) Travel distances of WT, *daf-16(mu86)*, and *hsf-1(sy441)* mutants. (D) Percent change in travel distance of strains from C. For maximum velocity and travel distance experiments, n = 30–45 worms per strain for each day (10–15 worms from 3 biological replicate plates). For percent change in maximum velocity and travel distance graphs, n = 3 biological replicate plates. Error bars indicate 95% confidence intervals. **P* < 0.05; ***P* < 0.01; ****P* < 0.001; ns, not significant; One-way ANOVA with Dunnett's post hoc test vs. WT.

5.3.2 Genetic interaction of *elpc-2(ix243)* with *hsf-1(sy441)*

The progressive declines in locomotor function of the *hsf-1(sy441)* mutant and the *elpc-2(ix243)* mutant occur during similar time frames (adult day 1 to 5). We wondered whether *elpc-2* and *hsf-1* work to maintain locomotor function by the same or independent mechanisms. If the two mutations cause locomotor deficits by independent mechanisms, the

hsf-1(sy441);elpc-2(ix243) double mutant should show more severe locomotor deficits than either of the single mutants. However, we observed no additive effects in the *hsf-1(sy441);elpc-2(ix243)* double mutant worms compared to the *hsf-1(sy441)* single mutant worms (Fig5.2A–D). This result suggests that the two mutations cause locomotor deficits by overlapping mechanisms. Another possibility is that the *elpc-2* mutation may lead to expression of a premature protein that may destabilize the whole Elongator complex and act as a seed for more widespread protein misfolding.

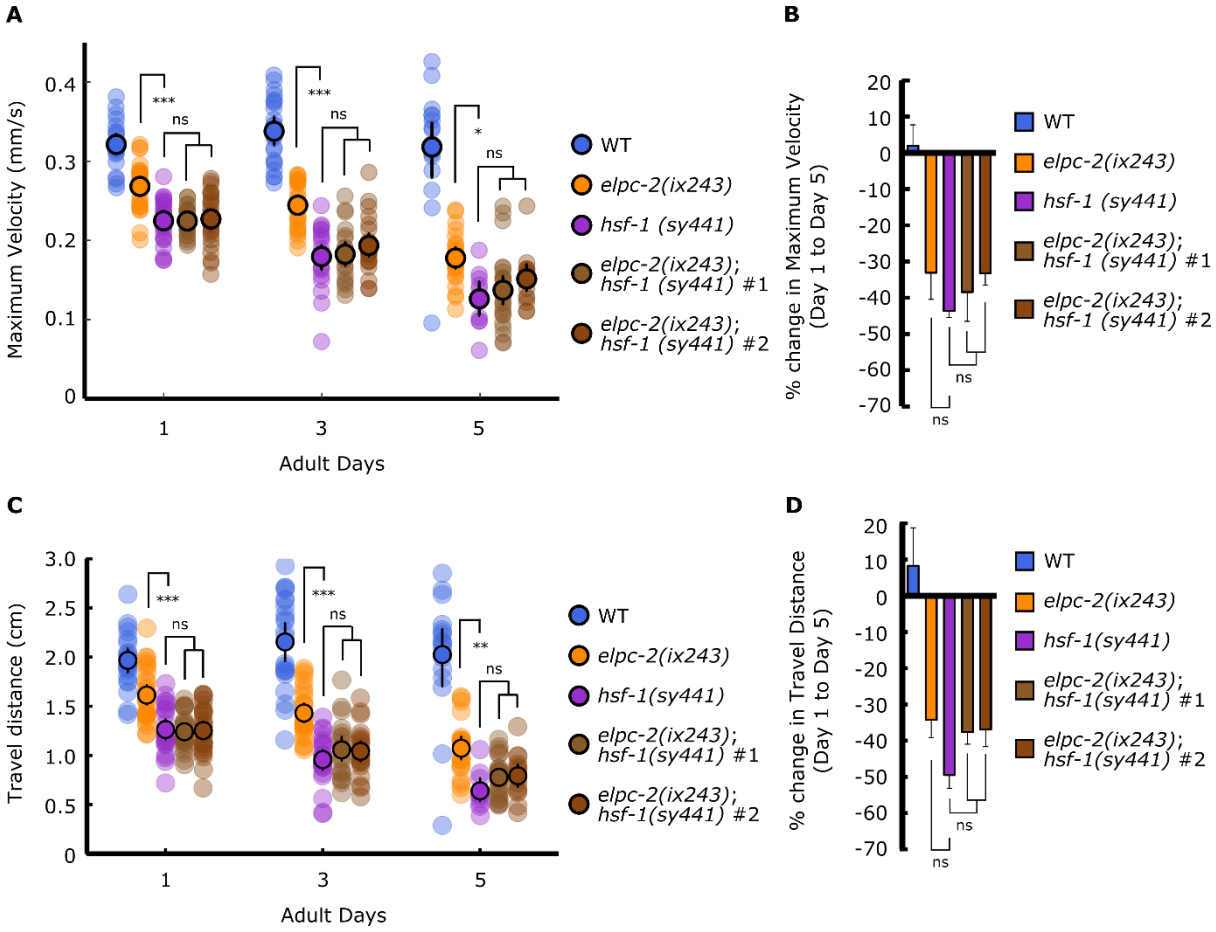

Figure 5.2 Locomotor function of *elpc-2(ix243);hsf-1(sy441)* double mutant worms

(A) Maximum velocities of WT, *elpc-2(ix243)*, *hsf-1(sy441)* and *elpc-2(ix243);hsf-1(sy441)* double mutant strains. (B) Percent change in maximum velocity of strains from left panel. (C) Travel distances of WT, *elpc-2(ix243)*, *hsf-1(sy441)* and *elpc-2(ix243);hsf-1(sy441)* double mutant strains. (D) Percent change in travel distance of strains from C. For maximum

velocity and travel distance experiments, n = 30–45 worms per strain for each day (10–15 worms from 3 biological replicate plates). For percent change in maximum velocity and travel distance graphs, n = 3 biological replicate plates. Error bars indicate 95% confidence intervals. *$P < 0.05$; **$P < 0.01$; ***$P < 0.001$; ns, not significant; One-way ANOVA with Tukey's post hoc test vs. WT.

5.3.3 Genetic interaction of *elpc-2(ix243)* with *tut-1(tm1297)*

In *C. elegans, elpc-1* and *elpc-3* have previously been reported to be involved in tRNA modifications (Chen et al., 2009a). tRNA modifications have been linked to protein folding by altering the speed of translation in yeast (Nedialkova and Leidel, 2015). We wondered whether other *C. elegans* tRNA modification mutants would cause progressive declines in locomotor function. TUT-1 also modifies the wobble uridine of tRNA by thiolation (Chen et al., 2009a). We measured the locomotor function of *tut-1(tm1297)* worms that are defective in tRNA thiolation. The *tut-1(tm1297)* mutant worms showed a significantly greater decline in locomotor function during adulthood compared to wild type (Fig. 5.3A–D).

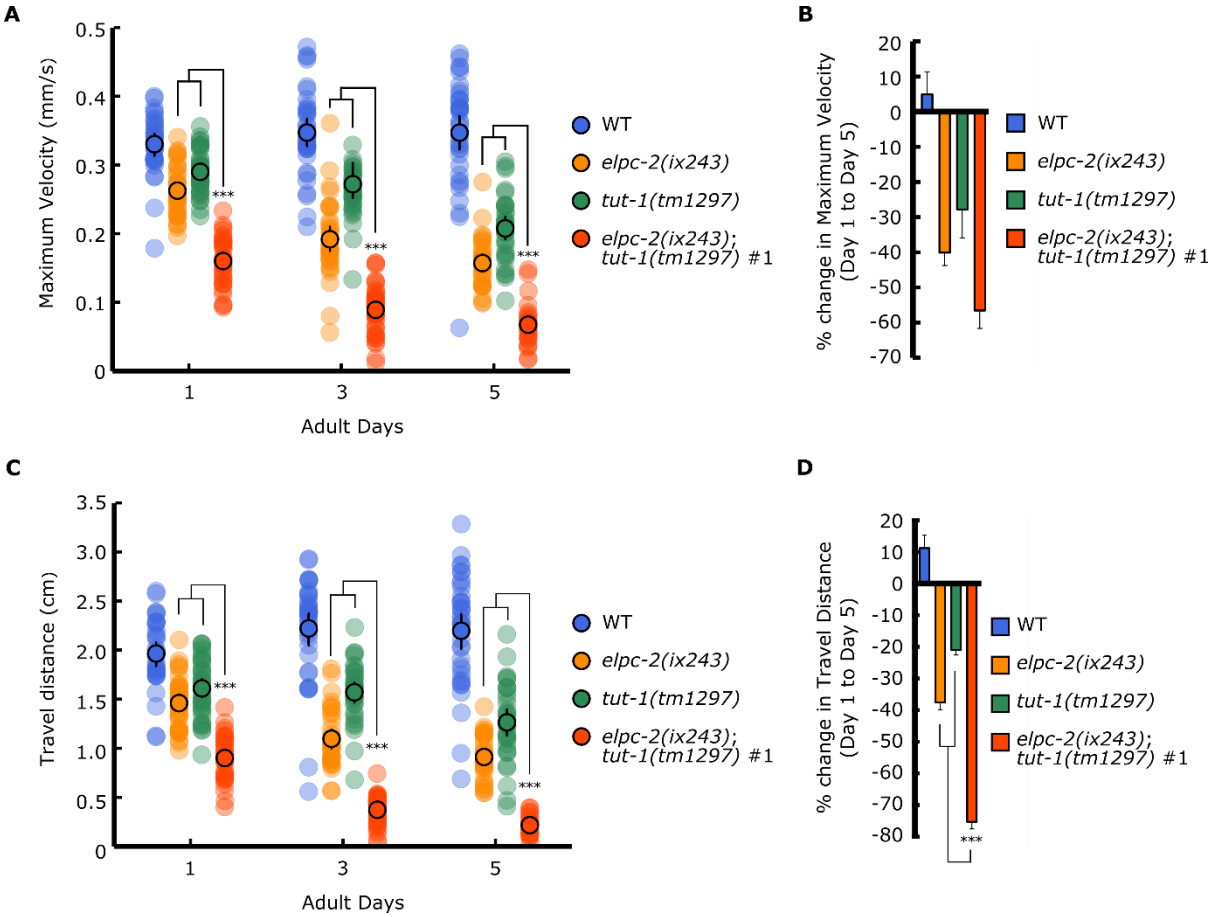

Figure 5.3 Locomotor function of *elpc-2(ix243);tut-1(tm1297)* double mutant worms

(A) Maximum velocities of WT, *elpc-2(ix243)*, *tut-1(tm1297)*, and *elpc-2(ix243);tut-1(tm1297)* double mutant strains. (B) Percent change in maximum velocity of strains from A. (B) Travel distances of WT, *elpc-2(ix243)*, *tut-1(tm1297)*, and *elpc-2(ix243);tut-1(tm1297)* double mutant strains. (D) Percent change in travel distance of strains from C. For maximum velocity and travel distance experiments, n = 30–45 worms per strain for each day (10–15 worms from 3 biological replicate plates). For percent change in maximum velocity and travel distance graphs, n = 3 biological replicate plates. Error bars indicate 95% confidence intervals. ***$P < 0.001$; One-way ANOVA with Tukey's post hoc test vs. WT.

The *elpc-2(ix243);tut-1(tm1297)* double mutant showed synthetic effects for development and locomotor function. The *elpc-2(ix243);tut-1(tm1297)* double mutant worms took almost double the time to reach adulthood (145.4 h) compared to the *elpc-2(ix243)* worms (80.2 h) or the *tut-1(tm1297)* worms (82.0 h) (Table 5.1). The *elpc-2(ix243);tut-*

1(tm1297) double mutant worms showed a significantly greater reduction in maximum velocity and travel distance from the first to fifth days of adulthood relative to either of the single mutants (Fig. 5.3A–D). These results suggest that *elpc-2*-dependent ncm and mcm modifications and *tut-1*-dependent thiolation of tRNA may have non-overlapping roles for both development and the maintenance of locomotor function.

Table 5.1 Development times of *tut-1(tm1297) and elpc-2(ix243);tut-1(tm1297)* mutants
Development time from egg to first egg-lay (n = 5 worms per strain).

Strain	Development Time (h)	% of WT
WT	70.4	100.0%
tut-1(tm1297)	82.0	116.5%
elpc-2(ix243);tut-1(tm1297)	145.4	206.5%

5.3.4 Induction of heat shock response is increased in *elpc-2(ix243)* worms

Since the Elongator complex has been reported to bind with RNA polymerase II, we wondered whether it may play a role in activating the heat shock response (Otero et al., 1999). We measured the induction of the heat shock response in *elpc-2(ix243)* worms that express *hsp16.2*p*::GFP*, a heat shock reporter. The ability to induce a heat shock response is not compromised in the *elpc-2(ix243)* mutant, with *elpc-2(ix243)* worms showing a greater induction of the heat shock reporter (Fig. 5.4A, B). This may indicate that ELPC-2 is a negative regulator of the heat shock response, or that loss of ELPC-2 may cause a larger burden of misfolded proteins, and require a higher expression level of molecular chaperones. In support of the latter possibility, yeast strains with mutations in the Elongator complex accumulated a higher level of misfolded proteins and expressed a higher level of heat shock response proteins (Nedialkova and Leidel, 2015).

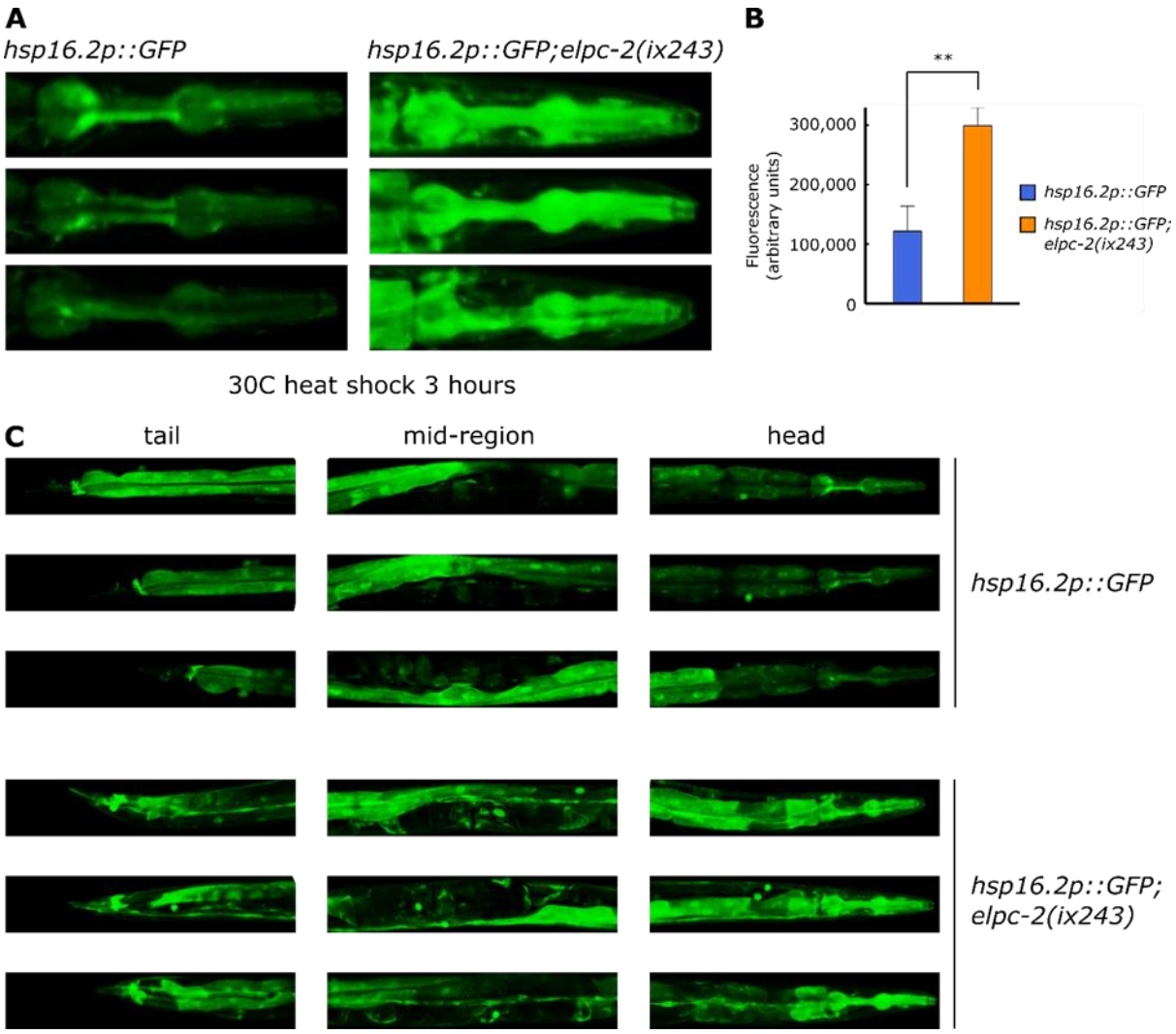

Figure 5.4 *hsp16.2*p*::GFP* reporter expression after 30C 3-h heat shock

(A) Images of *hsp16.2*p*::GFP* and *hsp16.2*p*::GFP;elpc-2(ix243)* worms after 3-h heat shock at 30°C. (B) Quantification of fluorescence intensity of *hsp16.2*p*::GFP* and *hsp16.2*p*::GFP;elpc-2(ix243)* worms (n = 3 worms per strain). ***P* < 0.01; Unpaired Student's *t* test.

5.3.5 Increased heat shock response in aged *elpc-2(ix243)* worms

Aged *elpc-2(ix243)* mutants without heat shock showed some expression of the *hsp16.2*p*::GFP* reporter in muscles and neurons (Fig. 5.5A, B). This may indicate that misfolded proteins are accumulating in the *elpc-2(ix243)* mutant even in the absence of heat

stress. *elpc-2(ix243);Ex[elpc-2(+)]* worms that carried a WT version of *elpc-2* showed minimal expression of the *hsp16.2*p*::GFP* reporter (Fig. 5.5A, B).

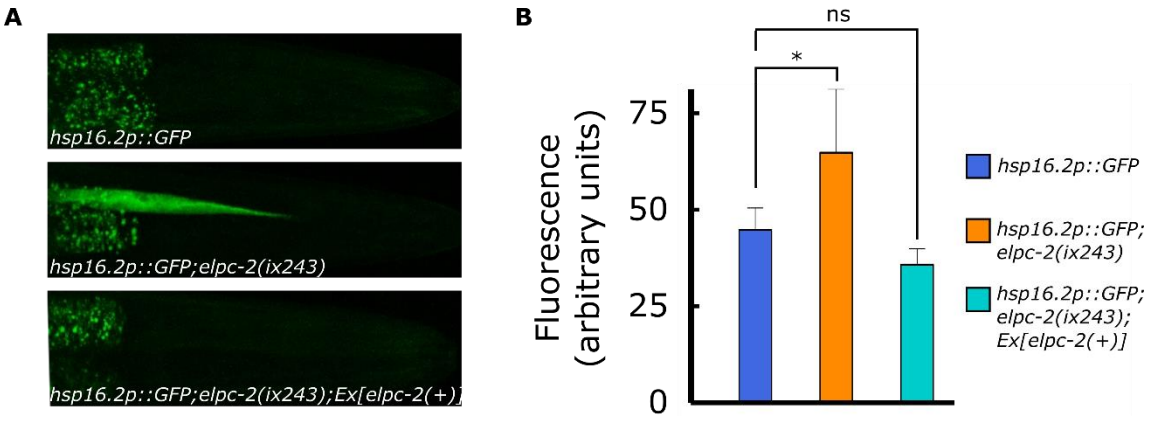

Figure 5.5 Induction of heat shock response in non-heat shocked, aged animals
(A) Representative images of *hsp16.2*p*::GFP, hsp16.2*p*::GFP;elpc-2(ix243),* and *hsp16.2*p*::GFP;elpc-2(ix243);Ex[elpc-2(+)]* worms on adult day 5. (B) Maximum fluorescence intensity of head region for *hsp16.2*p*::GFP, hsp16.2*p*::GFP;elpc-2(ix243),* and *hsp16.2*p*::GFP;elpc-2(ix243);Ex[elpc-2(+)]* worms on adult day 5 (n = 7 worms per strain). **P* < 0.05; One-way ANOVA with Dunnett's post hoc test vs. WT.

5.4. Discussion

5.4.1. *elpc-2* and *hsf-1* mutations cause progressive locomotor decline by an overlapping mechanism

The *hsf-1(sy441);elpc-2(ix243)* double mutant did not show additive effects for the progressive decline in locomotor function compared to the single *hsf-1(sy441)* mutant. This suggests that the mechanism of locomotor decline in both mutants may overlap. Another possibility is that the *elpc-2(ix243)* mutation may lead to destabilization of the Elongator complex, and denaturation of the entire protein complex. This misfolded protein complex may act as a seed to trigger the misfolding of other proteins. In either case, a greater burden of misfolded proteins are likely present in the *elpc-2(ix243)* mutant.

Since the *hsf-1(sy441)* mutant shows more deficits on the first day of adulthood, loss of protein chaperones downstream of HSF-1 may have a stronger requirement for development compared to the developmental requirement of the Elongator complex. tRNA modifications may partially contribute to disruptions in proteostasis, but complete loss of the heat shock response may cause a stronger effect on proteostasis. The greater requirement for *hsf-1* for proteostasis may explain why the *hsf-1(sy441)* worms show greater deficits in locomotor function on the first day of adulthood.

The Elongator complex was originally discovered as a protein complex bound to RNA polymerase II (Otero et al., 1999). Therefore, we wondered whether the non-additive effects seen in the *hsf-1(sy441);elpc-2(ix243)* mutant strain may be due to the Elongator complex's involvement in the activation of the heat shock response. However, loss of *elpc-2* did not reduce the expression of the *hsp16.2*p*::GFP* heat shock response reporter. On the contrary, *elpc-2(ix243)* mutant worms showed a stronger induction of the heat shock response. This result suggests that there may be an increased burden of misfolded proteins in the *elpc-2(ix243)* worms. Aged *elpc-2(ix243)* worms also showed greater expression of the *hsp16.2*p*::GFP* heat shock response reporter. Aged states may reflect similar cellular burdens as heat stressed states.

The shared effects on protein folding may explain why the *hsf-1(sy441);elpc-2(ix243)* double mutant worms did not show any additive effects compared to the single *hsf-1(sy441)* mutant as measured by the percent change in maximum velocity and total travel distance. However, *hsf-1(sy441)* worms showed a reduced locomotor ability on the first, third and fifth days of adulthood as measured by maximum velocity and travel distance. Therefore, loss of *hsf-1* may have greater effects in terms of development of the neuromuscular system compared to loss of *elpc-2*.

5.4.2. tRNA modifications may be involved in maintenance of locomotor healthspan

In addition to the Elongator complex, Urm1p was also found to modify tRNA on the wobble uridine of tRNA in yeast (Leidel et al., 2009). TUT-1, the ortholog of URM1 in *C. elegans,* also thiolates tRNA on the wobble uridine (Chen et al., 2009a). Similar to the *C. elegans elpc* mutants, we observed that *tut-1(tm1297)* mutant worms are unable to maintain lcoomotor function during adulthood. tRNA modifications may be an important mechanism to maintain locomotor function of *C. elegans* during adulthood.

The *elpc-2(ix243);tut-1(tm1297)* double mutant showed a strong delay in development to adulthood, and also showed additive effects in the progressive decline of locomotor function. These additive effects suggest that loss of both *elpc-2* and *tut-1* is strongly detrimental for development. Loss of ncm and mcm tRNA modifications may be somewhat buffered by the presence of tRNA modification by thiolation and vice versa. In wild-type *C. elegans* worms, ncm^5U and mcm^5s^2U nucleosides were detected (Chen et al., 2009a). In *elpc-1(tm2149)* and *elpc-3(tm3120)* mutant worms, neither ncm^5U nor mcm^5s^2U were detected (Chen et al., 2009a). Instead, s^2U nucleosides, which are not present in wild-type worms, were detected in *elpc* mutants (Chen et al., 2009a). The presence of the s^2U nucleoside may partially rescue the negative effects from loss of the mcm^5s^2U nucleoside. In *elpc-1(tm2149);tut-1(tm1297)* worms, no ncm^5U, mcm^5s^2U, or s^2U nucleosides were present (Chen et al., 2009a). The loss of the partially functional s^2u nucleoside may cause the severe developmental delay and strong progressive decline in locomotor function of the *elpc-1(tm2149);tut-1(tm1297)* worms.

Alternatively, *tut-1* may have different functions outside of tRNA modifications that may negatively affect the development and locomotor function of worms during adulthood.

The *elpc-2(ix243)* worms show a reduced maximum velocity on adult day 1, 3 and 5 compared to *tut-1(tm1297)* worms. However, the percent change in maximum velocity is not significantly different between *elpc-2(ix243)* and *tut-1(tm1297)* worms. This result indicates that the developmental requirement for *elpc-2* may be stronger than that of *tut-1*.

Studies using *elpc-1* and *elpc-3* mutants have observed deficits in a salt chemotaxis learning and memory assay (Chen et al., 2009a). There may be general neural dysfunctions from loss of the Elongator complex. Interestingly, *tut-1(tm1297)* worms did not show the deficit in salt chemotaxis learning (Chen et al., 2009a). This suggests that the Elongator complex and *tut-1* pathway may have some non-overlapping roles.

From the phenotypic analysis of the *elpc, tut-1*, and *hsf-1* mutants, we propose a working model where the Elongator complex and TUT-1 pathway modify tRNA at the wobble uridine position to optimize translation speeds, and works together with the HSF-1 pathway to maintain proteostasis and locomotor healthspan (Fig. 5.6).

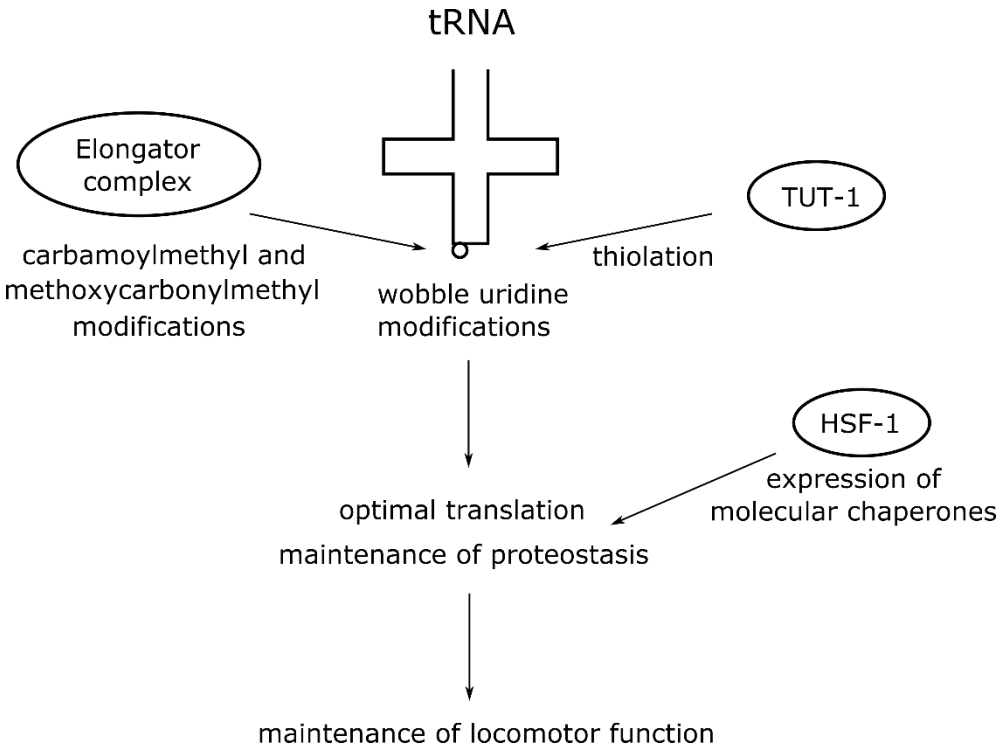

Figure 5.6 Working model of Elongator, TUT-1 and HSF-1 involvement in locomotor healthspan

6. Concluding remarks

To our knowledge, this is the first unbiased forward genetic screen for progressive decline in locomotor function in *C. elegans.* In order to carry out the screen, we developed the Edge Assay to measure the locomotor function of many worms at once. The Edge Assay may be a useful assay to quickly test the locomotor function of populations of worms for future genetic screens.

The isolated mutants from our screen demonstrate progressive declines in locomotor function from inherited mutations. The mutants are valuable tools to explore how an inherited mutation can have delayed onset of toxic effects. In the first mutant we analyzed, we identified a mutation in *elpc-2,* and found that the Elongator complex is a required protein complex to maintain locomotor healthspan in *C. elegans.* The Elongator complex has minimal requirements for the development of the *C. elegans* locomotor circuit, but is required to maintain the functional capacity of the neuromuscular system during adulthood.

The second mutant we analyzed carries a mutation in *dys-1,* but further experiments are needed to determine whether other mutations may be involved in the progressive decline in locomotor function. Future characterization of the second mutant strain may provide insights into mechanisms that affect the toxic effects of the *dys-1* mutation. In this case, findings may be applicable to understanding pathogenesis of Duchenne and Becker muscular dystrophies.

Similar to how gene-environment interactions are important to understand an individual organism's phenotype, the study of mutation-environment interactions may help us understand the phenomenon of a delayed onset of toxic symptoms. Some mutations may possibly be characterized as "aging-sensitive mutations" which can be considered analogous to temperature-sensitive mutations that are well-characterized in bacteria, yeast, *C. elegans,*

and *Drosophila* (Gordon and King, 1994; Grigliatti et al., 1973; Lovato et al., 2009; Lowry et al., 2015). For temperature-sensitive mutations, a mutation is present, but not toxic at permissive temperatures. However, when a certain temperature is reached, the mutation exerts its toxic effects. An aging-sensitive mutation could be any mutation or single nucleotide polymorphism that exerts an increased level of toxic effects due to aging or adulthood (Fig. 6.1).

In support of this model, temperature-sensitive misfolding mutations in paramyosin are induced into misfolded states in the presence of poly-glutamine proteins (Gidalevitz, 2006). Temperature-sensitive misfolding mutations in paramyosin and myosin are more prone to aggregation in aged worms (Ben-Zvi et al., 2009). Many temperature-sensitive mutations may therefore also be aging-sensitive mutations.

In future studies, we would like to characterize how genetic and environmental manipulations of aging can affect the toxicity of the *elpc* mutants and other mutants that show a progressive decline in locomotor function. It is especially advantageous to study mutation-environment interactions in *C. elegans* due to the short lifespan and well-studied genetic regulators of lifespan and aging. A collapse in proteostasis has been reported to occur during early adulthood in *C. elegans* (Labbadia and Morimoto, 2014b), Many aging-sensitive mutations may be triggered into toxicity during this period. We believe that the isolated mutants from our screen may serve as tools to study of how inherited mutations can lead to a delayed onset of toxicity, whether through gradual accumulation of damage, or through an interaction with changes related to aging or adulthood.

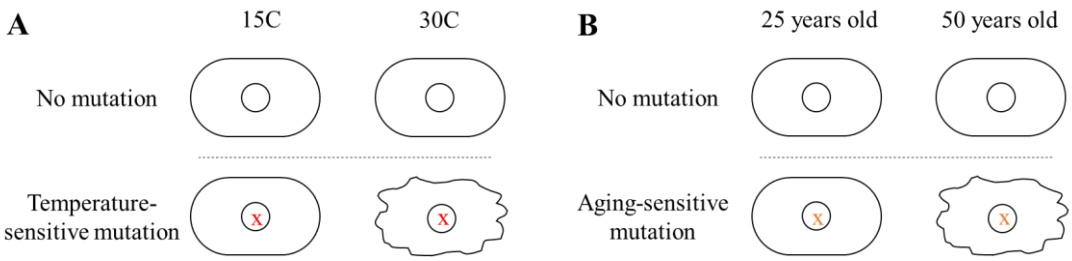

Figure 6.1 Mutation-environment interactions

(A) Simplified image of temperature-sensitive mutation. (B) Simplified image of aging-sensitive mutation.

Potential ways to improve healthspan is of great interest in a society in which the average lifespan is increasing. Understanding the genetic and environmental factors that maintain healthspan may provide clues for improving healthspan. Loss-of-function or reduction-of-function mutations in the Elongator complex leads to various types of disease (Cohen et al., 2015; Rubin and Anderson, 2017; Strug et al., 2009), and reduced expression of ELP3 can exacerbate the disease progression of ALS (Bento-Abreu et al., 2018). This indicates that the Elongator complex in some cases may be the causative mutation for disease, while in other contexts, it can alter the toxicity of other mutations. From our study, we find that the whole Elongator protein complex is required for the maintenance of locomotor function in *C. elegans.* The Elongator complex may become a promising target for therapeutic approaches to maintain healthspan in animals.

7. References

Anderson, S.L., Coli, R., Daly, I.W., Kichula, E.A., Rork, M.J., Volpi, S.A., Ekstein, J., and Rubin, B.Y. (2001). Familial Dysautonomia Is Caused by Mutations of the IKAP Gene. Am. J. Hum. Genet. *68*, 753–758.

Andresen, J.M., Gayán, J., Djoussé, L., Roberts, S., Brocklebank, D., Cherny, S.S., Cardon, L.R., Gusella, J.F., MacDonald, M.E., Myers, R.H., et al. (2007). The relationship between CAG repeat length and age of onset differs for Huntington's disease patients with juvenile onset or adult onset. Ann. Hum. Genet. *71*, 295–301.

Aroian, R. V, Koga, M., Mendel, J.E., Ohshima, Y., and Sternberg, P.W. (1990). The let-23 gene necessary for Caenorhabditis elegans vulval induction encodes a tyrosine kinase of the EGF receptor subfamily. Nature *348*, 693–699.

Bansal, A., Zhu, L.J., Yen, K., and Tissenbaum, H.A. (2015). Uncoupling lifespan and healthspan in *Caenorhabditis elegans* longevity mutants. Proc. Natl. Acad. Sci. U. S. A. *112*, E277-286.

Ben-Zvi, A., Miller, E.A., and Morimoto, R.I. (2009). Collapse of proteostasis represents an early molecular event in *Caenorhabditis elegans* aging. Proc. Natl. Acad. Sci. U. S. A. *106*, 14914–14919.

Bento-Abreu, A., Jager, G., Swinnen, B., Rué, L., Hendrickx, S., Jones, A., Staats, K.A., Taes, I., Eykens, C., Nonneman, A., et al. (2018). Elongator subunit 3 (ELP3) modifies ALS through tRNA modification. Hum. Mol. Genet. *27*, 1276–1289.

Bessou, C., Giugia, J., and Franks, C. (1998). Mutations in the Caenorhabditis elegans dystrophin-like gene dys-1 lead to hyperactivity and suggest a link with cholinergic transmission. Neurogenetics *261*, 102–115.

Blankenberg, D., Kuster, G. Von, Coraor, N., Ananda, G., Lazarus, R., Mangan, M., Nekrutenko, A., and Taylor, J. (2010). Galaxy: A web-based genome analysis tool for experimentalists. Curr. Protoc. Mol. Biol. 1–21.

Boal, A.K., Grove, T.L., McLaughlin, M.I., Yennawar, N.H., Booker, S.J., and Rosenzweig, A.C. (2011). Structural basis for methyl transfer by a radical SAM enzyme. Science (80-.). *332*, 1089–1092.

Bolukbasi, E., Vass, S., Cobbe, N., Nelson, B., Simossis, V., Dunbar, D.R., and Heck, M.M.S. (2012). Drosophila poly suggests a novel role for the Elongator complex in insulin receptor-target of rapamycin signalling. Open Biol. *2*, 110031.

Brenner, S. (1974). *Caenorhabditis elegans*. Genetics *77*, 71–94.

Bruijn, L.I., Miller, T.M., and Cleveland, D.W. (2004). Unraveling the mechanisms involved in motor neuron degeneration in ALS. Annu. Rev. Neurosci. *27*, 723–749.

Burch, J.B., Augustine, A.D., Frieden, L.A., Hadley, E., Howcroft, T.K., Johnson, R., Khalsa, P.S., Kohanski, R.A., Li, X.L., MacChiarini, F., et al. (2014). Advances in geroscience: Impact on healthspan and chronic disease. Journals Gerontol. - Ser. A Biol. Sci. Med. Sci. *69*, 1–3.

Calixto, A., Chelur, D., Topalidou, I., Chen, X., and Chalfie, M. (2010). Enhanced neuronal RNAi in C. elegans using SID-1. Nat. Methods *7*, 554–559.

Cesari, M., Pahor, M., Lauretani, F., Zamboni, V., Bandinelli, S., Bernabei, R., Guralnik, J.M., and Ferrucci, L. (2009). Skeletal muscle and mortality results from the InCHIANTI study. Journals Gerontol. - Ser. A Biol. Sci. Med. Sci. *64*, 377–384.

Chen, C., Tuck, S., and Byström, A.S. (2009a). Defects in tRNA Modification Associated with Neurological and Developmental Dysfunctions in *Caenorhabditis elegans* Elongator

Mutants. PLoS Genet. *5*, e1000561.

Chen, Y.-T., Hims, M.M., Shetty, R.S., Mull, J., Liu, L., Leyne, M., and Slaugenhaupt, S.A. (2009b). Loss of Mouse Ikbkap, a Subunit of Elongator, Leads to Transcriptional Deficits and Embryonic Lethality That Can Be Rescued by Human IKBKAP. Mol. Cell. Biol. *29*, 736–744.

Cingolani, P., Platts, A., Wang, L.L., Coon, M., Nguyen, T., Wang, L., Land, S.J., Lu, X., and Ruden, D.M. (2012). A program for annotating and predicting the effects of single nucleotide polymorphisms, SnpEff: SNPs in the genome of *Drosophila melanogaster* strain *w* 1118; *iso-2*; *iso-3*. Fly (Austin). *6*, 80–92.

Cirulli, E.T., Lasseigne, B.N., Petrovski, S., Sapp, P.C., Dion, P.A., Leblond, C.S., Couthouis, J., Lu, Y.-F., Wang, Q., Krueger, B.J., et al. (2015). Exome sequencing in amyotrophic lateral sclerosis identifies risk genes and pathways. Science (80-.).

Cohen, E., Bieschke, J., Perciavalle, R.M., Kelly, J.W., and Dillin, A. (2006). Opposing activities protect against age-onset proteotoxicity. Science *313*, 1604–1610.

Cohen, J.S., Srivastava, S., Farwell, K.D., Lu, H.M., Zeng, W., Lu, H., Chao, E.C., and Fatemi, A. (2015). ELP2 is a novel gene implicated in neurodevelopmental disabilities. Am. J. Med. Genet. Part A *167*, 1391–1395.

Cong, L., Ran, F.A., Cox, D., Lin, S., Barretto, R., Habib, N., Hsu, P.D., Wu, X., Jiang, W., Marraffini, L.A., et al. (2013). Multiplex genome engineering using CRISPR/Cas systems. Science *339*, 819–823.

Coovert, D.D., Le, T.T., McAndrew, P.E., Strasswimmer, J., Crawford, T.O., Mendell, J.R., Coulson, S.E., Androphy, E.J., Prior, T.W., and Burghes, A.H.M. (1997). The survival motor neuron protein in spinal muscular atrophy. Hum. Mol. Genet. *6*, 1205–1214.

Creppe, C., and Buschbeck, M. (2011). Elongator: an ancestral complex driving transcription and migration through protein acetylation. J. Biomed. Biotechnol. *2011*, 924898.

D'Amico, A., Mercuri, E., Tiziano, F.D., and Bertini, E. (2011). Spinal muscular atrophy. Orphanet J. Rare Dis. *6*, 71.

Dalakas, M.C., and Hohlfeld, R. (2003). Polymyositis and dermatomyositis. Lancet *362*, 971–982.

Dauden, M.I., Kosinski, J., Kolaj- Robin, O., Desfosses, A., Ori, A., Faux, C., Hoffmann, N.A., Onuma, O.F., Breunig, K.D., Beck, M., et al. (2017). Architecture of the yeast Elongator complex. EMBO Rep. *18*, 264–279.

Dietrich, P., Yue, J., Shuyu, E., and Dragatsis, I. (2011). Deletion of exon 20 of the familial dysautonomia gene ikbkap in mice causes developmental delay, cardiovascular defects, and early embryonic lethality. PLoS One *6*, 1–10.

Doitsidou, M., Poole, R.J., Sarin, S., Bigelow, H., and Hobert, O. (2010). C. elegans mutant identification with a one-step whole-genome-sequencing and SNP mapping strategy. PLoS One *5*, 1–7.

Elden, A.C., Kim, H.-J., Hart, M.P., Chen-Plotkin, A.S., Johnson, B.S., Fang, X., Armakola, M., Geser, F., Greene, R., Lu, M.M., et al. (2010). Ataxin-2 intermediate-length polyglutamine expansions are associated with increased risk for ALS. Nature *466*, 1069.

Ewald, C.Y., Castillo-Quan, J.I., and Blackwell, T.K. (2018). Untangling Longevity, Dauer, and Healthspan in Caenorhabditis elegans Insulin/IGF-1-Signalling. Gerontology *64*, 96–104.

Friedman, D.B., and Johnson, T.E. (1988). A Mutation in the *age-1* Gene in *Caenorhabditis elegans* Lengthens Life and Reduces Hermaphrodite Fertility. Genetics *118*, 75–86.

Garcia-Valles, R., Gomez-Cabrera, M., Rodriguez-Mañas, L., Garcia-Garcia, F.J., Diaz, A.,

Noguera, I., Olaso-Gonzalez, G., and Viña, J. (2013). Life-long spontaneous exercise does not prolong lifespan but improves health span in mice. Longev. Heal. *2*, 14.

Giardine, B., Riemer, C., Hardison, R.C., Burhans, R., Elnitski, L., Shah, P., Zhang, Y., Blankenberg, D., Albert, I., Taylor, J., et al. (2005). Galaxy: A platform for interactive large-scale genome analysis. Genome Res. *15*, 1451–1455.

Gidalevitz, T. (2006). Progressive Disruption of Cellular Protein Folding in Models of Polyglutamine Diseases. Science (80-.). *311*, 1471–1474.

Gidalevitz, T., Krupinski, T., Garcia, S., and Morimoto, R.I. (2009). Destabilizing protein polymorphisms in the genetic background direct phenotypic expression of mutant SOD1 toxicity. PLoS Genet. *5*, e1000399.

Gieseler, K., Grisoni, K., and Ségalat, L. (2000). Genetic suppression of phenotypes arising from mutations in dystrophin-related genes in Caenorhabditis elegans. Curr. Biol. *10*, 1092–1097.

Gil, J.M., and Rego, A.C. (2008). Mechanisms of neurodegeneration in Huntington's disease. Eur. J. Neurosci. *27*, 2803–2820.

Glass, C.K., Saijo, K., Winner, B., Marchetto, M.C., and Gage, F.H. (2010). Mechanisms underlying inflammation in neurodegeneration. Cell *140*, 918–934.

Goecks, J., Nekrutenko, A., and Taylor, J. (2010). Galaxy: a comprehensive approach for supporting accessible, reproducible, and transparent computational research in the life sciences. Genome Biol. *11*, R86.

Gönczy, P., Echeverri, C., Oegema, K., Coulson, A., Jones, S.J., Copley, R.R., Duperon, J., Oegema, J., Brehm, M., Cassin, E., et al. (2000). Functional genomic analysis of cell division in C. elegans using RNAi of genes on chromosome III. Nature *408*, 331–336.

Gonzalez-Freire, M., de Cabo, R., Studenski, S.A., and Ferrucci, L. (2014). The neuromuscular junction: Aging at the crossroad between nerves and muscle. Front. Aging Neurosci. *6*, 1–11.

Gordon, C.L., and King, J. (1994). Genetic properties of temperature-sensitive folding mutants of the coat protein of phage P22. Genetics *136*, 427–438.

Grigliatti, T.A., Hall, L., Rosenbluth, R., and Suzuki, D.T. (1973). Temperature-sensitive mutations in Drosophila melanogaster. MGG Mol. Gen. Genet. *120*, 107–114.

Grotewiel, M.S., Martin, I., Bhandari, P., and Cook-Wiens, E. (2005). Functional senescence in *Drosophila melanogaster*. Ageing Res. Rev. *4*, 372–397.

Hahm, J.-H., Kim, S., DiLoreto, R., Shi, C., Lee, S.-J. V., Murphy, C.T., and Nam, H.G. (2015). *C. elegans* maximum velocity correlates with healthspan and is maintained in worms with an insulin receptor mutation. Nat. Commun. *6*, 8919.

van Ham, T.J., Holmberg, M. a., van der Goot, A.T., Teuling, E., Garcia-Arencibia, M., Kim, H.E., Du, D., Thijssen, K.L., Wiersma, M., Burggraaff, R., et al. (2010). Identification of MOAG-4/SERF as a regulator of age-related proteotoxicity. Cell *142*, 601–612.

Hartl, F.U., Bracher, A., and Hayer-Hartl, M. (2011). Molecular chaperones in protein folding and proteostasis. Nature *475*, 324–332.

Hedgecock, E.M., Sulston, J.E., and Thomson, J.N. (1983). Mutations affecting programmed cell deaths in the nematode Caenorhabditis elegans. Science (80-.). *220*, 1277–1279.

Herndon, L. a, Schmeissner, P.J., Dudaronek, J.M., Brown, P. a, Listner, K.M., Sakano, Y., Paupard, M.C., Hall, D.H., and Driscoll, M. (2002). Stochastic and genetic factors influence tissue-specific decline in ageing C. elegans. Nature *419*, 808–814.

Heron, M.P. (2013). Deaths: leading causes for 2010.

Hims, M.M., Ibrahim, E.C., Leyne, M., Mull, J., Liu, L., Lazaro, C., Shetty, R.S., Gill, S., Gusella, J.F., Reed, R., et al. (2007). Therapeutic potential and mechanism of kinetin as a treatment for the human splicing disease familial dysautonomia. J. Mol. Med. *85*, 149–161.

Hoffman, E.P., Brown, R.H., and Kunkel, L.M. (1987). Dystrophin: The protein product of the duchenne muscular dystrophy locus. Cell *51*, 919–928.

Hsu, A.-L., Murphy, C.T., and Kenyon, C. (2003). Regulation of aging and age-related disease by DAF-16 and heat-shock factor. Science *300*, 1142–1145.

Huang, B., Johansson, M.J.O., and Byström, A.S. (2005). An early step in wobble uridine tRNA modification requires the Elongator complex. RNA *11*, 424–436.

Iwasa, H., Yu, S., Xue, J., and Driscoll, M. (2010). Novel EGF pathway regulators modulate *C. elegans* healthspan and lifespan via EGF receptor, PLC-γ, and IP3R activation. Aging Cell *9*, 490–505.

Jones, M.A., Gargano, J.W., Rhodenizer, D., Martin, I., Bhandari, P., and Grotewiel, M. (2009). A forward genetic screen in Drosophila implicates insulin signaling in age-related locomotor impairment. Exp. Gerontol. *44*, 532–540.

Jorgensen, E.M., and Mango, S.E. (2002). The art and design of genetic screens: caenorhabditis elegans. Nat. Rev. Genet. *3*, 356–369.

Joseph, B.B., Blouin, N.A., and Fay, D.S. (2018). Use of a Sibling Subtraction Method for Identifying Causal Mutations in *Caenorhabditis elegans* by Whole-Genome Sequencing. G3 (Bethesda). *8*, 669–678.

Justice, J.N., Carter, C.S., Beck, H.J., Gioscia-Ryan, R.A., McQueen, M., Enoka, R.M., and Seals, D.R. (2014). Battery of behavioral tests in mice that models age-associated changes in human motor function. Age (Omaha). *36*, 583–595.

Kaeberlein, M. (2018). How healthy is the healthspan concept? GeroScience *40*, 361–364.

Kashyap, L., Perera, S., and Fisher, A.L. (2012). Identification of novel genes involved in sarcopenia through RNAi screening in Caenorhabditis elegans. J. Gerontol. A. Biol. Sci. Med. Sci. *67*, 56–65.

Kazemi-Esfarjani, P., and Benzer, S. (2000). Genetic suppression of polyglutamine toxicity in Drosophila. Science *287*, 1837–1840.

Kenyon, C., Chang, J., Gensch, E., Rudner, A., and Tabtiang, R. (1993). A C. elegans mutant that lives twice as long as wild type. Nature *366*, 461–464.

Kimura, K.D., Tissenbaum, H.A., Liu, Y., and Ruvkun, G. (1997). *daf-2*, an insulin receptor-like gene that regulates longevity and diapause in *Caenorhabditis elegans*. Science *277*, 942–946.

Klass, M.R. (1983). A method for the isolation of longevity mutants in the nematode *Caenorhabditis elegans* and initial results. Mech. Ageing Dev. *22*, 279–286.

Koboldt, D.C., Chen, K., Wylie, T., Larson, D.E., McLellan, M.D., Mardis, E.R., Weinstock, G.M., Wilson, R.K., and Ding, L. (2009). VarScan: Variant detection in massively parallel sequencing of individual and pooled samples. Bioinformatics *25*, 2283–2285.

Koenig, M., Beggs, A.H., Moyer, M., Scherpf, S., Heindrich, K., Bettecken, T., Meng, G., Müller, C.R., Lindlöf, M., Kaariainen, H., et al. (1989). The molecular basis for Duchenne versus Becker muscular dystrophy: correlation of severity with type of deletion. Am. J. Hum. Genet. *45*, 498–506.

Labbadia, J., and Morimoto, R.I. (2014a). The Biology of Proteostasis in Aging and Disease. Annu. Rev. Biochem. *84*, 150317182619002.

Labbadia, J., and Morimoto, R.I. (2014b). Proteostasis and longevity: when does aging really

begin? F1000Prime Rep. *6*, 7.

Leidel, S., Pedrioli, P.G.A., Bucher, T., Brost, R., Costanzo, M., Schmidt, A., Aebersold, R., Boone, C., Hofmann, K., and Peter, M. (2009). Ubiquitin-related modifier Urm1 acts as a sulphur carrier in thiolation of eukaryotic transfer RNA. Nature *458*, 228–232.

Leinwand, S.G., Yang, C.J., Bazopoulou, D., Chronis, N., Srinivasan, J., and Chalasani, S.H. (2015). Circuit mechanisms encoding odors and driving aging-associated behavioral declines in Caenorhabditis elegans. Elife *4*, 1–26.

Li, H., and Durbin, R. (2009). Fast and accurate short read alignment with Burrows-Wheeler transform. Bioinformatics *25*, 1754–1760.

Li, H., Handsaker, B., Wysoker, A., Fennell, T., Ruan, J., Homer, N., Marth, G., Abecasis, G., and Durbin, R. (2009). The Sequence Alignment/Map format and SAMtools. Bioinformatics *25*, 2078–2079.

Liachko, N.F., Guthrie, C.R., and Kraemer, B.C. (2010). Phosphorylation promotes neurotoxicity in a Caenorhabditis elegans model of TDP-43 proteinopathy. J. Neurosci. *30*, 16208–16219.

Liu, J., Zhang, B., Lei, H., Feng, Z., Liu, J., Hsu, A.-L., and Xu, X.Z.S. (2013). Functional aging in the nervous system contributes to age-dependent motor activity decline in C. elegans. Cell Metab. *18*, 392–402.

Lovato, T.L., Adams, M.M., Baker, P.W., and Cripps, R.M. (2009). A molecular mechanism of temperature sensitivity for mutations affecting the Drosophila muscle regulator myocyte enhancer factor-2. Genetics *183*, 107–117.

Lowry, J., Yochem, J., Chuang, C., Sugioka, K., and Connolly, A. a (2015). High-Throughput Cloning Of Temperature-Sensitive C . elegans Mutants With Adult Syncytial

Germline Membrane Architecture Defects. G3 Genes|Genomes|Genetics *5*, 2241–2255.

MacLeod, A., Karn, J., and Brenner, S. (1981). Molecular analysis of the *unc-54* myosin heavy-chain gene of *Caenorhabditis elegans*. Nature *291*, 386–390.

Maruyama, I.N., and Brenner, S. (1991). A phorbol ester/diacylglycerol-binding protein encoded by the *unc-13* gene of *Caenorhabditis elegans*. Proc. Natl. Acad. Sci. *88*, 5729–5733.

Mello, C.C., Kramer, J.M., Stinchcomb, D., and Ambros, V. (1991). Efficient gene transfer in C.elegans: extrachromosomal maintenance and integration of transforming sequences. EMBO J. *10*, 3959–3970.

Milman, S., Atzmon, G., Huffman, D.M., Wan, J., Crandall, J.P., Cohen, P., and Barzilai, N. (2014). Low insulin-like growth factor-1 level predicts survival in humans with exceptional longevity. Aging Cell *13*, 769–771.

Minevich, G., Park, D.S., Blankenberg, D., Poole, R.J., and Hobert, O. (2012). CloudMap: a cloud-based pipeline for analysis of mutant genome sequences. Genetics *192*, 1249–1269.

Morimoto, R. (1993). Cells in stress: transcriptional activation of heat shock genes. Science (80-.). *259*, 1409–1410.

Morley, J.F., Brignull, H.R., Weyers, J.J., and Morimoto, R.I. (2002). The threshold for polyglutamine-expansion protein aggregation and cellular toxicity is dynamic and influenced by aging in Caenorhabditis elegans. Proc. Natl. Acad. Sci. U. S. A. *99*, 10417–10422.

Mormino, E.C., Sperling, R.A., Holmes, A.J., Buckner, R.L., De Jager, P.L., Smoller, J.W., Sabuncu, M.R., and Alzheimer's Disease Neuroimaging Initiative (2016). Polygenic risk of Alzheimer disease is associated with early- and late-life processes. Neurology *87*, 481–488.

Mulcahy, B., Holden-Dye, L., and O'Connor, V. (2012). Pharmacological assays reveal age-

related changes in synaptic transmission at the Caenorhabditis elegans neuromuscular junction that are modified by reduced insulin signalling. J. Exp. Biol. 492–501.

Murakami, T., Yang, S.-P., Xie, L., Kawano, T., Fu, D., Mukai, A., Bohm, C., Chen, F., Robertson, J., Suzuki, H., et al. (2012). ALS mutations in FUS cause neuronal dysfunction and death in Caenorhabditis elegans by a dominant gain-of-function mechanism. Hum. Mol. Genet. *21*, 1–9.

Nedialkova, D.D., and Leidel, S.A. (2015). Optimization of Codon Translation Rates via tRNA Modifications Maintains Proteome Integrity. Cell *161*, 1606–1618.

Newell Stamper, B.L., Cypser, J.R., Kechris, K., Kitzenberg, D.A., Tedesco, P.M., and Johnson, T.E. (2018). Movement decline across lifespan of *Caenorhabditis elegans* mutants in the insulin/insulin-like signaling pathway. Aging Cell *17*, 1–14.

Oeda, T., Shimohama, S., Kitagawa, N., Kohno, R., Imura, T., Shibasaki, H., and Ishii, N. (2001). Oxidative stress causes abnormal accumulation of familial amyotrophic lateral sclerosis-related mutant SOD1 in transgenic Caenorhabditis elegans. Hum. Mol. Genet. *10*, 2013–2023.

Oh, K.H., and Kim, H. (2013). Reduced IGF signaling prevents muscle cell death in a Caenorhabditis elegans model of muscular dystrophy. Proc. Natl. Acad. Sci. U. S. A. *110*, 19024–19029.

Otero, G., Fellows, J., Yang, L., De Bizemont, T., Dirac, A.M.G., Gustafsson, C.M., Erdjument-Bromage, H., Tempst, P., and Svejstrup, J.Q. (1999). Elongator, a multisubunit component of a novel RNA polymerase II holoenzyme for transcriptional elongation. Mol. Cell *3*, 109–118.

Patten, S.A., Aggad, D., Martinez, J., Tremblay, E., Petrillo, J., Armstrong, G.A.B., La

Fontaine, A., Maios, C., Liao, M., Ciura, S., et al. (2017). Neuroleptics as therapeutic compounds stabilizing neuromuscular transmission in amyotrophic lateral sclerosis. JCI Insight *2*.

Phizicky, E.M., and Hopper, A.K. (2010). tRNA biology charges to the front. Genes Dev. *24*, 1832–1860.

Podshivalova, K., Kerr, R.A., and Kenyon, C. (2017). How a Mutation that Slows Aging Can Also Disproportionately Extend End-of-Life Decrepitude. Cell Rep. *19*, 441–450.

Reilich, P., Schoser, B., Schramm, N., Krause, S., Schessl, J., Kress, W., Müller-Höcker, J., Walter, M.C., and Lochmuller, H. (2010). The p.G154S mutation of the alpha-B crystallin gene (CRYAB) causes late-onset distal myopathy. Neuromuscul. Disord. *20*, 255–259.

Reiner, D.J., Newton, E.M., Tian, H., and Thomas, J.H. (1999). Diverse behavioural defects caused by mutations in *Caenorhabditis elegans unc-43* CaM kinase II. Nature *402*, 199–203.

Renton, A.E., Majounie, E., Waite, A., Simón-Sánchez, J., Rollinson, S., Gibbs, J.R., Schymick, J.C., Laaksovirta, H., van Swieten, J.C., Myllykangas, L., et al. (2011). A hexanucleotide repeat expansion in C9ORF72 is the cause of chromosome 9p21-linked ALS-FTD. Neuron *72*, 257–268.

Rollins, J.A., Howard, A.C., Dobbins, S.K., Washburn, E.H., and Rogers, A.N. (2017). Assessing health Span in *Caenorhabditis elegans*: Lessons from short-lived mutants. Journals Gerontol. - Ser. A Biol. Sci. Med. Sci. *72*, 473–480.

Ross, C.A., Wood, J.D., Schilling, G., Peters, M.F., Nucifora, F.C., Cooper, J.K., Sharp, A.H., Margolis, R.L., and Borchelt, D.R. (1999). Polyglutamine pathogenesis. Philos. Trans. R. Soc. Lond. B. Biol. Sci. *354*, 1005–1011.

Rubin, B.Y., and Anderson, S.L. (2017). IKBKAP/ELP1 gene mutations: Mechanisms of

familial dysautonomia and gene-targeting therapies. Appl. Clin. Genet. *10*, 95–103.

Rubinsztein, D.C., Leggo, J., Coles, R., Almqvist, E., Biancalana, V., Cassiman, J.J., Chotai, K., Connarty, M., Crauford, D., Curtis, a, et al. (1996). Phenotypic characterization of individuals with 30-40 CAG repeats in the Huntington disease (HD) gene reveals HD cases with 36 repeats and apparently normal elderly individuals with 36-39 repeats. Am. J. Hum. Genet. *59*, 16–22.

Rudolf, R., Khan, M.M., Labeit, S., and Deschenes, M.R. (2014). Degeneration of neuromuscular junction in age and dystrophy. Front. Aging Neurosci. *6*, 1–11.

Samuelson, A. V, Carr, C.E., and Ruvkun, G. (2007). Gene activities that mediate increased life span of C. elegans insulin-like signaling mutants. Genes Dev. *21*, 2976–2994.

Selcen, D., and Engel, a G. (2003). Myofibrillar myopathy caused by novel dominant negative alpha B- crystallin mutations. Ann Neurol *54*, 804–810.

Sievers, F., Wilm, A., Dineen, D., Gibson, T.J., Karplus, K., Li, W., Lopez, R., McWilliam, H., Remmert, M., Söding, J., et al. (2011). Fast, scalable generation of high-quality protein multiple sequence alignments using Clustal Omega. Mol. Syst. Biol. *7*.

Siller, E., Dezwaan, D.C., Anderson, J.F., Freeman, B.C., and Barral, J.M. (2010). Slowing Bacterial Translation Speed Enhances Eukaryotic Protein Folding Efficiency. J. Mol. Biol. *396*, 1310–1318.

Silva, M.C., Fox, S., Beam, M., Thakkar, H., Amaral, M.D., and Morimoto, R.I. (2011). A genetic screening strategy identifies novel regulators of the proteostasis network. PLoS Genet. *7*.

Simpson, C.L., Lemmens, R., Miskiewicz, K., Broom, W.J., Hansen, V.K., van Vught, P.W.J., Landers, J.E., Sapp, P., Van Den Bosch, L., Knight, J., et al. (2009). Variants of the

elongator protein 3 (ELP3) gene are associated with motor neuron degeneration. Hum. Mol. Genet. *18*, 472–481.

Slaugenhaupt, S.A., Blumenfeld, A., Gill, S.P., Leyne, M., Mull, J., Cuajungco, M.P., Liebert, C.B., Chadwick, B., Idelson, M., Reznik, L., et al. (2001). Tissue-specific expression of a splicing mutation in the IKBKAP gene causes familial dysautonomia. Am. J. Hum. Genet. *68*, 598–605.

Solinger, J.A., Paolinelli, R., Klöß, H., Scorza, F.B., Marchesi, S., Sauder, U., Mitsushima, D., Capuani, F., Stürzenbaum, S.R., and Cassata, G. (2010). The *Caenorhabditis elegans* Elongator Complex Regulates Neuronal α-tubulin Acetylation. PLoS Genet. *6*, e1000820.

Von Stetina, S.E., Treinin, M., and Miller, D.M. (2005). The Motor Circuit. Int. Rev. Neurobiol. *69*, 125–167.

Strug, L.J., Clarke, T., Chiang, T., Chien, M., Baskurt, Z., Li, W., Dorfman, R., Bali, B., Wirrell, E., Kugler, S.L., et al. (2009). Centrotemporal sharp wave EEG trait in rolandic epilepsy maps to Elongator Protein Complex 4 (ELP4). Eur. J. Hum. Genet. *17*, 1171–1181.

Taylor, R.C., and Dillin, A. (2011). Aging as an event of proteostasis collapse. Cold Spring Harb. Perspect. Biol. *3*, 1–17.

Therrien, M., Rouleau, G. a, Dion, P. a, and Parker, J.A. (2013). Deletion of C9ORF72 Results in Motor Neuron Degeneration and Stress Sensitivity in C. elegans. PLoS One *8*, e83450.

Tissenbaum, H.A. (2012). Genetics, Life span, Health Span, and the Aging Process in *Caenorhabditis elegans*. J. Gerontol. A. Biol. Sci. Med. Sci. *67*, 503–510.

Toth, M.L., Melentijevic, I., Shah, L., Bhatia, A., Lu, K., Talwar, A., Naji, H., Ibanez-Ventoso, C., Ghose, P., Jevince, A., et al. (2012). Neurite sprouting and synapse deterioration

in the aging Caenorhabditis elegans nervous system. J. Neurosci. *32*, 8778–8790.

Vaccaro, A., Tauffenberger, A., Aggad, D., Rouleau, G., Drapeau, P., and Parker, J.A. (2012). Mutant TDP-43 and FUS cause age-dependent paralysis and neurodegeneration in C. elegans. PLoS One *7*, e31321.

Wang, E., Wang, J., Chen, C., and Xiao, Y. (2015). Computational evidence that fast translation speed can increase the probability of cotranslational protein folding. Sci. Rep. *5*, 15316.

White, J., Southgate, E., Thomson, J., and Brenner, S. (1986). The structure of the nervous system of the nematode Caenorhabditis elegans. Philos. Trans. R. Soc. Lond. B. Biol. Sci. *314*, 1–340.

Wu, Y., Wu, Z., Butko, P., Christen, Y., Lambert, M.P., Klein, W.L., Link, C.D., and Luo, Y. (2006). Amyloid-beta-induced pathological behaviors are suppressed by Ginkgo biloba extract EGb 761 and ginkgolides in transgenic Caenorhabditis elegans. J. Neurosci. *26*, 13102–13113.

Zhang, X.H., Tee, L.Y., Wang, X.G., Huang, Q.S., and Yang, S.H. (2015). Off-target effects in CRISPR/Cas9-mediated genome engineering. Mol. Ther. - Nucleic Acids *4*, e264.

Zhao, Y., Gilliat, A.F., Ziehm, M., Turmaine, M., Wang, H., Ezcurra, M., Yang, C., Phillips, G., Mcbay, D., Zhang, W.B., et al. (2017). Two forms of death in ageing Caenorhabditis elegans. Nat. Commun. *8*, 1–8.

Zobel, A.T.C., Loranger, A., Marceau, N., Thériault, J.R., Lambert, H., and Landry, J. (2003). Distinct chaperone mechanisms can delay the formation of aggresomes by the myopathy-causing R120G αB-crystallin mutant. Hum. Mol. Genet. *12*, 1609–1620.

Zuryn, S., and Jarriault, S. (2013). Deep sequencing strategies for mapping and identifying

mutations from genetic screens. Worm *2*, e25081.